Preparation and Characterization of Polypropylene-Cellulose Composites

By

Ulaş ATİKLER

**A Dissertion Submitted to the
Graduate School in Partial Fulfillment of the
Requirements for the Degree of**

MASTER OF SCIENCE

**Department: Chemical Engineering
Major: Chemical Engineering**

**İzmir Institute of Technology
İzmir,Turkey**

July, 2004

We approve the thesis of **Ulaş ATİKLER**

Date of Signature

..... **23.07.2004**

Assoc. Prof. Dr. Funda TIHMINLIOĞLU
Supervisor
Department of Chemical Engineering

..... **23.07.2004**

Prof. Dr. Devrim BALKÖSE
Co-Supervisor
Department of Chemical Engineering

..... **23.07.2004**

Prof. Dr. Semra ÜLKÜ
Co-Supervisor
Department of Chemical Engineering

..... **23.07.2004**

Assoc.Prof.Dr. Metin TANOĞLU
Department of Mechanical Engineering

..... **23.07.2004**

AsstProf.Dr. Erol Şeker
Department of Chemical Engineering

..... **23.07.2004**

AsstProf.Dr. Sedat Akkurt
Department of Mechanical Engineering

..... **23.07.2004**

Prof.Dr. Devrim BALKÖSE
Head of Department

ACKNOWLADGEMENTS

I would like to thank tomy supervisor Funda Tıhmınlıoğlu for her support, trust and reccomendations during my thesis study. I would also thank to my co-advisors Devrim BALKÖSE for her understanding, support and symphaty and Semra ÜLKÜ.

I would also thank to Metin TANOĞLU, Sedat AKKURT and Erol ŞEKER for their reccomendations.

Thanks to Hasan DEMİR who makes everything easier, tolerable and enjoyable for me.

Also thanks to MAM stuff for their patience and helpingness. I also want to thank to PETKİM Quality Control stuff, especially Ali ÖZİŞ and Feridun ŞENOL for their endless support to my study.

ABSTRACT

In recent years, much effort has been driven to replace glass fibers, which were used to reinforce thermoplastic composites, with natural fibers. In this study, three natural fibers, namely cellulose (CE), sawdust (SD) and wheat straw (WS) were employed as reinforcement to polypropylene (PP) polymer matrix. The most important problem encountered with natural fiber/PP composites is the inherent incompatibility between hydrophilic natural fibers and hydrophobic PP matrix, thus coupling agents were employed to alter incompatibility between fiber and matrix. Coupling agents enhance interfacial interactions by chemical and physical bonding between fiber and matrix. Surface treatment of natural fibers were carried out with two kinds of silanes; (3-aminopropyl)-triethoxysilane (AS) and methacriloxy propyl trimethoxy silane (MS), and maleic anhydride grafted polypropylene (MAPP). Silane coupling agents were agitated in aqueous ethanol solution in the presence of fibers at weight percents of 0.5, 1 and 2.5 with respect to fiber weight. MAPP was compounded during melt mixing of fiber and PP at weight percents of 2.5, 5 and 10 with respect to PP weight.

PP/fiber composites were prepared in a rheomixer equipped with two rotor blades and adjustable temperature, mixing rate and mixing time. Composites were prepared at 185 ^{o}C, 50 rpm mixing rate and 10 minutes mixing time. Torque values of each composite formulation were recorded with respect to time to determine changes in rheological properties of composites. It was found that increase in fiber loading increases stabilization torque of composites.

Mechanical properties of PP/fiber composites were significantly enhanced by employment of coupling agents and MAPP was found to be the most effective coupling agent. Mechanical properties of SD composites were found to exhibit the best performance compared to C and WS. Extent of interfacial interactions were evaluated with Pukanszky and Nielsen model and superior performance of MAPP in enhancing interfacial interactions was confirmed by these two models. Optimum conditions for coupling agents were found to be 1 wt % for silane coupling agents and 5 wt % for MAPP.

It was found that water sorption and void fraction of the composites decreased with employment of coupling agents. Among the coupling agents, MAPP exhibited the best performance in decreasing water sorption and void fraction of composites confirming results of mechanical tests. Scanning electron micrographs (SEM) used to

illustrate the effect of coupling agents on adhesion between fiber and matrix and fracture modes of the composites. In addition, FTIR analysis revealed the decrease in hydrophilicity of fibers with silane treatment and new bond formations with employment of MAPP.

ÖZ

Geçtiğimiz yıllarda termoplastik kompozitleri güçlendirmek amacıyla cam elyafı yerine doğal fiberlerin kullanımı konusu önem kazanmıştır. Bu çalışma da selüloz, talaş ve buğday sapı olmak üzere üç çeşit doğal fiberin polipropilen matrisi güçlendirmek amacıyla kullanımını içermektedir. Doğal fiberler içeren polipropilen (PP) kompozitlerinin hazırlanmasında en büyük problem olan ve hidrofilik yapıdaki doğal fiberlerin hidrofobik PP matrisle uyumsuzluğundan kaynaklanan bağlanma güçlüğünü gidermek için üç çeşit bağlayıcı kullanıldı. Bağlayıcılar fiber ile matris arayüzeyinde fiziksel ve kimyasal bağlar oluşturarak iki yüzey arasındaki yapışmayı güçlendirmektedir. Bunu sağlamak amacıyla doğal fiberler iki tür silan ve maleik anhidrid kaplanmış polipropilen (MAPP) ile yüzey işlemlerine tabi tutuldu. Silan bağlayıcı olarak kullanılan (3-aminopropil)-trietoksisilan (AS) ve metoksipropil trimetoksi silan (MS), fiber ağırlığına göre 0.5, 1 ve 2.5 % oranlarında fiberlerle karıştırılarak sulu alkol çözeltisi içinde reaksiyona sokuldu. MAPP ise doğal fiberlerin PP eriyiğine karıştırılması işlemi sırasında PP ağırlığına göre 2.5, 5 ve 10% oranlarında eklenerek kullanıldı.

PP/fiber kompozitler iki rotorlu bir karıştırıcı ünitesi bulunan, karıştırma hızı, karıştırma zamanı ve sıcaklığı ayarlanabilir bir reomikserde hazırlandı. Kompozitlerin hazırlanmasında sıcaklık 185 ºC, karıştırma hızı ve zamanı ise 50 rpm ve 10 dakika olmak üzere sabit tutuldu. Karıştırma işlemi sırasında uygulanan formülasyonların tork değerleri zamana karşı kaydedildi ve böylece örneklerin reolojik özelliklerindeki değişimler belirlendi.

Bağlayıcı kullanıldığında PP/ fiber kompozitlerin mekanik özelliklerinin iyileştiği ve en etkili bağlayıcının MAPP olduğu görüldü. Selüloz ve buğday sapıyla karşılaştırıldığında talaşla hazırlanan örneklerin daha iyi mekanik özelliklere sahip olduğu gözlendi. Arayüzey etkileşimleri Pukanski ve Nielsen modellerine göre değerlendirildi ve MAPP'nin gösterdiği üstün performans bu modellerle de doğrulandı. Bağlayıcılar için ideal ağırlık oranları silan için 1 % ve MAPP için 5 % olarak belirlendi.

Örnek kompozitlerin su çekişinin ve boşluk oranlarının bağlayıcı kullanıldığında azaldığı ve mekanik testlerde olduğu gibi su çekişi ve boşluk oranı bakımından da en iyi sonuçların MAPP ile alındığı gözlendi. Fiber ve matris arasındaki yapışma özellikleri üzerinde bağlayıcıların etkisi ve kompozitlerin kırılma modu SEM görüntüleriyle

desteklendi. FTIR analizi sonuçları doğrultusunda silan uygulamasıyla fiberlerin hidrofobik özelliklerinin azaldığı ve MAPP katkısıyla gerçekleşen yeni bağ oluşumları bulgulandı.

TABLE OF CONTENTS

LIST OF FIGURES

LIST OF TABLES

Chapter 1

INTRODUCTION

A recent approach have focused on the idea of employing natural fibers, particularly lignocellulosic fibers, as an alternative to inorganic counterparts, mostly glass fibers, as reinforcing agents in composite materials based on thermoplastic matrices (Zafeiropoulos et al, 2002). Although not popular yet as mineral and inorganic fillers and fibers, lignocellulosic fibers have several advantages over traditional fillers and fibers such as low density, flexibility during processing with no harm to equipment, acceptable specific strength properties, and low cost per volume basis (Ichazo et al, 2001). Several companies now manufacture lignocellulosic fiber/thermoplastic composites for use as synthetic lumber in applications such as decking and window frames (Selke and Wickman, 2003) .

Frequently employed polymer in lignocellulosic fiber/thermoplastic composites is polypropylene (PP) because of superior mechanical properties and compatible processing temperatures with lignocellulosic fibers avoiding degradation of cellulose.

There have been numerous attempts to use lignocellulosic fibers as an alternative in PP matrices including wood flour (Ichazo et al, 2001), wood pulp (Bataille et al, 1989), sisal fiber (Joseph at al, 1999) and sawdust (Suarez et al, 2003). Incorporation of lignocellulosic fibers were found to improve stiffness, dimensional stability and sometimes strength of PP matrix.

A major issue in achieving true reinforcement with the incorporation of lignocellulosic fibers into thermoplastic matrices is the inherent incompatibility between the hydrophilic fibers and the hydrophobic polymers. This results in poor adhesion between fiber and matrix, and therefore in poor ability to transfer stress from the matrix to the fiber. To increase the quality of the fiber-matrix interface in composite materials, surface modification of fibers is required to achieve maximum compatibility and thereby good adhesion. Thus, in the case of matrices bearing nonpolar properties, such as PP, chemical modifications were employed in order to transform polar hydroxyl groups on lignocellulosic fibers capable of creating hydrogen or chemical bonds with the matrix (Gauthier et al, 1998). Surface modification of the fibers also imparts in

hydrophobization of lignocellulosic fibers, a cause of hydroxyl groups on the fibers, decreasing moisture sensitivity of the fibers.

The most effective coupling agents to achieve good adhesion between lignocellulosic fibers and thermoplastic matrices were found to be silanes and maleic anhydride grafted polyolefins (Bledzki and Gassan, 1999)

Ichazo et al (2001) studied the effect of modification of wood flour as the lignocellulosic fiber on mechanical and water sorption properties of wood flour/PP composites. They employed vinil-tris-(2-metoxietoxi)-silane and maleic anhydride grafted polypropylene as coupling agent. They achieved significant improvements in tensile strength and stiffness with incorporation of wood flour. Surface treatments, especially (MAPP) further increased tensile strength of composites. Water sorption of composites decreased with surface treatment as well.

Bataille et al (1989) studied the effect of two silane coupling agents, namely metacryloxy-propyl trimethoxy silane and amino-propyl trimethoxy silane on mechanical performance of PP/cellulose fiber composites. They used methanol/water mixture as the aqueous medium for silanation of the fibers at 3:10 coupling agent: cellulose fiber ratio. They achieved about 20% improvements in yield stress with employment of silane coupling agents.

Castellano et al (2004) studied the extent of reaction between cellulose and two silane coupling agents by means of contact angle measurements, FTIR and inverse gas chromotography (IGC). Two silanes employed were cyanoethyltrimethoxy silane and methacryloxypropyltrimethoxy silane. They have observed a decrease in contact angle of cellulose which is a measure of decreased hydrophilicity of cellulose. They have also observed new bands in FTIR spectra caused by bonding between silanes and cellulose. IGC results revealed that polar contribution of surface energy is decreased from 25.8 to 6.3 mJ/m^2 with cyanoethyltrimethoxy silane coupling agent treatment which was an evidence for decreased hydrophilicity of cellulose.

Keener et al (2003) studied the effect of maleic anhydride content and molecular weight of MAPP on mechanical properties of PP composites containing jute and flax as lignocellulosic fiber. They obtained that maleic anhydride content and molecular weight of MAPP must be optimized in order to achieve balanced mechanical properties.

The objective of this study is to prepare PP/lignocellulosic fiber composites from cellulose, sawdust and wheat straw and to improve mechanical properties of PP/fiber composites by employment of coupling agents. Two silane coupling agents; (3-

aminopropyl)-triethoxysilane (AS) and methacriloxy propyl trimethoxy silane (MS), and maleic anhydride grafted polypropylene (MAPP) were employed in order to increase compatibility between fiber and matrix. Water sorption and microstructural characterization of the composites were also investigated.

The thesis is organized in the following fashion: In Chapter 2, background information about lignocellulosic fibers and PP is given. In Chapter 3 theoretical aspects of adhesion is introduced, strategies to improve compatibility was revised and characterization of interface was explained. Chapter 4 and Chapter 5 cover experimental procedure and analysis, and results of the thesis, respectively. Conclusions and recommendations are given in the final chapter of the thesis.

Chapter 2

POLYPROPYLENE/CELLULOSE COMPOSITES

In this chapter, polymer composites and their applications will be covered. Properties of our matrix material; polypropylene and fiber; cellulose will be introduced. Application areas of cellulose based natural fiber; thermoplastic composites will also be overviewed.

2.1. Polymer Composites

Composite materials may be defined as materials made up of two or more components and consisting of two or more phases. Such materials must be heterogeneous at least on a microscopic scale. A composite consists of fibers or fillers embedded in or bonded to a matrix with distinct interfaces between the two constituent phases. The matrix must keep fibers or fillers in a desired location or orientation, separating fillers and fibers from each other to avoid mutual abrasion during periodic straining of the composites. The matrix acts as a load transfer medium between fibers or fillers. Since the matrix is generally more ductile than fibers and fillers, it is the source of composite toughness. The matrix also serves to protect the fibers and fillers from environmental damage before, during and after composite processing (Jang , 1994).

In a composite, both fibers and fillers and the matrix largely retain their identities and yet result in many properties that cannot be achieved with either of the constituents acting alone. There are 3 general classes of composite materials;

i) Particulate filled materials consisting of a continuous matrix phase and a discontinuous filler phase. e.g. talc filled PP
ii) Fiber-filled composites e.g. glass fiber filled PP
iii) Interpenetrating composites made up of two continuous phases PP-PE polymer blend

Mineral fillers, such as calcium carbonate, clays, silicas, mica, talc, alumina trihydrate and titanium dioxide account for about 90% of the demand for the fillers and

extenders, with calcium carbonate being by far the most commonly used filler(Rothon, 1999). Non-mineral fillers include carbon black, glass beads and various organic materials such as cellulose. Fibers also find various application areas in composite technology. The most commonly used fibers in polymer matrices are various types of carbon, glass and aramid (e.g., Kevlar®) fibers. Boron fibers are expensive and are used currently in military and aerospace applications only. Also still in limited use are silicon nitride, silicon carbide, mullite and other ceramic fibers and metal wires (Jang , 1994). There are several reasons to use polymer composites rather than single polymers. These include

i) Increased stiffness and strength
ii) Increased dimensional stability
iii) Increased heat deflection temperature
iv) Increased electrical conductivity
v) Improved impact strength
vi) Reduced flammability
vii) Reduced permeability to gasses
viii) Reduced cost

There are also disadvantages encountered with addition of fillers to polymer matrices such as complex rheological properties, difficult fabrication techniques and reduction in some physical and mechanical properties. An optimization must be made between advantages and disadvantages of composites for balanced end use properties. In the present study, PP as the polymer matrix material and cellulosic fibers, namely cellulose, sawdust and wheat straw as the filler or fiber were used in the preparation of the composites.

2.2. Matrix: Polypropylene

Polypropylene is a polyolefin which are an important class of polymers. Polyolefins, which are defined as polymers based on alkene-1 monomers or α-olefins, are the most widely used group of thermoplastic polymers today. Based on their monomeric units and their chain structures, they can be divided into the following subgroups (Gahleitner , 2001):

i) Ethylene based materials –polyethylenes(PE s)-produced under low pressure conditions with transition metal catalysts of various types and showing a linear chain structure. This subgroup includes high density PE (HDPE), medium density PE (MDPE), linear low- density PE (LLDPE).

ii) Ethylene based polymers (PE s) produced in a radical polymerization under high pressure with oxygen or peroxides as chain initiators and showing a branched chain structure. According to their reduced crystallinities and densities, these materials are termed low density polyethylenes (LDPE s).

iii) Propylene- based polymers produced with transition-metal catalysts-polypropylene (PP) and its copolymers-showing a linear chain structure with stereo specific arrangement of the propylene units. Mostly the isotactic species (iPP) is used today, but also syndiotactic (sPP) species are also available.

iv) Polymers based on higher α-olefins,(e.g. poly-butene-1) produced with transition metal catalysts and having a linear and stereospecific chain structure.

v) Olefinic elastomers based on transition metal or single-site catalysts. These polymers are based on ethylene and propylene, amorphous with high molecular masses.

More than 60% of produced polyolefins (PP, PE) have been introduced to the market as compounds, while only about 23% of the volume of the other thermoplastics have been used for compounding. Polypropylene is considered one of the primary candidates to become the matrix of the choice for engineering new thermoplastic compounds, replacing many small volume engineering plastics.

Polypropylene (PP) is a semi crystalline commodity thermoplastic produced by coordination addition polymerization of propylene monomer as seen in Figure 2.1. Most frequently, Ziegler-Natta catalysts are employed in industrial processes to produce crystalline isotactic (iPP) and syndiotactic (sPP) polymer with a small portion of amorphous atactic PP as a side product. Polymerization reaction can be summarized as follows;

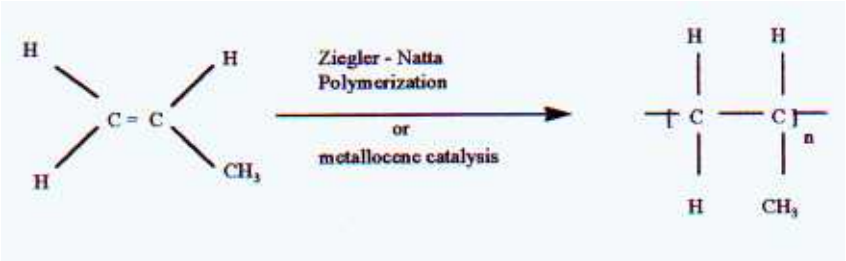

Figure 2.1. Synthesis of polypropylene.

Polypropylene has recently become an attractive candidate for many engineering applications. Relatively low price, excellent chemical resistance, good processability and the possibility of modifying its mechanical properties in a wide range by adding fillers and dispersions of secondary polymeric inclusions has contributed to its massive expansion into automotive, land transport, home appliances and other industries. Poor low temperature impact behavior relatively low stiffness are among the most important deficiencies prohibiting neat polypropylene replacing more expensive engineering thermoplastics in more demanding applications. Binary combinations of polypropylene with fillers or elastomers address generally only one concern and exhibit either increased stiffness or enhanced low temperature fracture resistance. It is, however, necessary, in order to increase PP marketability into more demanding markets, to increase both stiffness and toughness at the same time. Hence, attempts have been made to incorporate fiber, filler and elastomer inclusions into the PP matrix in the course of melt mixing. (Janjar, 1999)

2.3. Fiber: Natural fibers

Components of natural fibers are cellulose ,hemi-cellulose , lignin, pectin, waxes, and water soluble substances with cellulose , hemi-cellulose , and lignin as the basic components with regard to the physical properties of the fibers.

2.3.1.Cellulose

Cellulose is the essential component of all plant fibers. Cellulose is a linear condensation polymer consisting of glucose units jointed together by β-1,4- glycosidic bonds. The formula of cellulose is shown in Figure 2.2.

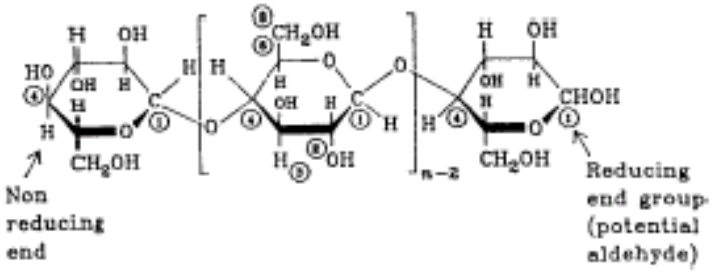

Figure 2.2. Chemical structure of cellulose (Bledzki and Gassan,1999).

The molecular structure of cellulose is responsible for its supramolecular which determines many of its chemical and physical properties.

The mechanical properties of natural fibers depend on its cellulose type and spiral angle, because each type of cellulose has its own cell geometry and geometrical conditions determine the mechanical properties.

Solid cellulose forms a microcrystalline structure with regions of high order i.e. crystalline regions. Naturally occurring cellulose crystallizes in monoclinic structure. The molecular chains are oriented in the fiber direction as seen in Figure 2.3.

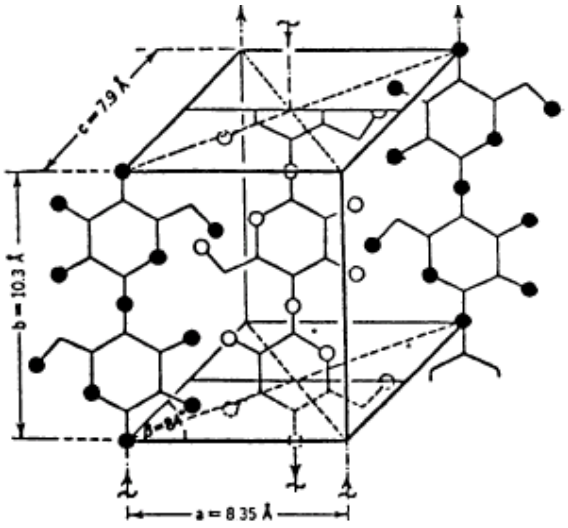

Figure 2.3. Crystal structure of cellulose (Bledzki and Gassan,1999).

2.3.2.Further Components

Hemi cellulose is a group of polysaccharides that remains associated with the cellulose after lignin has been removed. Hemi cellulose exhibits a considerable degree

of chain branching whereas cellulose is a strictly linear polymer. Unlike cellulose , the constituents of hemi cellulose differ from plant to plant:

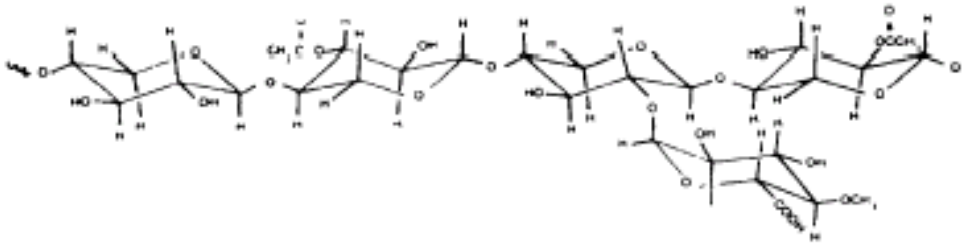

Figure 2.4. Chemical structure of hemicelluloses (Bledzki and Gassan,1999).

Lignins are complex hydrocarbon polymers with both aliphatic and aromatic constituents (Figure 2.5). Lignin acts as amorphous, ductile matrix in a natural fiber composite structure so the mechanical properties are lower than those of cellulose. Lignin also decreases water sorption capacity of cellulose by forming a layer on polar cellulose molecules.

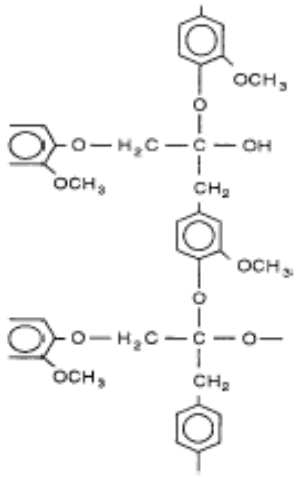

Figure 2.5. Chemical structure of lignin (Bledzki,1999).

2.3.3. Physical Structure of Cellulose Fibers

A single fiber of all plant based natural fibers consists of several cells. These cells are formed out of crystalline micro fibrils based on cellulose, which are connected to a complete layer, by amorphous lignin and hemi cellulose. This structure is a good

example of a composite with lignin hemi cellulose matrix and cellulose fiber reinforcement. Strength is supplied by highly crystalline cellulose whereas ductility is supplied by amorphous lignin and other components. Structure is depicted in Fig 2.6. Multiple of such cellulose –lignin/hemi cellulose layers in one primary and three secondary cell walls stick together in a multiple layer composite. These cell walls differ in composition and in the orientation (spiral angle) of the cellulose micro fibrils. The spiral angle of the fibrils and the content of cellulose determine mechanical properties of cellulose based natural fibers.

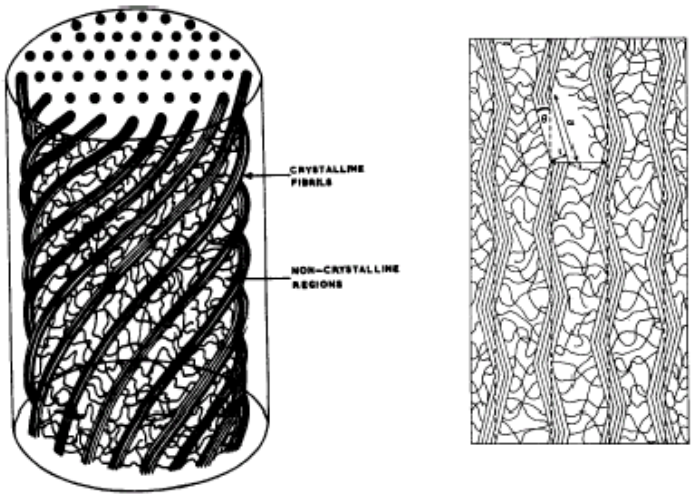

Figure 2.6. Structure of plant cell (Bledzki,1999).

Natural fibers are subdivided based on their origins, coming from plants, animals or minerals. Generally, plant or vegetable fibers are used to reinforce plastics. Plant fibers can be classified as follows as seen in Figure 2.7 (Michel, 1989):

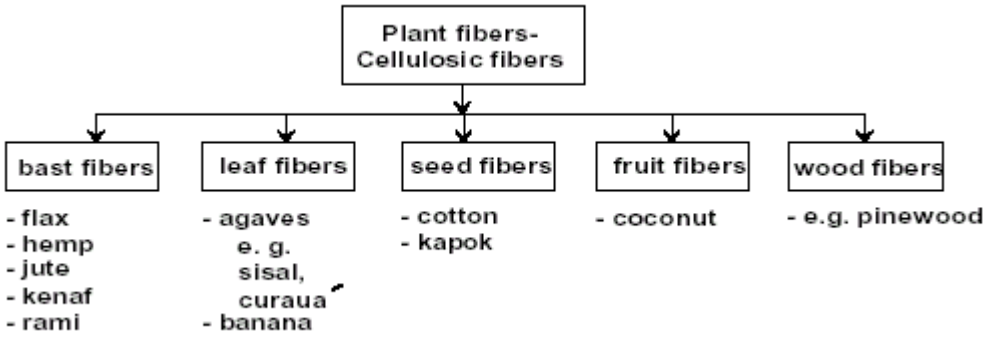

Figure 2.7. Classification of plant fibers (Michel, 1989).

The availability of large quantities of such fibers with well defined mechanical properties is a general prerequisite for successful use of these materials. Additionally for more technical oriented applications, the fibers have to be specially prepared or modified regarding (Bledzki and Gassan,1999):

i) homogenization of the fiber's properties;
ii) degrees of elementarization and degumming;
iii) degrees of polymerization and crystallization;
iv) good adhesion between fiber and matrix;
v) moisture repellence;
vi) flame retardant properties.

2.3.4. Mechanical Properties of Natural Fibers

Natural fibers are in general suitable to reinforce plastics (thermosets as well as thermoplastics) due to their high strength and stiffness and low density. Thermoplastic polymers are primarily reinforced by glass fibers due to superior mechanical and thermal properties of glass fibers. In recent years, much effort has been driven to replace glass fibers with natural fibers. Advantages of natural fibers over glass fibers can be seen in Table 2.1. As seen from the table, key manufacturing properties of natural fibers such as density, cost, renewebility and machine compatibility is superior than glass fibers, but one has to keep in mind that natural fibers have some disadvantages such as poor wetting, incompatibility between fiber and some polymeric

matrices and high moisture absorption. Strategies to overcome these disadvantages will be discussed in Chapter 3.

Table 2.1. Comparison of natural and glass fibers (Wambua et al, 2003).

	Natural fibres	Glass fibres
Density	Low	Twice that of natural fibres
Cost	Low	Low, but higher than NF
Renewability	Yes	No
Recyclability	Yes	No
Energy consumption	Low	High
Distribution	Wide	wide
CO_2 neutral	Yes	No
Abrasion to machines	No	Yes
Health risk when inhaled	No	Yes
Disposal	Biodegradable	Not biodegradable

Table 2.2. shows mechanical properties of natural fibers and competing synthetic fibers (Gurram et al, 2002). The characteristic values for flax and softwood fibers reach levels close to the values for glass fibers. Nevertheless, the range of the characteristic values, as one of the drawbacks for all natural products, is higher than those of glass fibers, which can be explained by differences in fiber structure due to overall environmental conditions during growth.

Table 2.2. Mechanical properties of natural fibers (Gurram et al, 2002).

Fiber	Density (g/cm3)	Elongation (%)	Tensile strength(MPa)	Modulus (Gpa)
Cotton	1,3-1,6	7.0–8.0	287–597	5.5–12.6
Jute	1,3	1.5–1.8	393–773	26.5
Flax	1,5	2.7–3.2	345–1035	27.6
Hemp	-	1.6	690	—
Ramie	-	3.6–3.8	400–938	61.4–128
Sisal	1,5	2.0–2.5	511–635	9.4–22.0
Coir	1,2	30.0	175	4.0–6.0
Viscose	-	11.4	593	11.0
Soft wood	1,5	—	1000	40.0
Glass	2,5	2.5	2000–3500	70.0
Aramide	1,4	3.3–3.7	3000–3150	63.0–67.0
Carbon	1,4	1.4–1.8	4000	230–240

2.4. Application Areas and Market Growth of Natural Fiber Based Plastic Composites

The use of natural fiber-plastic composites is growing rapidly as consumers experience their advantages over wood including no routine maintenance and no cracking, warping or splintering. Mostly employed natural fibers in natural fiber-plastic composites is wood wastes such as hardwood, softwood, plywood, peanut hulls, bamboo, straw, etc. mixed with various plastics (PP, PE, PVC). Natural fibers employed are kenaf, hemp, jute, sisal, flax and rice husk. The powder is extruded into pellets and then extruded to desired shape (SpecialChem, 2002).

Wood-plastic composites are used primarily in building products such as decking, fencing, siding and decorative trim. Other applications include infrastructures such as boardwalks, marinas and guardrails; transportation such as interior automotive panels and truck floors; and industrial and consumer applications such as pallets, playground equipment and benches. Market share of wood and natural fiber-plastic fillers and various applications can be seen in Figure 2.8.

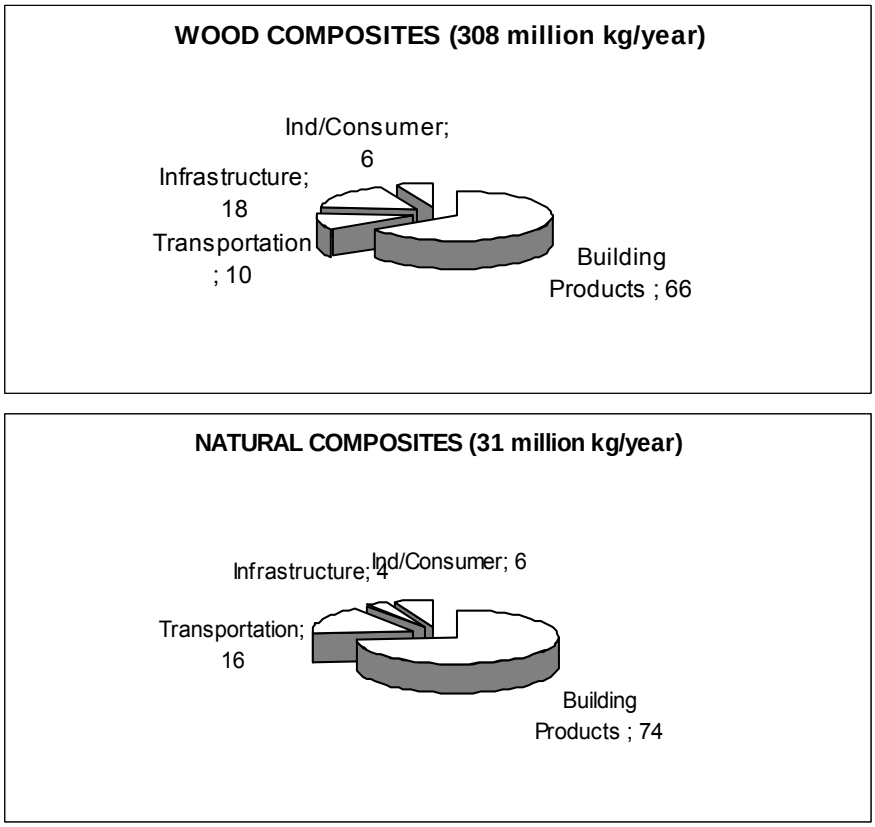

Figure 2.8. Markets for natural fiber and wood-plastic composites in 2001 in USA (SpecialChem, 2002).

In US, natural fiber and wood plastic composites have a total of 340 million kg/year capacity and it is predicted that it will reach a capacity of 635 million/year capacity at an annual growing rate of 12%. To meet the specified qualifications, additives such as coupling agents, colorants, lubricants consumption will grow accordingly.

Chapter 3

INTERFACE IN POLYMER COMPOSITES

Adhesion between fiber and matrix is achieved via different routes through the interface region. Interface refers to the boundary between two phases, namely fiber and matrix (Jang, 1994). Bonding between fiber and matrix is accomplished through the interface with different bonding mechanisms. The fiber or filler interfacial adhesion plays an important role in determining the mechanical properties of a polymer composite. A better interfacial bond will impart a composite improved properties such as interlaminar shear strength, fatigue and corrosion resistance.

Polymers used as matrices in thermoplastic composites as well as fillers and fibers have the most diverse physical and chemical structures, thus a wide variety of interactions may form between the two components. Two boundary cases of interactions can be distinguished: covalent bonds, which rarely form spontaneously, but can be created by special surface treatments and zero interaction, which does not exist in reality, since at least secondary, van der Waals forces always act between the components (Pukanszky and Fekete, 1999)

In practice the strength of the interaction is somewhere between the two boundary cases. Interaction between two surfaces in contact with each other can be created by primary or secondary bonds. The most important primary forces are the ionic, covalent and metallic bonds. The bonds formed by these forces are very strong, their strength is between 60-80 kj/mol for covalent and 600-1200 kj/mol for ionic bonds. The secondary bonds are created by van der Waals forces. The strength of these interactions is much lower; it is between 20 and 40 kj/mol. Hydrogen bonds form a transition between the two groups of interactions, both in character and strength. Besides the attractive forces created by the above mentioned secondary forces, repulsive forces also act between the interacting surfaces due to the interaction of their electron fields. The final distance of the atoms is determined by the equilibrium between attractive and repulsive forces (Pukanszky and Fekete, 1999).

3.1. Bonding Mechanisms

There are several bonding mechanisms between fiber or filler and matrix in polymer composites that impart in interfacial adhesion of the two phases.

3.1.1. Adsorption and Wetting

If the surface of two bodies come into contact when they are brought close to each other, then wetting is said to have taken place. Adhesion is primarily caused by van der Waals forces, although other type of bondings can co-exist. The occurrence of wetting can be explained by simple thermodynamics. In polymer composites, wetting is accomplished by wetting of liquid phase (polymer) onto a solid phase (filler or reinforcement). Contact between filler or reinforcement can be realized if the liquid is not too viscous and a thermodynamic driving force exits. This is expressed in terms of surface energies. The strength of the adhesive bond is assumed to be proportional to the reversible work of adhesion (W_{AB}), which is necessary to separate two phases with the creation of two new surfaces. The Dupre equation relates W_{AB} to the surface (φ_A and φ_B) and interfacial (φ_{AB}) tension of the components, i.e.:

$$W_a = \varphi_{SV} + \varphi_{LV} - \varphi_{SL} \tag{3.1}$$

The subscripts S,L and V refer to solid, liquid and vapor respectively. The vapor phase is commonly air. According to this equation, wetting is strongly favored if the surface energies of the two constituents are large and their interfacial surface energy is small. In practice, a large value of liquid surface energy restricts wetting of a liquid droplet. Wetting or contact angle θ is depicted by the Young equation obtained by a balance of horizontal forces as shown in Figure 3.1.

$$\varphi_{SV} = \varphi_{SL} + \varphi_{LV} \cos\theta \tag{3.2}$$

Complete wetting ($\theta=0^o$) occurs if the surface energy of the solid is equal to or greater than the sum of the liquid surface energy and interface surface energy. Much

effort has been driven to change surface energies of polymers or fillers and reinforcement so as to increase wetting between fiber and matrix (Hull and Clyne, 1996).

.

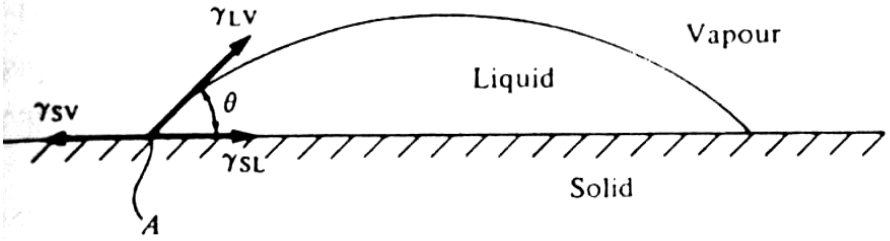

Figure 3.1. Contact angle and surface energy for a liquid drop on a solid surface (Hull and Clyne, 1996)

3.1.2. Interdiffusion and Chemical Reaction

There are different types of diffusional processes providing adhesion between filler and matrix along the interface. As seen in Figure 3.2.a. free chain ends of two polymers can diffuse at the interface providing chain entanglement and rising interfacial strength. This effect is employed in some coupling agents used on fibers in thermoplastic matrices. Interdiffusion can also take for non-polymeric systems accompanied by a chemical reaction. Various types of chemical reactions can occur at the interface. A representative scheme is depicted in Figure 3.2.d. New chemical bonds, namely A-B, are formed as a consequence of interfacial chemical reactions. These bonds can be ionic, covalent, metallic etc. A good example of this kind is chemical reactions provided by silane coupling agents, which will be discussed in detail in the following chapter. Also physical treatment of matrices can form active sides on the matrix capable of reacting with the filler or reinforcement.

3.1.3. Electrostatic Attraction

If the surfaces carry net charges of opposite signs, as shown in Figure 2.b., then adhesive forces are formed between filler or fiber and matrix. This effect is employed for certain fiber treatments such as glass fibers. The surface may exhibit anionic or

cationic properties, depending on the pH of the aqueous solution used in coupling agents. Thus, if ionic functional silanes are used, it is expected that cationic functional groups will be attracted to an anionic surface or vice versa as depicted in Figure 3.2.c.

3.1.4. Mechanical Keying

Surface roughness of the fibers can impart to the strength of the interface if good wetting has occurred as illustrated in Figure 3.2.e. The effects are much more pronounced under shear loading that, increases friction between fiber and matrix.

3.1.5. Residual Stresses

The nature of interfacial contact is strongly influenced by the presence of residual stresses. Residual stresses are mainly caused by plastic deformation of the matrix and phase transformations involving volume changes. One of the most important sources of residual stresses is thermal contraction occurring during cooling. Because of lower thermal expansivity of the fibers than the matrix, there exist compressive residual stresses on the fibers and tensile residual stresses on the matrix (Hull and Clyne, 1996).

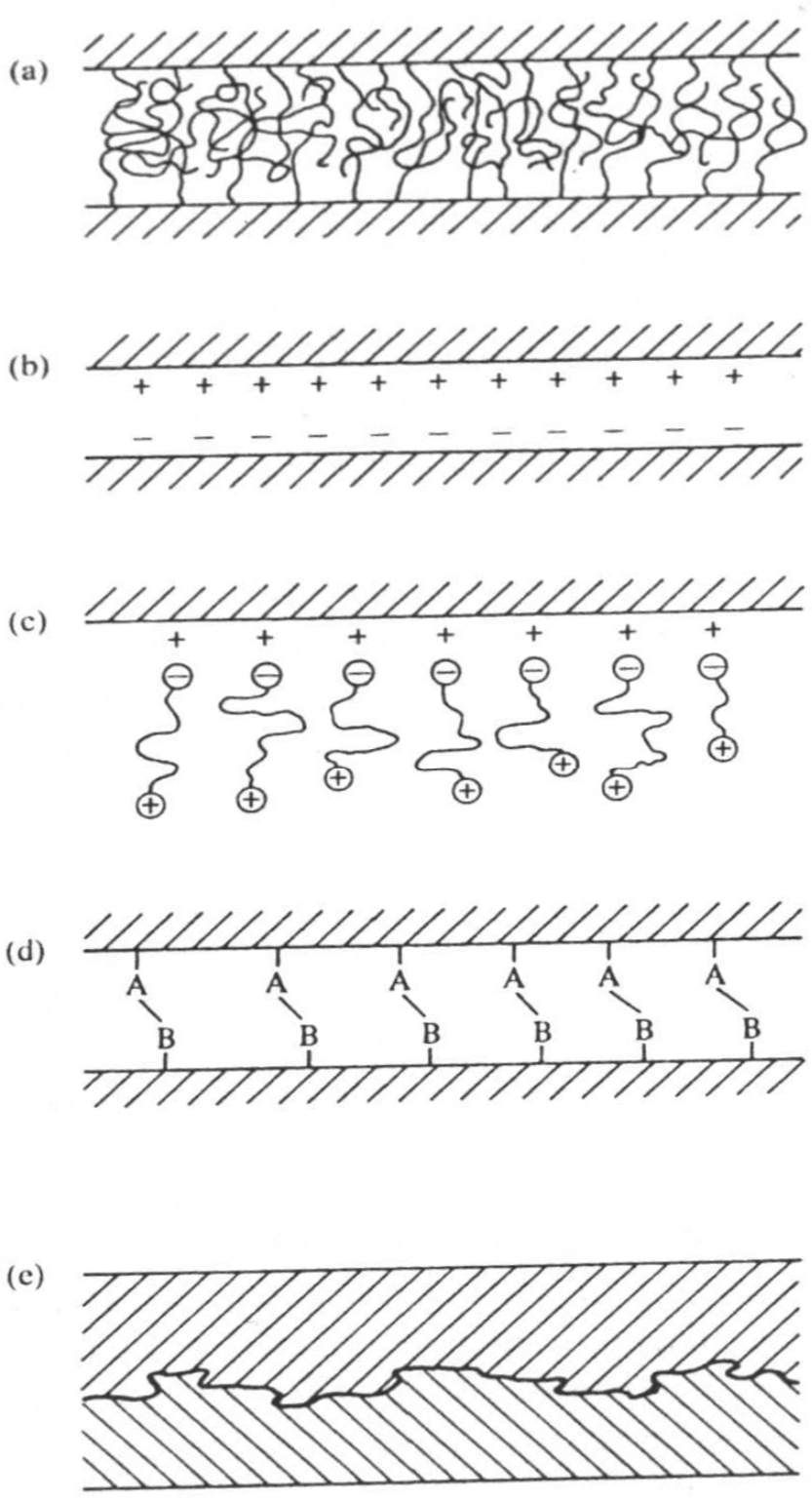

Figure 3.2. Interfacial bonds formed by a) Molecular entanglement followed by interdiffusion b)electrostatic attraction c) cationic- anionic interaction d)chemical reaction e) mechanical keying (Hull and Clyne, 1996).

3.2. Methods for Surface Modification

Surface properties have a critical importance in thermoplastic – cellulose composites because most of the problems encountered are because of incompatibility between fiber and matrix. Surface energy differences cause poor interfacial adhesion which deteriorates mechanical properties of the composite. Most effort is dedicated to modification of surface properties of cellulose in order to achieve good adhesion between fiber and matrix. The natural fiber or wood surface is a complex heterogeneous polymer composed of cellulose, hemi cellulose and lignin. The surface is influenced by polymer morphology, extractive chemicals and processing conditions.

The use of different kinds of reactive and non-reactive surface treatment methods leads to change in surface structure of the fibers as well as matrices. There are various methods for surface modification specific to the fiber, matrix employed, and processing conditions. It must be emphasized that filled polymer composites experiences two kinds of interactions: particle/particle and matrix/filler interaction. Surface treatment of both of the interactions and properties of composites are determined by inter-connected effect of the two (Pukanszky and Fekete, 1999). Type and amount of surface modifier, processing conditions must be optimized both from technical and economical aspects. Surface modification methods can be divided into three categories; non-reactive nad reactive surface treatments and elastomer employment.

3.2.1. Non-Reactive Treatment (Physical Methods)

Physical methods such as stretching, calendering, thermo treatment and production of hybrid yarns do not change the chemical composition of the fibers, but change structural and surface properties (Bledzki and Gassan,1999). These methods increase interfacial interactions between fiber and matrix by changing surface properties of the fibers.

Electrical discharge (corona and cold plasma) are employed for surface oxidation activation which changes surface energy of cellulose fibers. Surface cross linking and free radical formations are other means to achieve surface energy changes. These methods are also employed to non-active polymer substrates such as

polypropylene and polyethylene to activate surface of polymer. The tendency of interaction between substrate and matrix is increased so decreasing surface energy of the substrate or increasing surface energy of the matrix is achieved via these kinds of methods. Accordingly, mechanical properties of the composites were enhanced (Czvikovszky and Hargita, 1999; Albano, 2002).

Another method of surface modification of cellulose is alkali treatment to enhance absorption capacity of cellulose fibers by removing lignin and other soluble substances from surface of cellulose. (Valadez,1999; Mwaikambo, 2000; Joseph, 1999).

Other non-reactive treatment method for the modification of fillers is the coverage of their surface with a small molecular weight organic compound. Usually amphoteric surfactants are used which have one or more polar groups and a long alphatic chain. A typical example is the surface treatment of calcium carbonate with stearic acid (Pukanszky, 1999). The principle of treatment is the preferential adsorption of the polar groups of the surfactant onto the surface of the filler. The high energy surfaces of the inorganic fillers can often enter into interaction with the polar group of the surfactant. Preferential adsorption is promoted in a large extent by the formation of ionic bonds between stearic acid and the surface of calcium carbonate.

3.2.2. Reactive Treatment (Chemical Coupling)

Most of the fillers and fibers including cellulose fibers which are hydrophilic in nature are inherently incompatible with hydrophobic polymers. When two materials are incompatible, compatibility is achieved by introducing a third material that has properties intermediate between those of fiber and matrix. There are several chemical methods of coupling in materials (Bledzki and Gassan,1999)

i) Weak boundary layers – coupling agents eliminate weak boundary layers,

ii) Deformable layers – coupling agents produce a tough, flexible layer,

iii) Restrained layers – coupling agents develop a highly cross-linked interface region, with a modulus intermediate between that of substrate and of the polymer.

iv) Wettability – coupling agents improve the wetting between polymer and substrate (critical surface tension factor),

v) Chemical bonding coupling agents form covalent bonds with both materials.

vi) Acid–base effect – coupling agents alter acidity of substrate surface.

Reactive surface treatment assumes chemical reaction of the coupling agent with both of the components. In the next subsections, some of these reactive treatment methods, namely graft copolymerization, isocyanate and silane treatment will be explained in detail.

3.2.2.1. Graft Copolymerization

The most effective chemical method employed for polyethylene and polypropylene based composites is graft copolymerization. The coverage of fiber surface with a polymer layer which is capable of interdiffusion with the matrix proved to be very effective both in stress transfer and in forming a thick diffuse interphase with acceptable deformability. Increased polarity of matrix leads to better adhesion with polar fiber. In this treatment, the fiber is usually covered by a functionalized polymer, preferably by the same polymer as the matrix (Pukanszky and Fekete, 1999). This reaction is initiated by free radicals of the cellulose molecule. The cellulose is treated with an aqueous solution. Then the cellulose molecule cracks and radicals are formed. As seen in Figure 3.3, the resulting bonds with the esterification of cellulose would be either covalent or secondary (hydrogen) bonds. Mechanical interblocking would also occur. All of these bonds co-exist at varying degrees. It is the presence of relatively polar anhydride group on the olefin which imparts the unique set of properties to the graft polymer that make these polymers good couplers for natural fibers in polyolefins (Keener, 2003). Unlike acrylic or methacriylic acid, maleic anhydride does not readily react with itself. The decreased tendency to participate in side reactions and the versatility of the anhydride group over an acid group makes maleic anhydride the graft moiety of choice when grafting a reactive polar group onto PP. The resulting copolymers possesses properties characteristic of both, fibrous cellulose and grafted polymer. Solution technique is a difficult and time consuming technique compared to melt mixing since MAPP must be dissolved in toluene at about 100 ^{o}C with the fibers (Karnani et al, 1997). Generally functionalized polymer is hot blended with polymer and wood fiber in an extruder (reactive extrusion) or mixer. Reactions experienced are the same with solution technique (Ichazo, 2001; Sanadi, 1997; Mwaikambo, 2000; Bledzki and Gassan, 1999; Suarez, 2003). The polymer interdiffusion can be achieved grafted cellulose and matrix polymer by this simple mixing technique.

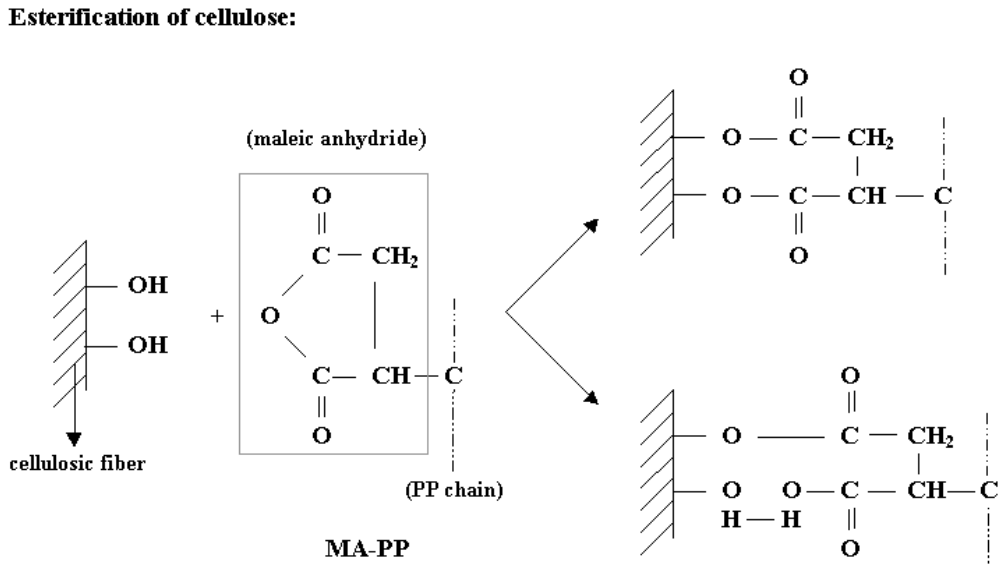

Figure 3.3. Grafting of cellulose with MAPP (Bledzki and Gassan,1999)

There are two important parameters affecting the grafting efficiency of fibers. Acid number that is the number of polar anhydride groups bonded to polymer backbone and molecular weight of grafted polymer. Low molecular weight will not allow the coupler to interact and entangle sufficiently with the polyolefin phase. Too high molecular weight may not allow the coupler to reside at the interface. A low acid number may not give the coupler enough sides for attachment to the polar filler. Too high of an acid number may hold the coupler too close to the polar surface and not allow sufficient interaction with the continuous non-polar phase (Keener, 2003). The effect of molecular weight of MAPP on tensile yield stress for PP/cellulose composites was clearly demonstrated in Figure 3.4 (Pukanszky, 1999). It is obvious that molecular weight of MAPP has a great impact on mechanical properties. Increase in molecular weight is accompanied by an increase in tensile strength of cellulose/PP composites.

The success of MAPP couplers pertains to their excellent balance of properties to bridge the interface between polar and nonpolar species. A coupler holds dissimilar materials together. In the case of MAPP, the coupler may co-crystallize with the continious polymer while the maleic anhydride portion of the molecule can interact with the more polar cellulose surface.

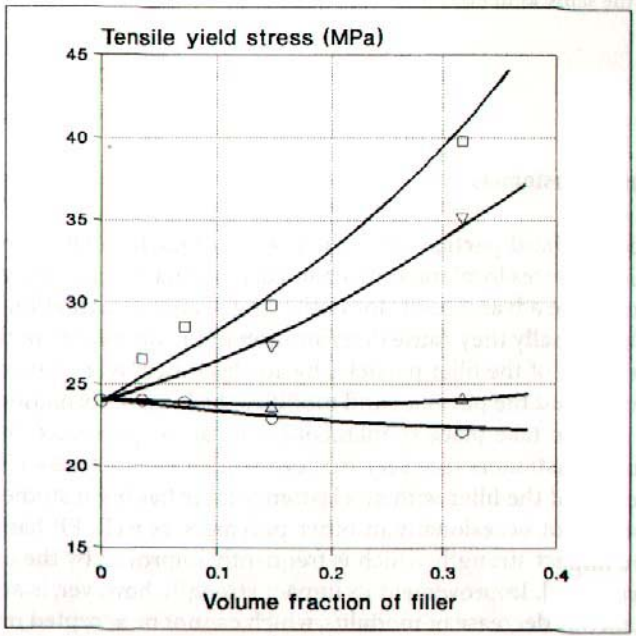

Figure 3.4. Effect of MAPP molecular weight on tensile yield stress of cellulose-PP composites. (O) non-treated, treatment with MAPP with a molcular weight of (Δ)350, (∇)4500, (□)3.9x 10^4. (Pukanszky, 1999)

3.2.2.2. Treatment with Isocyanates

The mechanical properties of composites reinforced with wood-fibers and PVC or PS as resin can be improved by an isocyanate treatment of those cellulose fibers or the polymer matrix. Polymethylene–polyphenyl–isocyanate (PMPPIC) in pure state or solution in plasticizer can be used. PMPPIC is chemically linked to the cellulose matrix through strong covalent bonds as seen in Figure 3.5 (Bledzki and Gassan,1999).

R - N = C = O + H - O - Cell - R - HN - C - O - Cell

Figure 3.5. Bonding between polymethylene–polyphenyl–isocyanate and cellulose

Both PMPPIC and PS contain benzene rings, and their delocalized p electrons provide strong interactions, so that there is an adhesion between PMPPIC and PS.

Isocyanites are also employed for wood flour/thermoplastic composites to alter OH bonds on cellulose which gives a hydrophilic character to cellulose but it did not work well in terms of increasing mechanical properties (Raj et al, 1989).

3.2.2.3.Silanes as Coupling Agents

Organosilanes are the main groups of coupling agents for cellulose fiber reinforced polymers. In fact, they are employed successfully to mineral fillers and fibers such as glass (Wambua, 2003) silica (Sae-Oui, 2003), alumina, mica and talc (Denac, 1999). Most of the silane coupling agents can be represented by the following formula:

$$R\text{-}(CH_2)_n\text{-}Si(OR')_3$$

where n=0-3 OR' is the hydrolysable alkoxy group such as amine, mercapto, vinyl group, and R the functional organic group such as methyl, ethyl or isopropyl group attached to silicon by an alkyd bridge. The general mechanism of how alkoxysilanes form bonds with the fiber surface which contains hydroxyl groups is shown in Figure 3.6.

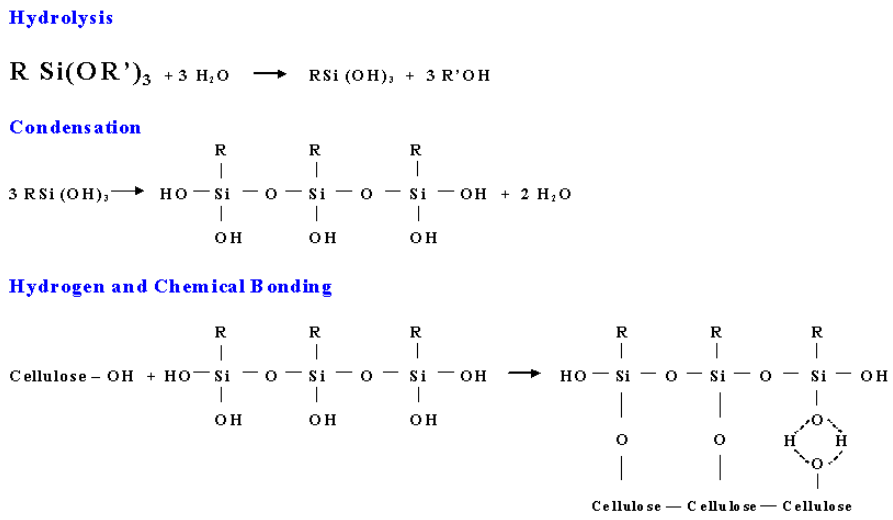

Figure 3.6. Chemical reaction sequence of silane treatment (Karnani, 1997)

The first step in silane coupling is hydrolysis reaction. Silanes react with water and form silanols. Second step is the condensation of silanols to form polysiloxanes. In the last step, polysiloxanes either form covalent bonds or hydrogen bonds. This means that silanes adhere to the surface of fiber with chemical and physical bonds. It has to be noted that functional organic group (R) must be capable of interacting with the matrix material or must be capable of interdiffusing through the polymer matrix. Hydrolysis reactions can be catalyzed by peroxides. The exact mechanism of bonding will depend on several factors including: the relative acidity or basicity at the interface, the thermodynamic compatibility of the polymer with the organosilane and its condensation products, the temperature dependence of hydrolysis and condensation, the temperature dependence of polymer creep compliance and chain disentanglement (to facilitate interpenetration), and the activation energy for achieving a covalent bond between the polymer matrix and the organic functionality of the silane molecule (Plueddemann, 1982). Since hydrolysis reactions can occur in the presence of water, water content is another important parameter that determines extent of hydrolysis reaction. Mixing times, temperature and drying conditions are all important parameters determining overall physical and chemical properties of composites. Silanes are the most common coupling agents to any filler or fiber composites in thermoplastics and thermosets. Accordingly, there exists a numerous literature knowledge on employment of silane coupling agents to PP- natural fiber composites(Ichazo, 2001; Fernanda, 1999).

Most commonly, silanes are employed in aqueous solutions at 1-2wt% of silane with respect to fiber irrespective of silane type. Karnani et al (1997) employed amino-ethyl amino-propyl trimethoxy silane in aqueous solution at 2wt% with respect to kenaf fibers and they achieved about 57% increase in tensile strength, but Ichazo et al (2001) employed the same procedure to wood flour at 1wt% with respect to filler with vinil-tris-(2-metoxietoxi)-silane and did not achieve a significant increase in mechanical properties.

Castellano et al (2004) had employed two silanes, namely cyanoethyl trimethoxisilane and metacryloxy propyltrimetoxisilane stressed on the conditios to facilitate reaction between cellulose and silane coupling agents. They have employed various solvent systems with the aim of testing different mediums with different polarities. Solvents employed were heptane, dioxane, toluene/methanol mixture with and without small amounts of added water. They have employed FTIR and IGC to determine reactions between silanes and cellulose and they have concluded that the

most important parameter effecting coupling agent efficiency was the amount of water. Increased water content is accompanied by increase in extent of reaction between condensed polysilaxanes and cellulose surface.

Ethanol/water mixtures were most frequently employed reaction medium for silane reactions (Felix, 1993, Pickering, 2003) Acidity adjustments could also be beneficial to extend of reactions between cellulose and silanes, especially for aminofunctional silanes (Felix, 1993). Fernanda et al (1999) employed methanol without water as the reaction medium for 3 different silanes but they could not obtain significant improvements in mechanical properties for polypropylene-wood fiber composites.

3.2.3. Soft interlayer: Elastomers

Incorporation of hard particles or fibers into the polymer matrix creates stress concentration, which induced local micromechanical deformation processes. Usually this causes deterioration in properties of composites. Encapsulation of fillers or fibers by an elastomer layer changes the stress distribution along the fibers or fillers and modifies local deformation process (Pukanszky and Fekete, 1999).

The coverage of filler or fiber with an elastomer layer is mostly employed for PP composites. PP has a poor low temperature impact strength, which is frequently improved by the introduction of elastomers. Improvement of impact strength is accompanied by a simultaneous decrease of modulus, which is compensated by incorporation of fibers or fillers. Rana et al. (2002) studied effect of coupling agent (MAPP) and elastomer on mechanical properties of PP-jute composites and found that compatibilizer increased tensile and flexural properties whereas elastomer increased impact strength of composites.

3.3. Effect of Surface Treatment on Mechanical Properties

Mechanical properties such as tensile strength and modulus, flexural strength and modulus, impact strength are primary parameters that were considerably enhanced by employment of surface treatment of fiber or matrix. Other mechanical properties developed by modification of interfacial interactions between cellulosic fibers and PP are dynamic mechanical properties (Manchado and Arroya, 2000; Joseph, 2003; Amash,

2000; Cho, 1999; Wielage, 2003), creep behavior (Park and Belatincz, 1998; Rowel, 1998), and fatigue properties (Gassan and Bledzki, 2000; Bledzki and Gassan,1999).

It has to be emphasized that in general tensile and flexural strength of natural fiber filled PP composites decreases with increasing fiber content and Young's modulus generally increases. There are expectations where tensile strength increases with increasing fiber content (Ichazo, 2001). Coupling agents would decrease the decline in tensile properties with increasing fiber content. In some cases, an increasing trend could be achieved with employment of coupling agents. Impact strength generally decreases with addition of fibers therefore, generally elastomers are incorporated in order to compensate the decrease in impact strength.

Rowel et al (1998) studied effect of MAPP treatment on flexural, tensile and impact properties in aspen-PP composites. Results of this study can be seen in Table 3.1.

Table 3.1. Effect of MAPP on mechanical properties of 30 wt% aspen filled-PP composites (Rowel et al, 1998)

Property	30% aspen 70% PP	30% aspen 68% PP 2% MAPP
Flexural strength (MPa)	53.7 (+/- 0.4)	76.6 (+/- 0.5)
Flexural modulus (GPa)	3.1 (+/- 0.1)	3.4 (+/- 0.1)
Tensile strength (MPa)	29.6 (+/- 0.1)	48.2 (+/- 0.3)
Tensile modulus (GPa)	2.5 (+/- 0.4)	2.7 (+/- 0.1)
Izod-notched (J/m)	28 (+/- 1)	27 (+/- 6)
Izod-unnotched (J/m)	119 (+/- 11)	149 (+/- 11)
Rockwell hardness	79.1	92.3
Taber Wear Index	152	102

It was clearly observed that tensile and flexural strength was considerably increased by employing MAPP coupling agent. It was interesting to note that only 2% of coupling agent with respect to total mass increased the tensile and flexural strength over 50%.

Karnani and co-workers (1997) studied effect of MAPP and silane treatment on mechanical properties of kenaf/PP composites and achieved the results in Table 3.2. It can be extracted from the table that MAPP treatment provided 123% and 42% increase

in tensile and flexural strength, respectively at 60 wt% fiber loading. Tensile and flexural modulus had increased 70% and 44%, respectively at the same loading. Silane treatment also have a positive impact on tensile and flexural strength. Silanation increased tensile strength from 26.9 to 42.5 MPa which corresponds to a 58% increase compared to untreated composites at the same loading.

Table 3.2. Results of Mechanical Tests on Various PP-Kenaf Composite Blends. (Karnani et al 1997)

Material	Kenaf Fiber wt%	Modulus (GPa)	Tensile strength(MPa)
PP only	0	1.2	28.4
PP no MAPP	20	2.1	26.9
	40	2.6	27.1
	60	3.0	27.4
PP+2%MAPP	20	2.9	32.1
	40	3.4	41.3
	60	4.1	53.8
PP+5%MAPP	20	3.2	36.1
	40	4.3	49.4
	60	5.1	61.2
Silylated kenaf	20	3.3	42.5

Bataille and co-workers (1989) examined effect of two types of silanes and MAPP on tensile mechanical properties of wood fiber-PP composites. They found that aminopropyl triethoxy silane and MAPP increased yield strength about 20%. Silane coupling was achieved in a methanol-water solution. Silane concentration was 30% with respect to fiber weight which was rather high for a coupling agent concentration studied previously in literature. MAPP is incorporated during compounding at a 5% wt with respect to PP weight.

Ichazo et al (2001) employed two coupling agents, vinil-tris-2-metoxy-etoxy silane and two types of MAPP. They found that incorporation of untreated wood fibers into PP increased tensile strength more than 50% at 40 wt% loading. Silane treatment of the fibers did not work well since no difference in tensile strength was observed. This can be attributed to improper selection of mixing conditions of silane coupling agent and wood fibers such as mixing time and pH. MAPP with a higher molecular weight

yielded better results as expected. 20% increase in tensile strength was achieved via MAPP treatment. Impact strength decreased at about 100% and coupling agents accelerated the decline in impact strength .

Takase and Shiraishi (1989) modified PP with maleic anhydride via reactive kneading and evaluated effect of MAPP amount on mechanical properties. They have determined that MAPP impart in development of tensile strength and over 100% increase was achieved. They have also stressed on optimum amount of MAPP to be employed and 2.5% MAPP with respect to PP is the amount to attain maximum tensile strength. After that ratio, no change in mechanical properties was obtained. They have also found that covalent bonds were formed between cellulose and MAPP by extraction techniques.

Tjong and co-workers (1999) studied MAPP-methyl cellulose composites. Surface of methyl cellulose was modified with a titanate coupling agent. They have increased tensile strength over 40% at 25% fiber loading and 80% increase was achieved in Young's modulus at the same fiber loading when compared to pure MAPP was obtained. They have also observed an increase in storage modulus with fiber addition.

Gonzales et al (2003) studied effect of fiber surface treatment with NaOH and vinyltris(2-methoxy-ethoxy) silane on tensile strength of henequen fibers-PE composites and they have found that alkali treatment alone did not cause any improvement in tensile strength, silane treatment alone have caused a 15% increase in tensile strength and co-existence of two surface treatments yielded 25% increase in tensile strength at 20 v% fiber loading. Better adhesion between fiber and matrix was also confirmed by SEM photos.

Fernando et al (1997) investigated effect of processing conditions and treatment with silanes and MAPP on tensile and flexural properties of PP-wood fiber composites. They concluded that 180^{o}C is the optimum operating temperature in terms of mechanical properties. MAPP treatment with employment of vinyltris(2-methoxy-ethoxy) silane at 4 wt% based on fiber weight yielded the highest tensile and flexural strength.

Rana and co-workers (2002) investigated effect of surface and impact modifier on tensile, flexural and impact properties of jute fiber reinforced PP. They have employed MAPP as surface modifier and a polyolefinic elastomer based impact modifier containing carboxylic functions. They found that MAPP compatibilizer causes

improvements in tensile and flexural properties. Impact modifier considerably enhanced notched and un-notched impact strength at the expense of loosing tensile and flexural properties but co-employment of impact modifier and compatibilizer enhanced both tensile, flexural and impact properties.

3.4. Effect of Surface Treatment on Water Sorption Properties of PP-Natural Fiber Composites

The most important problem encountered while employing natural fibers as filler in thermoplastics is the high water sorption of composites caused by hydrophilic nature of natural fibers. High content of water in the composites would form a layer in the interface region, decreasing interfacial adhesion between fiber and matrix. Mechanical properties would decrease accordingly. To achieve minimum sorption of water through composites is to employ dry natural fibers while compounding fiber and polymer. Another precaution would be coating of composite with a thin polymer the same type with the matrix. But the most frequently inserted method is employment of coupling agents. It was mentioned that coupling agents increase interfacial adhesion between fiber and matrix by chemical or physical interaction. Water absorption in cellulose fibers is caused by hydrogen bonding between free hydroxyl groups on cellulose molecules and water molecules. Silane coupling agents and maleic anhdride group on MAPP form hydrogen or covalent bonds with some of free hydroxyl groups of cellulose decreasing water absorption capacity of cellulose. Another reason for decreased water absorption capacity of composites would be enhanced adhesion between fiber and matrix. Enhanced adhesion would decrease thickness of the interface which would restrict water penetration through cellulose molecules. Decrease in water absorption is a clear indicator of interaction between fiber and coupling agents. Silane and MAPP treated composites with lesser water absorption values have greater tensile strength confirming better interfacial adhesion via bonding between fiber and coupling agent (Gassan and Bledzki, 2000).

Ichazo and co-workers (2002) investigated effect of wood floor surface treatment with NaOH, vinyltris (2-methoxy-ethoxy) silane and two types of MAPP with different molecular weights on the water sorption properties of the woodflour/PP composites. The water sorption experiments were conducted for 40 days in distilled water. They achieved the following results in Table 3.3.

Table 3.3. Thickness swelling of PP/wood flour (WF) composites (Ichazo, 2002).

Material	Thickness swelling (%)
PP/untreated WF	2.2
PP/treated WF with NaOH	2.7
PP/treated WF with silane	1.4
PP/treated WF with MAPP	1.3

The results clearly showed that employment of MAPP and silane decreased water sorption about 80% because of the reasons mentioned above. Alkali treatment increased water sorption of composites because NaOH increases surface area of cellulose fibers by eliminating impurities and lignin on cellulose fibers.

3.5. Characterization of the Interface

The most important concept in composites is the understanding of the interface. Much of the effort in polymer matrix composites is devoted to understanding of the interface. Physical and chemical characterization of the interface is accomplished via direct or indirect methods. It is very difficult to detect any changes in the interface as an effect of interaction since the interlayer is very thin (Pukanszky, 1999). For the characterization of the interface, spectroscopic techniques, thermodynamic characterization and mechanical properties connected with interfacial adhesion are generally used.

3.5.2. Spectroscopic Techniques

Spectroscopic techniques are extremely useful for the characterization of filler or fiber surfaces treated with coupling agents in order to modify interactions in composites. Such an analysis makes possible the study of the chemical composition of the interlayer, the determination of surface coverage and possible coupling of the filler and polymer. This is especially important in the case of reactive coupling, since, for example, the application of organofunctionalsilanes may lead to a complicated polysiloxane interlayer of chemically and physically bonded molecules.

X-Ray photoelectron spectroscopy (XPS) gives a spectrum where the peaks are highly element specific, allowing direct elemental analysis. This property can provide information about surface composition, chemical environment and bonding of surface chemical species. An example of XPS usage is organafunctional silane modified and alkali treated henequen fibers. Figure 3.7 shows XPS spectra of unmodified (FIB), silane modified (FIBSIL) and NaOH treated (FIBNA) fibers.

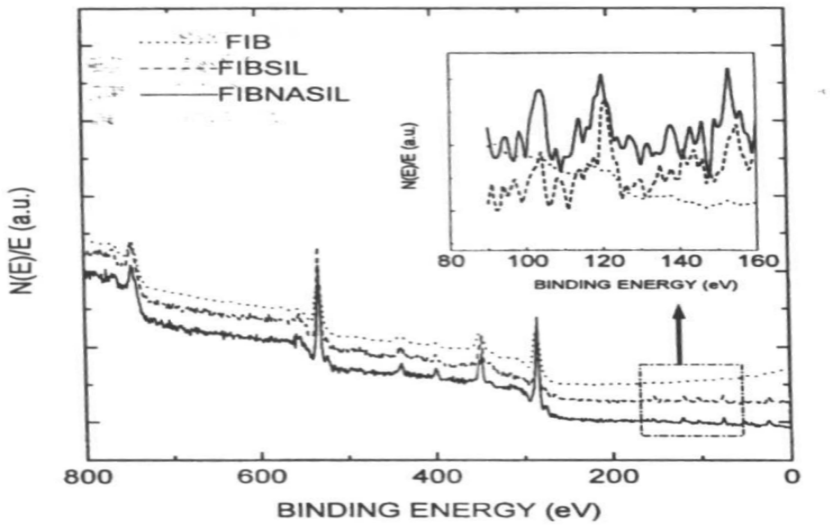

Figure 3.7. XPS spectra of henequen fibers (Gonzales, 2003)

Silicon on the surface of fibers caused by siloxane layer on the fiber has characteristic emission peaks in the region between 150-155 eV and 99-104 eV. Amplified 90-160 eV range clearly demonstrates presence of Si for silane treated fibers which can be treated as an evidence for effective surface coverage of the fibers.

Fourier transform infrared analysis (FTIR) is another important too for characterization of fiber surfaces. Changes in characteristic vibrations indicate chemical reactions, while a shift in an absorption band shows physico-chemical interaction (Pukanszky, 1999, Hull 1996) FTIR can be employed for determination of change in the chemical composition of fibers with treatment as well as composites. A typical example of FTIR employment is tracing chemical modification of cellulose fibers with silane, namely, cyanoethyl trimethoxy silane.

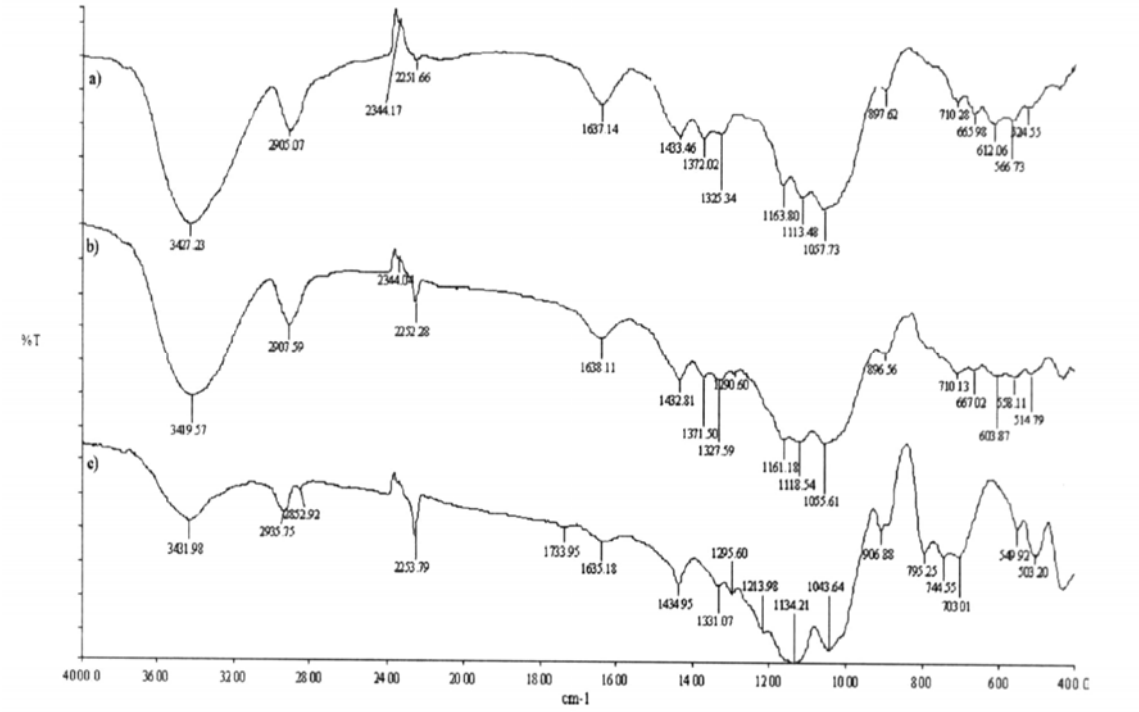

Figure 3.8. FTIR spectra of cellulose containing different degrees of moisture with respect to cellulose, treated with cyanoethyl trimethoxy silane a)5% b)50% c)100 % (Castellano, 2004)

Effect of water content in the silane solution with respect to fiber on CN formation was investigated by examining characteristic peak of –CN group at 2250 cm^{-1} (Figure 3.8). As observed, peak at 2250 cm^{-1} increases with increasing moisture content. It was found that water presence is a very important parameter on the surface coverage of fiber by a silane layer (Castellano, 2004) .

3.5.3. Thermodynamic Characterization

Surface characteristics of fillers can also be characterized by thermodynamic parameters. The significance of Dupre equation is discussed in Section 3.1. Reversible work of adhesion (W_{AB}), can be divided into two parts: a dispersion term (W_{AB}^{d}) and one characterizing the electron donor – acceptor interaction (W_{AB}^{ab}) (Pukanszky, 1999).

$$W_{AB} = W_{AB}^{d} + W_{AB}^{ab} \qquad (3.3)$$

Using Fowkes's approach, the reversible work of adhesion can be defined as:

$$W_{AB}=2(\varphi_A^d \varphi_B^d)^{1/2}+nf\Delta H^{ab} \quad (3.4)$$

Where, ΔH^{ab} is the change in free enthalpy due to acid/base interactions, n is the number of moles taking part in the interaction on a unit surface f is a correction factor close to unity.

According to Gutman's theory, ΔH^{ab} can be characterized by donor (DN) and acceptor (AN) numbers, which indicate acidity or bacicity of the material.

$$-\Delta H^{ab} = AN.DN/100 \quad (3.5)$$

Using these approaches, flow microcalorimetry is used where a small sample is put into the cell of the calorimeter and the probe molecule passes through it in an appropriate solvent. Adsorption of the probe results in an increase in temperature and integration of the area under the signal gives the heat of adsorption. This quantity can be used for the calculation of reversible work of adhesion according to Eq. (3.3).

The most frequently used technique for the determination of thermodynamic and acid base characteristics is inverse gas chromatography (IGC) (Asten et al, 2000; Tshabalala, 1997; Santos, 2001). In IGC technique, the unknown filler or fiber surface is characterized by solvents of known properties. Dispersion component of surface tension is characterized by non-polar solvents, namely n-alkanes. Polar component is characterized by polar solvents. Net retention volume (V_N) can be calculated from:

$$V_N=(t_r-t_o)Fj_o \quad (3.6)$$

where t_r is the retention and t_o is the reference time, F the flow rate of the carrier gas, and j_o is a correction factor taking into account the pressure difference. The dispersion component of the surface tension of the filler can be calculated from the retention volume of n-alkanes (Pukanszky, 1999):

$$-RTInV_n=Na(\varphi_{LV}\varphi_s^d)^{1/2} \quad (3.7)$$

where V_n is the retention volume of the alkanes, *a* is the surface area of the adsorbed molecule, φ_{LV} is the surface tension of the solvent and N is the Avogadro Number. The product of RT and logarithm of the retention volume is a linear function of $\varphi_{LV}^{1/2}$. If the measurements are carried out with polar solvents, the deviation from this straight line is proportional to the acid/base interaction potential of the solid surface (Pukanszky, 1999).

Abdelmouleh et al, (2004) investigated the effect of 4 different silanes, namely metacriloxypropyltrimethoxysilane (MPS), aminopropyltriethoxysilane (APS), hexadecyltrimethoxy silane (HDS), mercaptopropyltrimethoxysilane (MRPS) on dispersive component of surface energy and acid/base properties of cellulose surface. They achieved results on Table 3.4. They stressed on the change in acid base character with modification since dispersive components do not change much. Their conclusion was relatively high value of the AN/DN ratio for untreated cellulose reflected the acid character resulting from the strong density of the surface hydroxyl groups. After modification with MPS, MRPS and HDS, the decrease in AN/DN ratio reflected the progressive reduction in surface accessibility of hydroxyl groups to the probes. The APS treatment reversed the interaction balance and led to a surface ehich displayed a modest basic character, generated by the presence of amino groups.

Table 3.4. Dispersive surface energy and acid/base properties of cellulose before and after modification (Abdelmouleh et al, 2004)

Samples	γ_s^D	AN/DN
Cellulose	30.9	3.1
Cell+MPS	29.6	1.4
Cell+APS	31.2	0.8
Cell+MRPS	29.1	1.6
Cell+HDS	22.6	1.1

3.5.4. Mechanical properties

Interfacial adhesion of the components in filled polymers can be deduced from mechanical properties of composites with the help of models describing composition dependence. Such models must also take into account interfacial interactions. One of

these models considers interface thickness and yield stress of composite as the key parameters and defines a parameter related to stress transfer between components. Semi-empirical correlation developed for the quantitative description of the composition dependence of tensile yield stress in heterogeneous polymer systems (Pukanszky, 1999).

$$\sigma_y = \sigma_{yo}(1- \sigma_f)/(1+2.5\ \sigma_f)\ \exp\ (B\sigma_f) \qquad (3.8)$$

where σ_y and σ_{yo} are the yield stress of the composite and the matrix, respectively, σ_f is the volume fraction of the filler, and B is a parameter related to stress transfer between the components. The term $(1- \sigma_f)/(1+2.5\ \sigma_f)$ expresses the decrease of effective load bearing crossection on filling, while $\exp\ (B\sigma_f)$ describes interaction. The parameter B_y contains the thickness of the interface (l) and its yield stress (σ_{yi}):

$$B=(l+l\rho_f A_f)\mathrm{In}\ (\sigma_{yi}/\ \sigma_{yo}) \qquad (3.9)$$

where A_f and ρ_f are the specific surface area and the density of the filler, respectively. Parameter B_y can be determined from the composition dependence of tensile yield stress and if the experiments are carried out with at least two fillers of different particle sizes, l can be calculated from the results. Figure 3.9 illustrates use of parameter B as a measure of interfacial interactions.

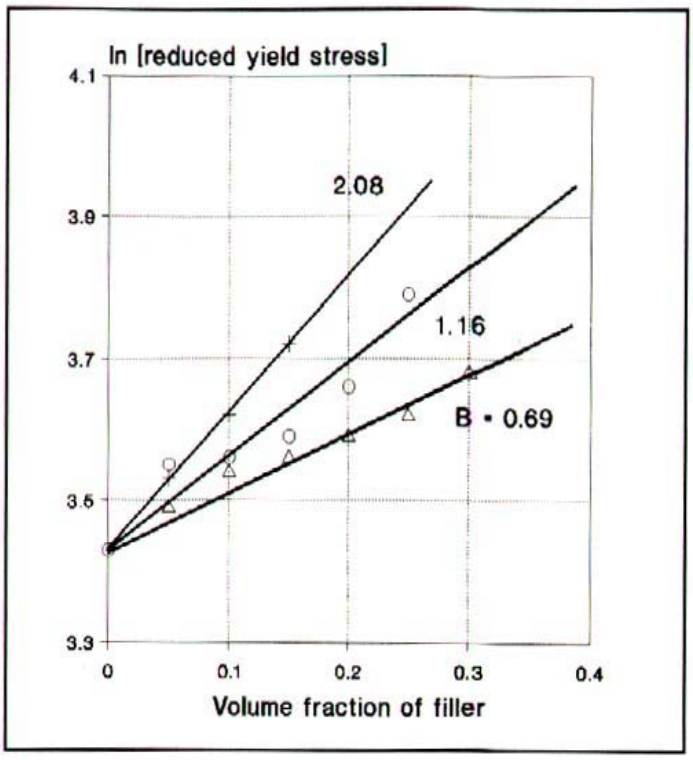

Figure 3.9. Effect of treatment on the tensile yield stress of PP/$CaCO_3$ composites. Treatment: (O) non-treated, (Δ) stearic acid, (+) aminosilane (Pukanszky, 1999).

Treatment of PP/ $CaCO_3$ composites with aminosilane and stearic acid revealed that interfacial adhesion was enhanced with aminosilane treatment. B parameter increased from 1.16 to 2.08 when compared to untreated composites. Stearic acid treatment exhibited an adverse effect on interfacial adhesion.

Nielsen Model also describes an interaction parameter taking into account interfacial adhesion in particulate filled polymers. The equation formulated in Equation 3.10 (Metin, 2002).

$$\sigma_c/\sigma_p = (1 - \Phi_f^{2/3})S \qquad (3.10)$$

where σ_c and σ_p are tensile strengths of the composite and matrix respectively. The parameter S in the Nielsen's model describes weakness in the structure created through stress concentration at the filler-matrix interface. Unity in the value of S means no stress

concentration effect, whereas smaller values means greater stress concentration effect or poorer adhesion.

Chapter 4

EXPERIMENTAL

4.1.Materials

Isotactic PP, (MH-418, PETKIM) in pellet form, with a density of 895 kg/m^3 was used as the polymeric matrix material. Cellulose (CE), sawdust (SD) and wheat straw (WS) were used as fiber in this study. Coupling agents employed were (3-aminopropyl)-triethoxysilane (AS) (Fluka Co.) , methacriloxy propyl trimethoxy silane (MS), (Merck Co.) and maleic anhydride grafted polypropylene (MAPP) with an acid value of 59 (Clairant Co.) Ethanol was used as a solvent in the surface modification of the filler.

4.2.Methods

Experimental methods can be classified in three categories;

- Size reduction and surface treatment of fibers
- Preparation of PP/fiber composites
- Characterization of fibers and PP/fiber composites

4.2.1. Size Reduction and Surface Treatment of Fibers

Cellulose (CE) powder was used as received. Sawdust was sieved through 250μm sieve before use. Wheat straw was first ground since fibers were too long and then they were obtained in the size range of below 250μm in diameter. Figure 4.1 shows microstructure of cellulose, sawdust and wheat straw which were takem by scanning electron microscopy (SEM). CE was in particulate form with a particle size range of 20-100μm. SD and WS were in fiber form with varying aspect ratios. Aspect ratios of WS are lower than SD. Length of the fibers would be up to 200 μm for SD and 300-400 μm for WS.

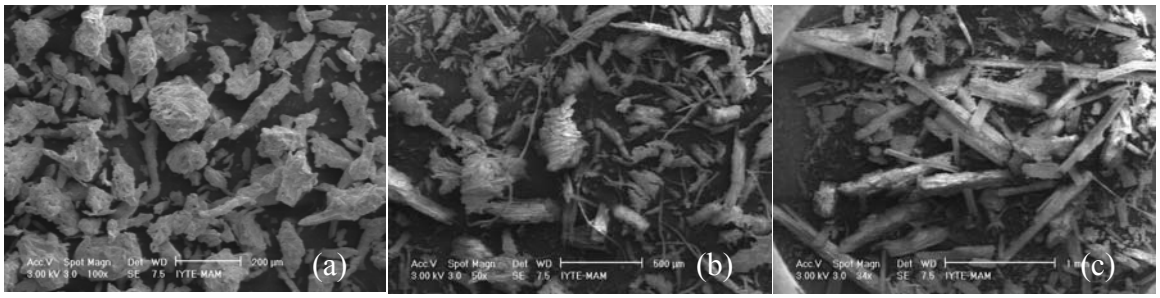

Figure 4.1: SEM pictures of (a) cellulose, (b) sawdust and (c) wheat straw.

Coupling agents were employed in order to increase compatibility between fiber and matrix and to decrease hyrophilicity of fibers, as explained in Chapter 3. From this point of view, silane coupling agents and MAPP were used as suitable candidates to alter incompatibility between fiber and matrix. Chemical formula of silane coupling agents employed can be seen in Figure 4.2. Surface modification of CE, SD and WS with silane coupling agent was carried out in solution. Aqueous ethyl alcohol solution (95/5 w/w) was prepared and silane coupling agent (0.5, 1, 2.5% w/w of fiber) was added to the solution. The solution was mixed with a mechanical mixer for 15 minutes for hydrolysis reaction of silane coupling agent to take place. Then the fibers were added to the solution of silane coupling agent and left for 45 minutes under agitation for condensation and chemical bonding of silanes and cellulose fibers as explained in Chapter 3. Weight ratio of solution to fiber was kept at about 5. Treated fibers were washed with ethanol to remove excess coupling agents. Afterwards, the solution was introduced into a rotary evaporator at 60^{o}C under vacuum for 1 h until fibers were dried. Employment of rotary evaporator had prevented agglomeration of particles via rotation action. The fibers were further dried in an oven at 70^{o}C for 24 h before composite preparation. Schematic representation of silane treatment can be seen in Figure 4.3.

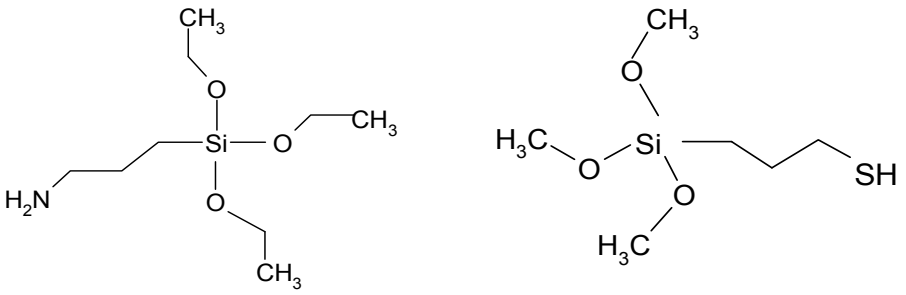

Figure 4.2. Chemical structure of (3-aminopropyl)-triethoxysilane (AS) and methacriloxy propyl trimethoxy silane (MS), respectively.

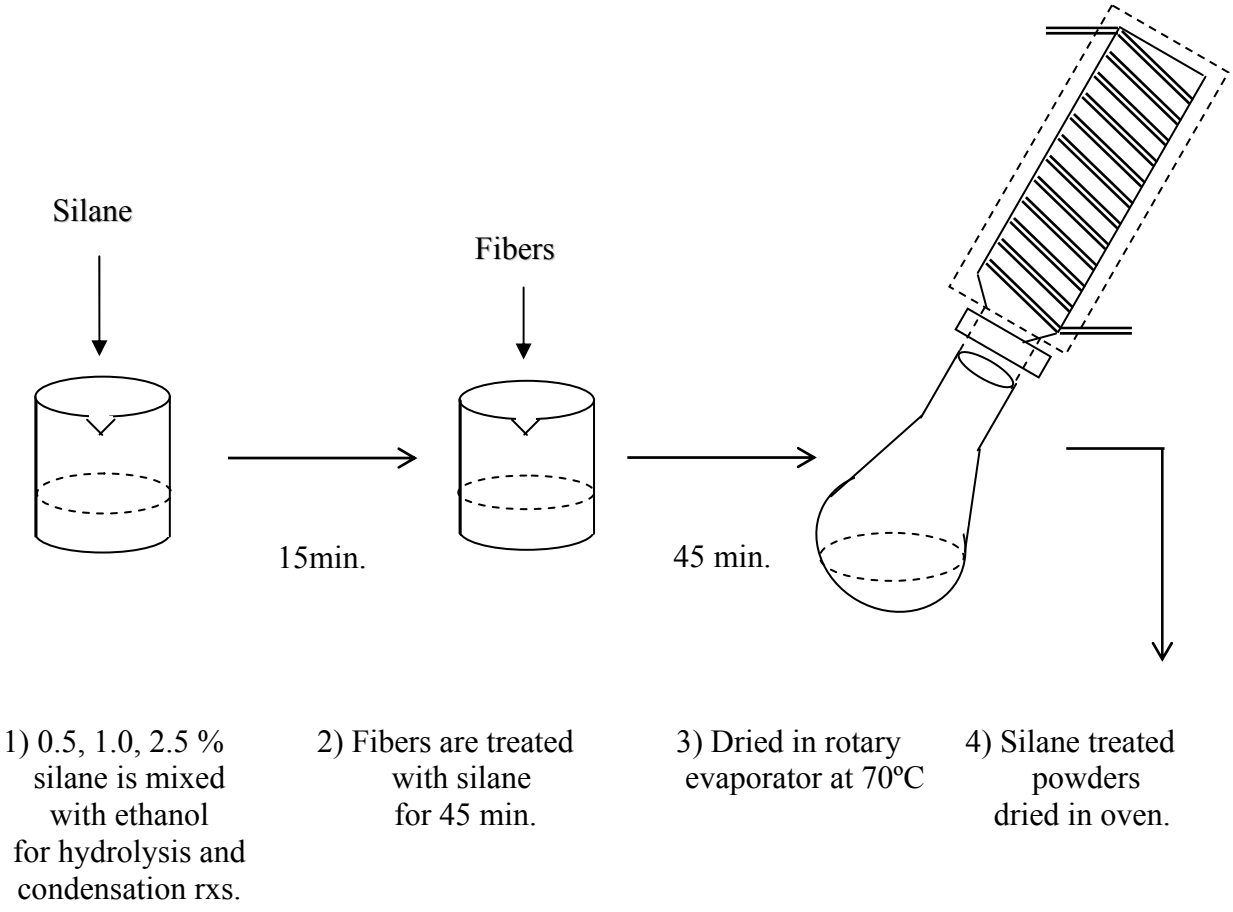

Figure 4.3. Schematic representation of silane treatment

MAPP was mixed in the proportion of 2.5, 5, 10w% of PP and mixed with melt PP in rheomixer during compounding.

4.2.2. Preparation of Composites

Composites were compounded in "Haake Rheomix 600". A general and detailed view of rheomixer is shown in Figure 4.4. This instrument enabled melt mixing of thermoplastic polymers and fillers or fibers. The rheomixer was equipped with two rotor blades rotating in opposite directions. This design enables good dispersion of fillers in the polymer matrix. The rotor speed could be adjusted for optimum mixing. There were three walls surrounding the chamber where filler and matrix melt. Temperature of the three walls could be adjusted separately for optimum temperature control. Time of mixing could also be adjusted to reach optimum mixing conditions.

Torque of the two rotors, which is a measure of resistance of the melt to flow, could be damped through "Convert Data" software with respect to time. Although viscosity of the melt could not be measured directly, torque of the melt at stabilization conditions is an indicator of viscosity of melt. Especially, relative rheological behavior of filled polymers with respect to loading or surface treatment could be determined by comparing stabilization torque data. The composites were prepared at mixing temperature of 185 ^{o}C, rotor speed of 50 rpm and mixing time of 10 minutes. First, PP was incorporated into the rheomixer, and then previously dried, treated or untreated fibers were introduced as soon as torque indicated melting of the polymer (about 2 min). 10 minutes of mixing was enough to reach to the stabilization torque, which indicates homogeneous mixing of filler and matrix. The composites were prepared with CE, SD and WS at 10, 20 30 and 40 wt% of fiber loadings. Combination of PP and fibers were arranged so that composite volume was 48.3 cm^3, which was 70% of the total volume of the mixing chamber. MAPP was mixed with PP before melting. The specimens taken from the rheomixer were compression molded in a Carver polymer press (Figure 4.5) to form rectangular sheet with dimensions 150x150x1 mm^3. Composites were heated without pressure for 4 minutes to 185^{o}C in order to avoid void formation and then pressed at 2000 psi pressure at the same temperature for 6 minutes. The specimens were cooled to 40 ^{o}C in 6 minutes under the same pressure in Carver polymer press.

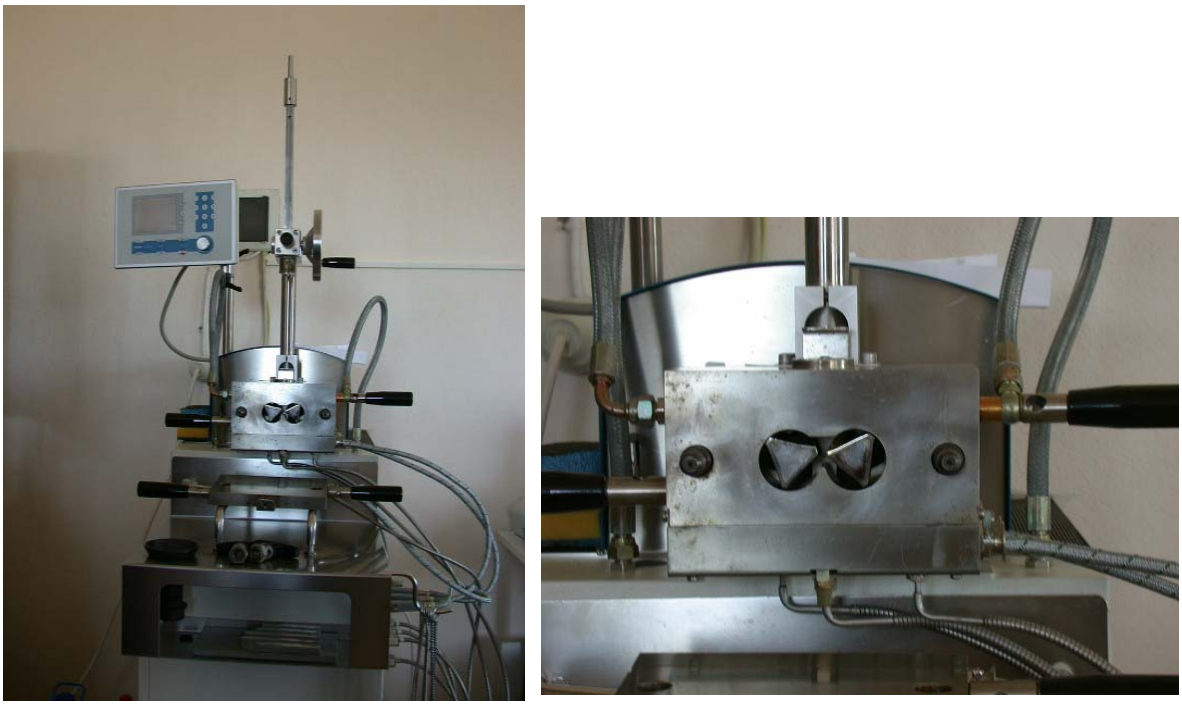

Figure 4.4. General and detailed view of rheomixer.

Figure 4.5. Picture of Carver polymer press

Flow sheet of preparation of polymer composites can be depicted as follows in Figure 4.6;

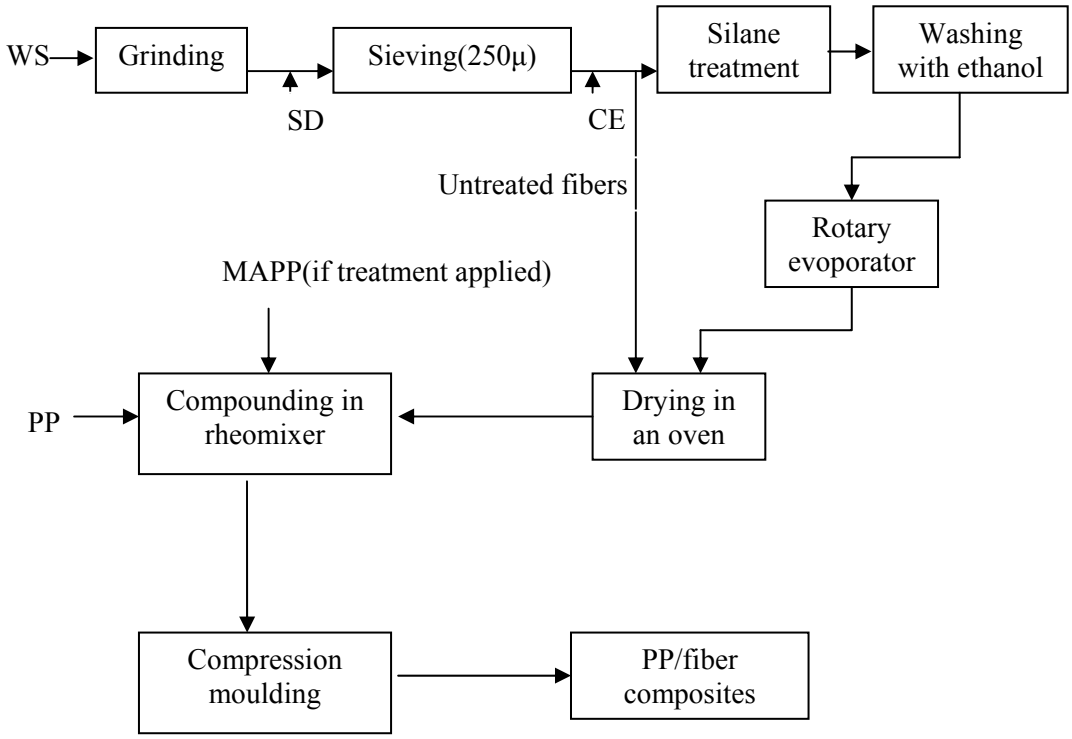

Figure 4.6. Flow sheet of preparation of composites.

4.2.3. Characterization of Composites

Characterization of the composites includes rheological behaviour of the composites during melt mixing in the rheomixer, mechanical testing, morphological properties through SEM examination of the fracture surfaces, water sorption properties, FTIR analysis and density measurements.

4.2.3.1. Rheological Properties of the Composites During Melt Mixing

Compounding of fiber and matrix was explained previously in section 4.2.2. During compounding, torque vs time data of the mix can be damped through "Convert Data" software program to determine rheological response of the composites. Torque is the rotational energy consumed by the rheometer to provide constant rotational speed (50 rpm in our experiments) at a specified temperature (185^{o}C) and time (10 minutes). Stabilization torque is the torque attained at the end of homogeneous mixing of fiber and the polymer which is somewhat proportional to the viscosity of the melt. Effect of fiber type and loading and treatment type on stabilization torque was investigated in order to determine relative rheological behaviour of the composites.

4.2.3.2. Mechanical Properties

Pressed sheets were cut with Ceast hollow die punch according to ASTM 638. Picture of Hollow Die Punch can be seen in Figure 4.7. Tensile properties such as tensile strength, Young's Modulus, strain and stress at break, energy to rupture were determined by Testometric mechanical test instrument. The full-scale load of mechanical test machine was 100kN and the cross head speed was 50mm/min for the mechanical tests. The test results were taken from WINTEST software program supplied from Testometric Co. Tests were performed at room temperature (23^{o}C) and at least five specimens for each composite formulation were tested.

Figure 4.7. Picture of Hollow Die Punch and sample cutter

4.2.3.3. Morphological properties

Fracture surface of fractured tensile specimens were investigated by Philips XL 30 SFEG Scanning Electron Microscobe (SEM). Bonding between fiber and matrix, dispersion of fiber in the matrix and fiber architecture were determined. Specimens investigated were 30wt% CE, SD and WS loaded composites treated with 1wt% silane and 5wt% MAPP treatment. Untreated composites were also investigated.

4.2.3.4. Water Sorption Properties

Samples were cut into 3x1.75x0.1 cm^3 sheets. First, the samples were dried at 70^oC for 24 hours to reach constant weight. The samples were then immersed into static distilled water bath at 25 ^oC for 24 hours for observing sorption of water. Mass of the samples was measured after removing them from the water bath after 24 hours. The samples were wiped with tissue paper to remove surface water before weighing. Water uptake of PP composites at time t was calculated from;

$$\text{Uptake } \% = (M_t - M_0)/M_0 \times 100 \qquad (4.1)$$

where

M_t : Mass of sample at time t

M_0: Mass of sample at t = 0

4.2.3.5. Density Measurements of Fibers and Composites

Densitiy measurements were carried out with a Sartorius YDK 01 picnometer proceeding on Archimedes principle. Alcohol was used as the liquid. Both of sample weights (W_s) and weights in alcohol (W_a) of PP/CE, PP/SD, PP/WS composites were recorded and densities of composites were calculated according to the equation below.

$$\rho_{c=} W_s * \rho_f / (W_s - W_a) \quad (4.2)$$

where ρ_c and ρ_f are densities of composite and alcohol, respectively. Densities of composites were compared with theoretical densities of composites calculated by gas picnometer to examine void fraction in the composites. Density measurements of the CE, SD and WS fibers were performed with a Ultrapycnometer 1000 Quantachroma gas pycnometer that uses Helium at 19 psia pressure. The pycnometer was equipped with a chamber with a known volume. Fiber of interest was filled to the chamber and Helium gas was purged onto the fiber with known mass. By this method, theoretical densities of fibers or powders can be determined. 5 runs were performed for each sample and average theoretical density with standard deviation was calculated by Software program " Pycwin Version 1.10" that is connected to the device.

Theoretical densities of fibers were as follows;

d_{CE}= 1.577 ± 0.018 g/cm^3

d_{SD}= 1.485 ± 0.017 g/cm^3

d_{WS}= 1.505 ± 0.020 g/cm^3

where numbers after ± represents standard deviations calculated for 5 runs.

4.2.3.6. FTIR Analysis of Fibers and Composites

FTIR analysis enables determination of chemical changes experienced during silane treatment of the fibers. Silane treated and untreated CE particles were studied by FTIR in order to examine chemical and physical changes of the fibers. FTIR studies were carried out with a Shimadzu 8601 Infrared Spectrophotometer with a resolution of 4.0 and a mirror speed of 2.8. Fibers were analyzed by preparing KBr pellets of the fiber. Wavelength of the device was varied between 400-4400 cm^{-1} and 20 scans between the specified wavelengths were made.

Composites were characterized by FTIR spectroscopy with the same method except that composite films were prepared without using KBr technique.

Chapter 5

RESULTS AND DISCUSSION

5.1. Rheological Properties of the Composites

It is well known that incorporation of rigid fillers increase melt viscosity of polymers. Particle size and shape, interactions between particles and interactive effect of filler with the surrounding matrix are important parameters determining rheological behavior of filled polymers (Hornsby, 1999). Rheological properties of PP/cellulose composites were studied by means of Haake Rheomixer, which give plots of Torque vs. mix time data. Torque is an indicator of viscosity which reveals relative rheological behaviour of composites with changing loading or surface treatment at stabilization conditions. Torque vs time data were recorded at mixing temperature of 185 ^{o}C, rotor speed of 50 rpm and mixing time of 10 minutes. It has to be noted that shear rate dependency of composites cannot be determined since turning rate of the rotor blades was kept constant. A typical Torque vs. time data for cellulose/PP composites can be seen in Figure 5.1.

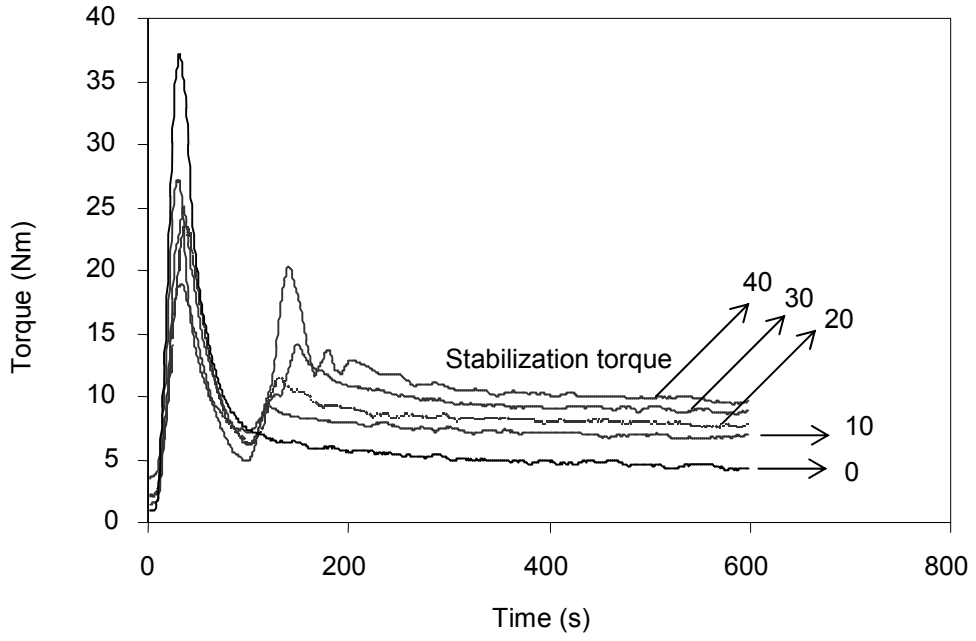

Figure 5.1. Torque vs time data for 0, 10, 20, 30, 40 wt% cellulose loaded PP composites

The initial torque increased rapidly by incorporation of polymer which is depicted as a peak at around 40 seconds. Peak heights decreased with increasing filler loading because polymer loading decreased with increasing filler loading. Torque decreased rapidly as soon as temperature of polypropylene increased and melting occured. After complete melting at around 90 seconds, cellulose was fed to rheomixer which was accompanied by an increase in viscosity. This second peak was proportional to the fiber loading. Wetting of the fibers by the polymer and dispersion decreased torque up to a stable value that is called stabilization torque. Composite reached stabilization torque at around 400 seconds. A stable torque is also an indicator of homogenization of filler in the melt (Joseph at al, 1999). When stabilization values were compared, it was clearly seen that an increase in fiber loading was accompanied by an increase in stabilization torque. Stabilization torque was 4.3 N.m for neat PP whereas 9.06 N.m for 40wt% cellulose filled PP which corresponds to a 111% increase. This result can be treated as an increase in viscosity with increasing fiber loading.

Figure 5.2 illustrates variation of stabilization torque with respect to fiber loading for PP/CE composites.

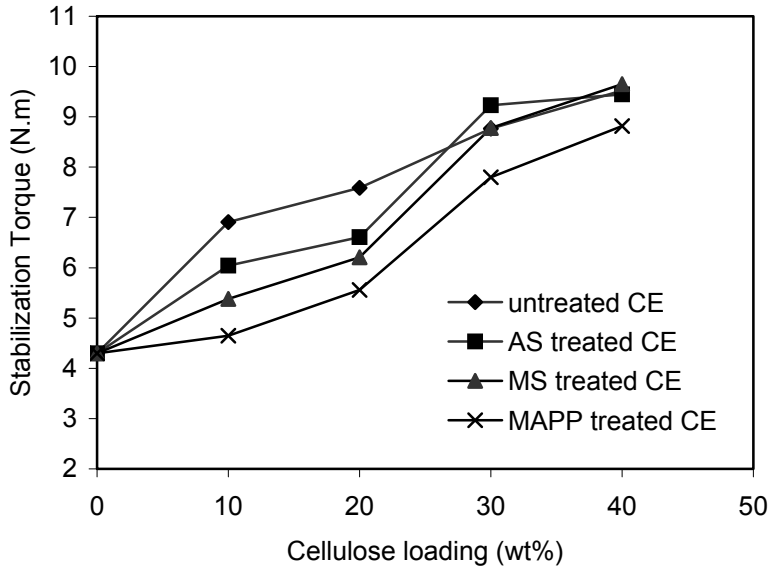

Figure 5.2. Variation of stabilization torque with respect to cellulose loading and treatment.

Surface treatment was employed to promote fiber dispersion and to enhance interfacial bonding between fiber and matrix. Frequently, surface modification of the fiber results in a reduction in shear viscosity relative to untreated material, which may be explained by reduced interaction between the filler and dispersion medium, although a decreased tendency towards filler network formation may also be a contributory factor. If present in polymer phase, these chemicals may also exert a lubricating effect causing a reduction in viscosity. There are instances where surface treatment of filler can result in increased melt viscosity due to enhanced interaction between filler and polymer. This can be considered in terms of a stable adsorption layer formed around the filler increasing its effective (Hornsby, 1999). In our stabilization torque data, all surface treatments have decreased stabilization torque, especially at low fiber loadings. As mentioned above, there are two interactions in a filled polymer system; Fiber-fiber interactions and fiber-matrix interactions. Silane coupling agents increase polarity and hydrophobicity of CE fibers, which yields to decreased particle-particle interactions. That is, agglomeration or network formation is decreased that would have a decreasing effect on viscosity. On the other hand, particle-matrix interaction is increased due to enhanced matrix-polymer adhesion. This would have a positive effect on viscosity. As seen in Figure 5.2, stabilization torque significantly decreased with AS and MS treatment of CE at 10 and 20wt% CE loadings, but stabilization torque was almost the same at 30 and 40% loadings. These results reveal that at lower fiber loadings, the dominating interaction is particle-particle interaction, but at higher loadings, particle-matrix interactions begin to dominate. MAPP treatment always had a negative effect on stabilization torque, which is more pronounced for low fiber loadings. To understand the nature of decrease in stabilization torque to due MAPP treatment, stabilization torque of neat PP and 10wt%MAPP treated PP were compared. The comparison was shown in Figure 5.3. It was observed that 10wt% MAPP incorporation into PP decreases torque from 4.30 to 3.36 which corresponds to a 22% decrease. This result proves that decrease in viscosity of composites is due to interaction of MAPP with PP. MAPP behaves as a lubricating agent in PP. This can be attributed to maleic anhydride groups on MAPP. These groups would lower shearing between polymer chains. Another possible reason for the decrease in viscosity with MAPP addition would be decreased interaction with the walls of Rheomixer . MAPP would have behaved as a slipping agent.

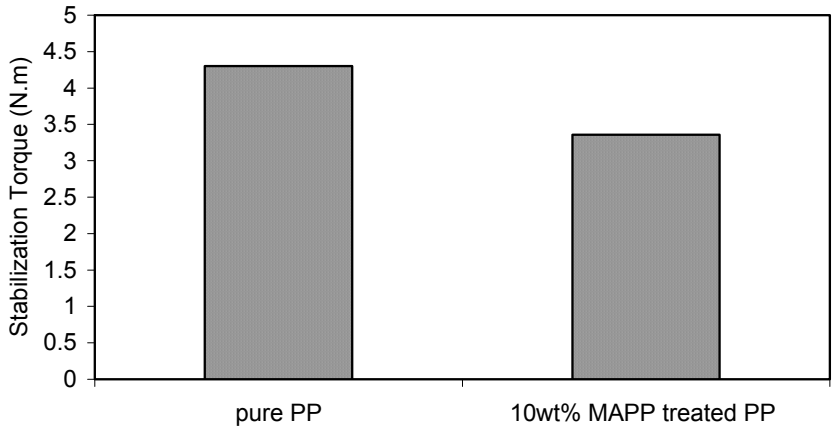

Figure 5.3. Comparison of stabilization torque of pure and MAPP treated PP.

Figure 5.4, 5.5 and 5.6 illustrate effect of treatment type, concentration and fiber type on stabilization torque at 30wt% loading for AS, MS and MAPP treated PP/CE composites, respectively.

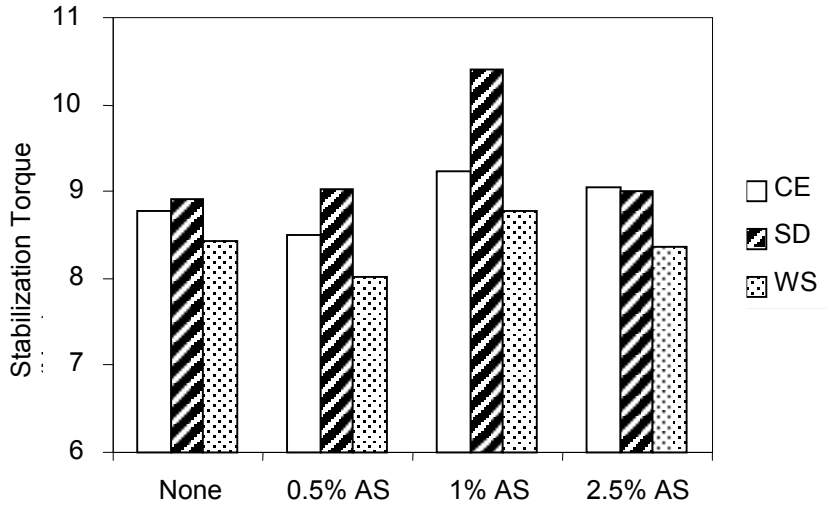

Figure 5.4. Effect of concentration of AS treatment on stabilization torque of 30wt% CE, SD and WS loaded PP composites.

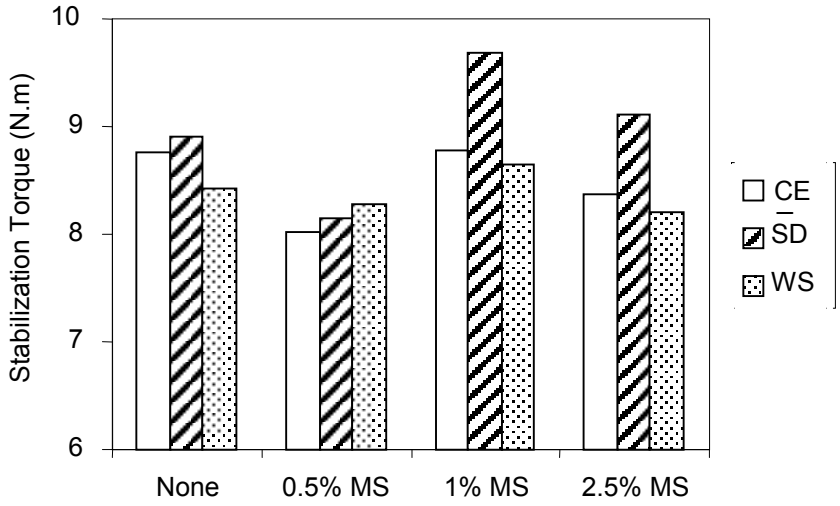

Figure 5.5. Effect of concentration of MS treatment on stabilization torque of 30wt% CE, SD and WS loaded PP composites.

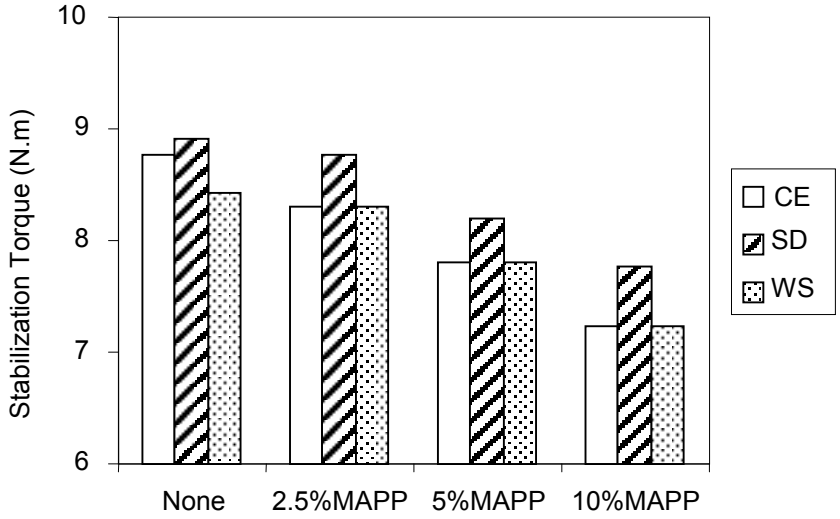

Figure 5.6 Effect of concentration of MAPP treatment on stabilization torque of 30wt% CE/SD/WS loaded PP composites.

Figures 5.4 and 5.5 show the influence of silane treatment concentration on the stabilization torque of the composites containing 30 wt% fiber. Stabilization torque were measured for 3 different silane concentrations (0.5, 1, 2.5 wt% of fiber). As observed from the figures, silane treatment leads to increase in stabilization torque values. The increase is maximum at 1 wt% silane treated composites. In all silane treated composites, stabilization torque values decreases at 2.5wt% silane concentration

regardless of fiber type. When AS and MS treated composites were compared, AS treatment provided higher stabilization torque values compared to MS treatment because particle-particle interactions are more pronounced in AS treatment. These results suggest that matrix-fiber interaction or adhesion between fiber and matrix is maximum at 1% silane treatment. It can also be concluded that 2.5% silane treatment would have formed a layer on the fibers which can be attributed to unreacted silanes or long chain siloxanes on fiber surface. This layer would restrict interaction between fiber and matrix decreasing stabilization torque. Viscosity of suspension of rigid spherical particles can be characterized by Eisenstein's equation which holds for rigid particles in dilute concentrations as seen in Equation 5.1 (Hornsby, 1999).

$$\eta / \eta_1 = (1 + k_E \Phi_2) \qquad (5.1)$$

where η is the viscosity of suspension (CE/PP composite in our case) , η_1 is the viscosity of suspending liquid (PP in our case), k_E is the Eisenstein coefficient (2.5 for dispersed spheres) and Φ_2 is the volume fraction of particles.

Taking relative torque values as the viscosity of CE/PP composite since shear rate and temperature was constant, experimental viscosities with changing filler volume fraction was compared with theoretical calculations according to Eisenstein's equation for PP/CE composites, as seen in Figure 5.7.

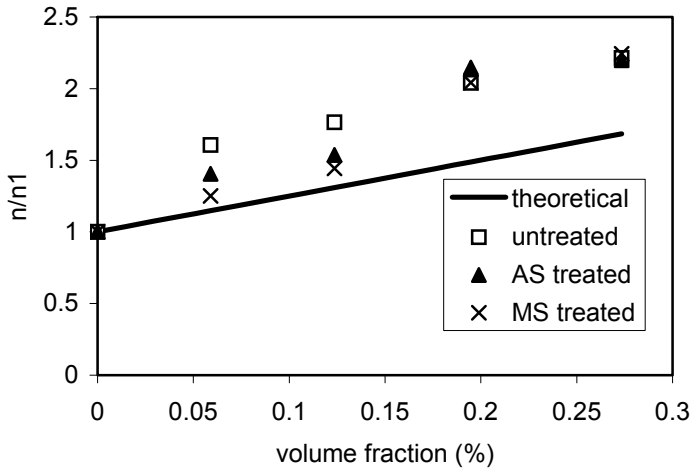

Figure 5.7. Variation of torque with respect to CE volume fraction for untreated and AS and MS treated CE.

AS seen in Figure 5.7, deviation of torque from theoretical value is high, especially at high volume fractions. Treatment of CE decreased deviation from theoretical value at low filler loading. It has to be kept in mind that Eisenstein's equation is valid for dilute suspensions. At high volume fractions, the model does not predict experimental values well as a result of particle-particle interactions. Increase in volume fractions increased particle-particle interactions, thus deviation from Eisenstein's equation was increased. It was also noted that silane treatment decreased deviation from the model because of decreased interactions between particles. The decrease in interactions would be treated as an evidence of enhanced dispersion of fillers in the matrix via silane treatment, especially at low volume fractions.

5.2. Mechanical Properties of Composites

Tensile tests were conducted in order to determine effect of fiber loading and type, surface treatment type and amount on mechanical properties of composites. The most important tensile test responses are tensile strength, Young's Modulus, elongation at break and energy to break. At least 5 specimens were tested for each sample. Experimental tensile test results were given in Appendix A.1. Figure 5.8 is a typical example of stress-strain curve where mentioned mechanical responses were extracted.

Stress-strain curves belong to PP/SD composites at 30wt% of fiber loading and optimum treatment conditions.

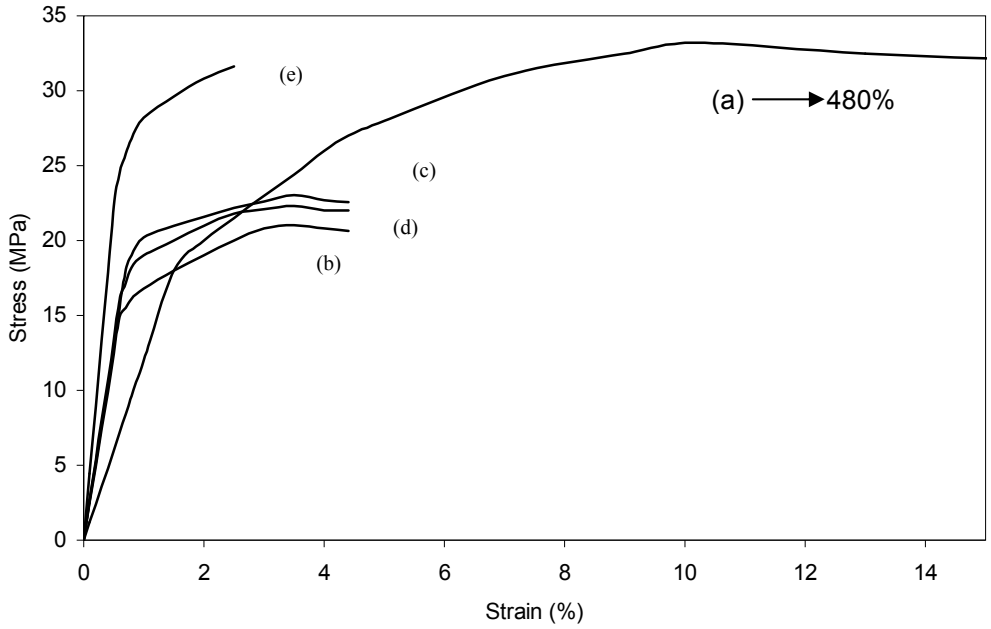

Figure 5.8. A typical stress-strain diagram of PP/SD composite at 30wt% fiber loading (a) pure PP (b) untreated (c) AS treated (d) MS treated (e) MAPP treated composites.

Generally speaking, incorporation of CE into PP had decreased tensile strength as well as toughness and strain at break of the materials. Young's Modulus of composites increased with employment of CE. AS and MS treatment had increased tensile strength to some extend, but MAPP treatment had a distinct positive effect on tensile strength. Composites treated with MAPP had almost recovered the tensile strength loss due to incorporation of fibers. Increase in Young's Modulus is also much more pronounced for MAPP treated composites. AS and MS did not have a distinct effect on Young's Modulus and strain at break. Strain at break of MAPP treated composites had decreased compared to untreated, silane treated composites. Another interesting point is MAPP treatment prevented stress relaxation in the composites, that is there was no yielding in MAPP treated composites whereas untreated, AS and MS treated exhibited yielding phenomenon. Next sections will present a detailed analysis of

tensile testing responses. Effect of different parameters on mechanical response will be evaluated.

5.2.1. Tensile Strength of Composites

The effect of fiber type and loading and surface treatment on tensile strength of composites were studied. Figure 5.9 demonstrates that tensile strength of CE, SD and WS loaded composites as a function of fiber loading. It was obtained that tensile strength decreased with increasing fiber loading irrespective of fiber type. At 40wt% fiber loading, the decline was 41.9, 42.4 and 44.4% for CE, SD and WS/PP composites, respectively. The decline in tensile strength with increasing fiber content is the usual case for natural fiber reinforced thermoplastics (Battaille, 1989, Johan, 1991). However, there are some expectations where true reinforcement of the matrix, thus an increasing trend in tensile strength with increasing fiber content can be achieved with specific fiber types. For example, Ichazo et al (2001) studied wood flour/PP composites and they have achieved around 50% enhancement in tensile strength at 40wt% fiber loading compared to neat PP. In our case, neither of fibers provided an increase with incorporation of fibers to PP matrix.

Effect of coupling agent concentration on the tensile strength of the composites was investigated. % increase in tensile strength of 30 wt% loaded composites with surface treatment was tabulated in Table 5.1. As a general trend, it can be observed that AS and MS treatments provided maximum tensile strength increase at 1wt% silane treatment with respect to fiber weight. Tensile strength increase between 6 and 11.6% could be achieved at 1wt% level of silane treatment. Silane treatment above 1% decreased tensile strength of composites to the levels of untreated composites. In silane treatment, the formation of silanol as a result of hydrolysis and the respective siloxane as an effect of condensation were to be expected. This should favor the formation of hydrogen bonds with the hydroxyl groups that are on the surface of cellulose. Probably, siloxane chains were formed and they become so excessively long that suffered crosslinking reactions and therefore, the formation of a weak interface (Ichazo, 2001) Similarly, optimum condition for MAPP was 5wt % with respect to polypropylene content. It was also observed that MAPP provided a much more efficient reinforcement compared to two types of silane treatments. At optimum conditions, MAPP had increased tensile strength 32.6, 50.4 and 49.4% for CE, SD and WS composites,

respectively. The increase in tensile strength with silane treatment at optimum conditions did not exceed 14.2%.

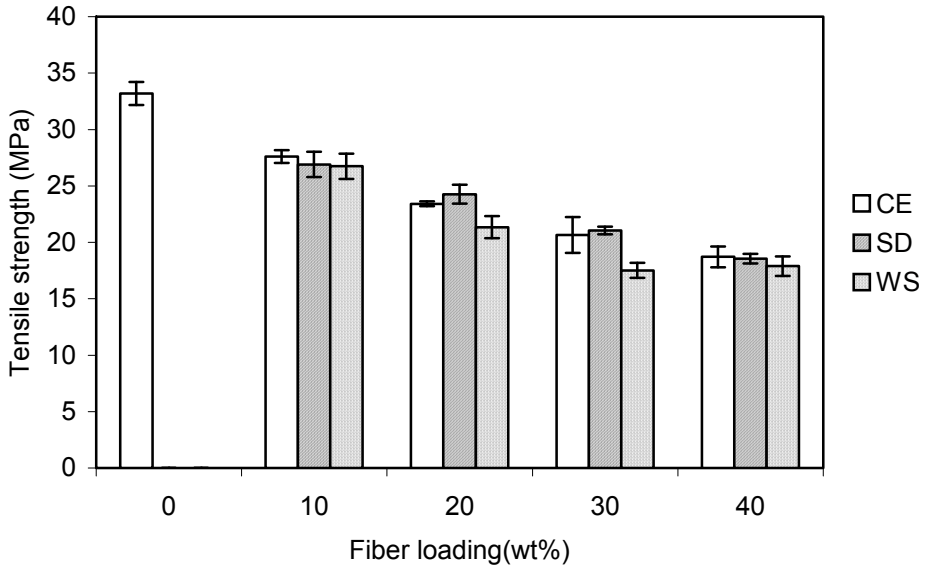

Figure 5.9. Effect of fiber loading on tensile strength of PP/C, SD and WS composites.

Table 5.1. % increase in tensile strength with varying treatment type and amount for 30wt% fiber loaded composites compared to untreated composites.

% increase	AS treatment			MS treatment			MAPP treatment		
	0.5%	1%	2.5%	0.5%	1%	2.5%	2.5%	5%	10%
CE	2.2	8.8	0	0.6	8.3	2.2	28.0	32.7	25.1
SD	2.2	9.4	0	1.0	6.0	1.0	46.1	50.4	35.8
WS	14.2	10.2	8.2	6.8	11.6	-6.2	51.0	49.4	49.6

Figure 5.10 illustrates the effect of coupling agents on tensile strength of CE, SD and WS/PP composites at 30wt% loading. This graph shows that MAPP has a great coupling efficiency compared to AS and MS. Another conclusion is MAPP is more effective coupling agent for SD/PP composites since increase in tensile strength is much more pronounced for SD/PP composites compare to two other composite systems. Although 30wt% fiber was employed, there was almost no tensile strength decrease for SD/PP composites compared to neat PP.

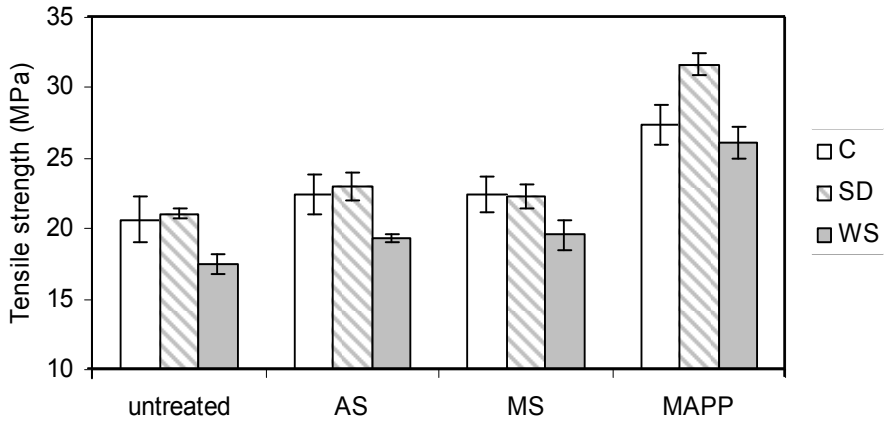

Figure 5.10. Effect of coupling agent on tensile strength of PP/CE, SD and WS composites.

Tensile strength or tensile yield stress is an excellent parameter for interfacial interactions in heterogeneous polymer systems. It is possible to determine a parameter related to stress transfer of composites by using tensile strength.

Factor with σ_f takes into account the smaller effective load-bearing cross section by replacing matrix polymer by dispersed phase. Parameter B considers stress transfer between dispersed phase and matrix. Strong interfacial interactions lead to high values of B and consequently to high tensile strength of corresponding system. Pukanzky model was given in Equation 3.8 . Equation can be rearranged;

$$(\sigma_y / \sigma_{yo}(1+2.5\ \sigma_f / 1- \sigma_f)/)) = \text{In}\ \sigma_{y(rel)} = (B\sigma_f) \qquad (5.2)$$

If In $\sigma_{y(rel)}$ is plotted against volume fraction of dispersed phase, as seen in Figure 5.11, parameter B can be calculated as a line slope, with intercept in cross section of coordinate axis. The equation was also solved non-linearly by using Solver program in Excel. Calculated B values with linearization and Excel solver are tabulated in Table 5.2.

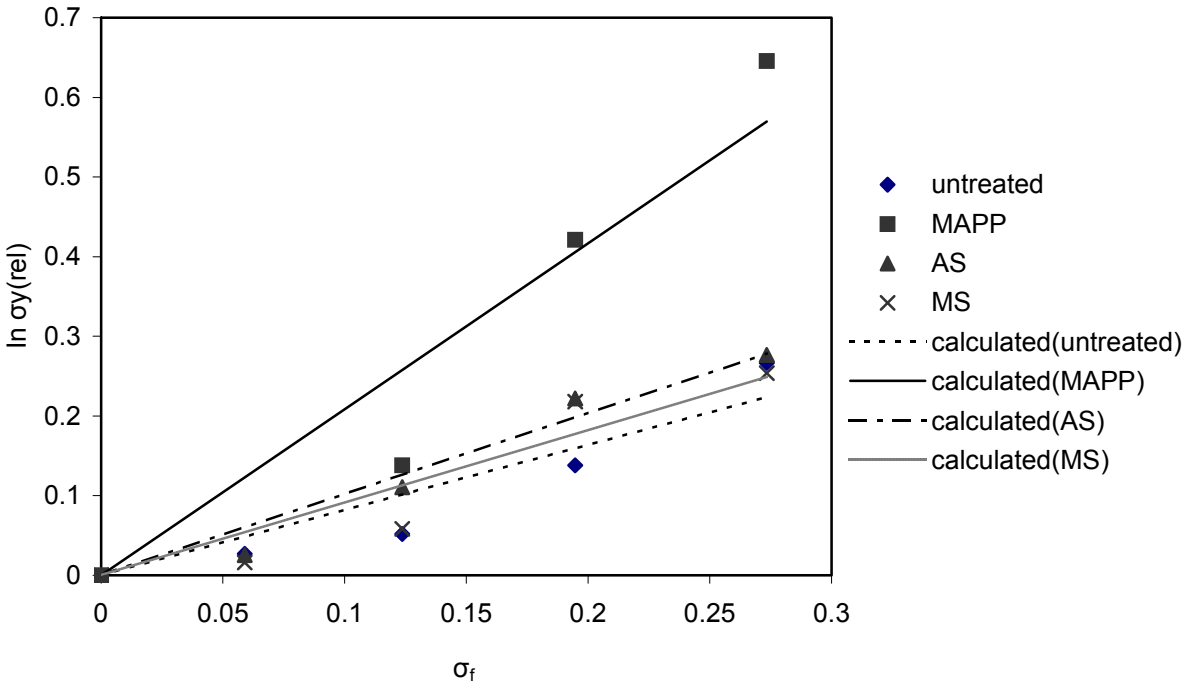

Figure 5.11. Dependence of linearized yield stress as a function of CE volume fraction.

Table 5.2. Values of parameter B calculated by linearization and Solver.

Treatment	B with linearization	B with solver
untreated	0.8198	0.8202
AS	1.0199	0.9914
MS	0.9128	0.9240
MAPP	2.0839	2.0552

It is evident that two approaches lead similar results as seen in Table 5.2. It can be concluded that MAPP treatment had the highest value of B, thus greatly enhanced stress transfer between fiber and matrix. AS and MS treatment also enhanced stress transfer but efficiency was very low compared to MAPP treatment since B value increase was rather low compared to MAPP treatment.

Denac and Musil (1999) had employed Pukanszky model to investigate the effect of aminosilane treatment on talc/PP composites. B value had increased from 2.72 to 3.20 with employment of silane treatment. They have also confirmed enhanced adhesion by SEM micrographs.

Metin et al (2003) employed three types of silane coupling agents for the surface modification of zeolites and observed increased B values with employment of silane coupling agents.

Figure 5.12 shows experimental and calculated yield stress values of C/PP composites with varying volume fraction of CE.

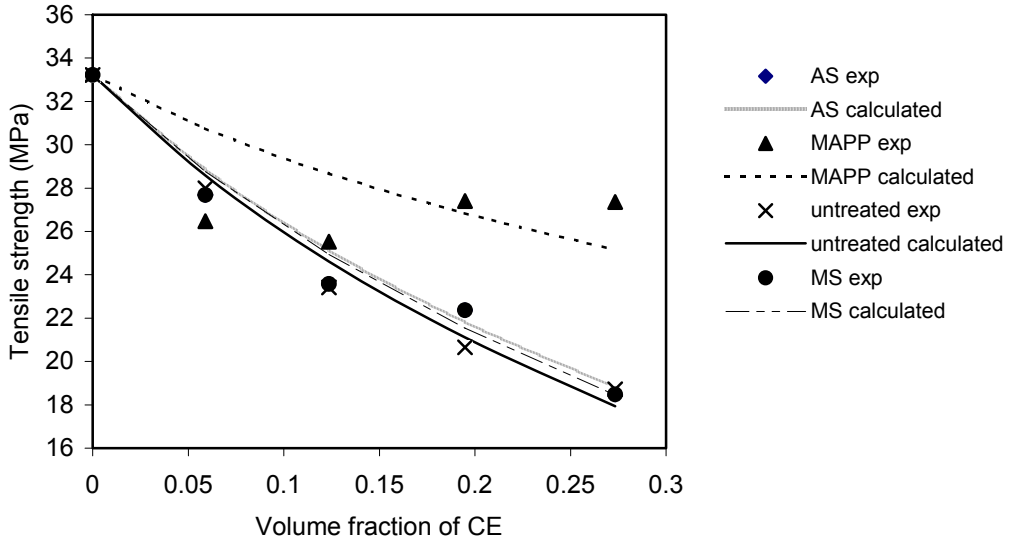

Figure 5.12. Effect of coupling agent on the experimental and calculated yield stress values of PP/CE composites with respect to volume fraction.

As seen in Figure 5.12, untreated, AS and MS treated composites were in good agreement with the calculated values, but MAPP had established high deviations especially at low fiber loadings. MAPP was incorporated into PP matrix at 5wt% loading with respect to PP. The aim was to add fibers into matrix with the same composition, that is matrix always contains 5wt% MAPP with respect to PP. But MAPP in the matrix is highly polar due to maleic anhydride groups. Highly polar MAPP may have clustered around polar cellulose particles because of polar attraction forces. Too high amount of maleic anhydride may hold the coupler too close to the polar surface

and not allow sufficient interaction with the continuous non-polar phase (Keener, 2003). In other words, MAPP may have covered CE particles and MAPP couldn't have diffused into matrix due to high amount of MAPP at low fiber loadings. It would be a better choice to add MAPP with respect to amount of filler in the matrix.

Nielsen model explained in Chapter 3 was also applied to CE/PP composites at 30 wt% loading. S parameters were 0.965, 1.050, 1.046 and 1.281 for untreated, AS, MS and MAPP treated composites, respectively. Increasing trend with coupling agent treatment could be observed. Values greater than unity indicate lesser stress concentration effect, thus better adhesion between fiber and matrix, hence MAPP exhibited the best performance in terms of enhanced interfacial adhesion.

5.2.2. Young's Modulus of Composites

The effect of filler content and type and coupling agents on Young's Modulus of the composites were studied. It was well known that incorporation of fillers or fibers into a ductile thermoplastic matrix increases Young's Modulus since fillers or fibers decrease deformation capacity of thermoplastic matrix in the elastic zone (Colom, 2003). Adhesion between fiber and matrix can have additional effects on Young's Modulus since interface has a great impact on deformation capacity of composites.

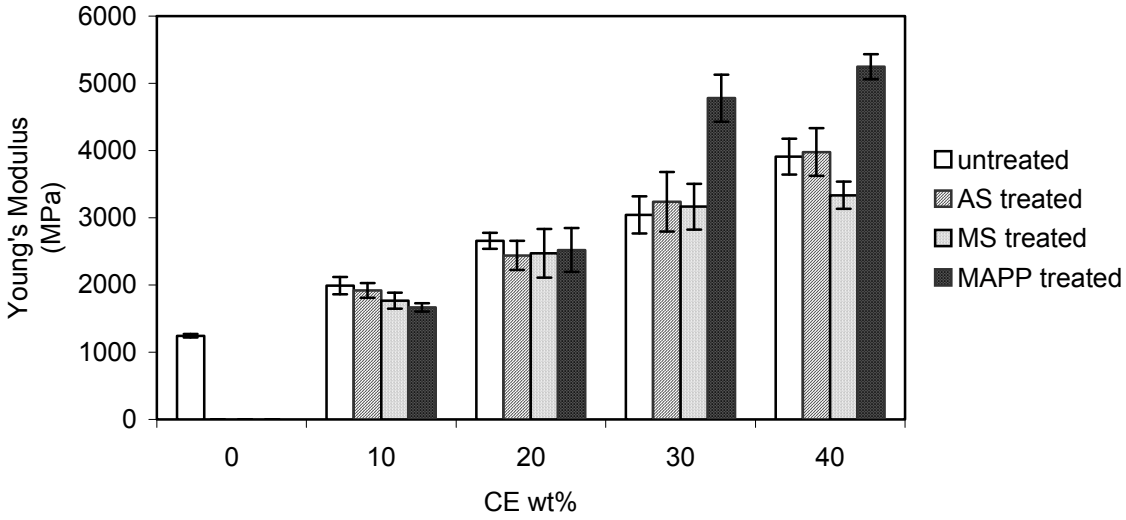

Figure 5.13. Effect of fiber loading and treatment type on Young's Modulus of PP/C composites.

As seen in Figure 5.13, Young's Modulus tends to increase with increasing CE loading. 40 wt% of CE had increased Young's Modulus from 1243 MPa to 3910 MPa which corresponds to a 214% increase. When effect of coupling agents on Young's Modulus of PP/CE composites was investigated (Figure 5.14) , it can be deduced that none of the coupling agents had a significant influence on Young's Modulus except for MAPP. There were fluctuations in Young's modulus of composites treated with AS or MS compared to untreated composites but these fluctuations were generally in the range of error. This is an evidence that AS and MS did not change interface or deformation capacity of the composites, thus Young's Modulus was not significantly affected. MAPP had a great influence on Young's Modulus of CE/PP composites, especially at high loadings. The same discussion of effect of MAPP on tensile strength is valid for the discussion of Young's Modulus. At low loadings, too high amount of MAPP had covered CE particles and interfacial strength was decreased, thus Young's Modulus of composites was not affected significantly by employment of MAPP. However, at 30 and 40wt% CE loading, Young's Modulus increased 57.1 and 34.2 % compared to untreated composites at the same loading, respectively. This is an indicator of better adhesion between fiber and matrix.

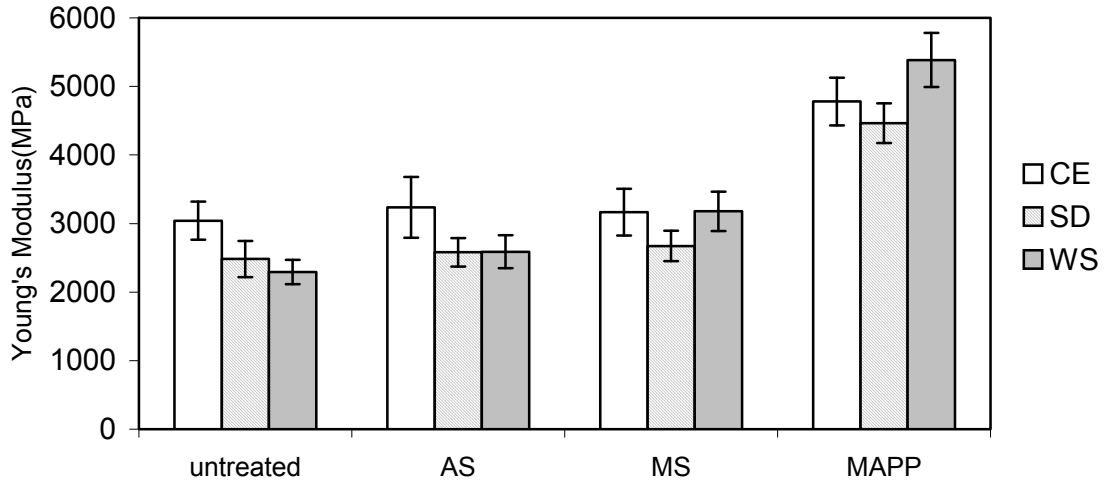

Figure 5.14. Effect of fiber and treatment type on Young's Modulus of PP/CE, SD, WS composites at 30wt% fiber loading.

5.2.3. Strain at Break and Energy to Break of Composites

Strain at break of composites is a measure of ductility in polymer composites. High values of elongation at break indicate that composite is ductile where as low values indicate that composite is brittle. Energy to break is the area under the stress-strain curve and is the amount of energy absorbed up to fracture and is a measure of toughness.

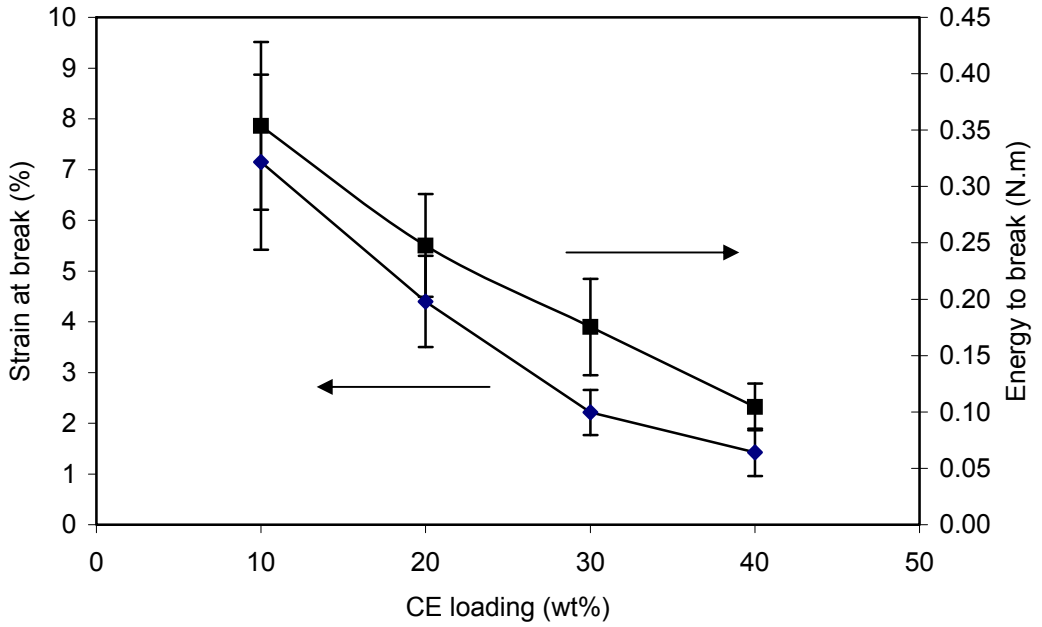

Figure 5.15. Effect of CE loading on strain at break and energy to break of PP/CE composites.

Figure 5.15 illustrates effect of fiber loading on elongation at break and energy to break of PP/CE composites. It was clearly observed that loading had an adverse effect on both elongation at break and energy to break. It has to be mentioned that elongation at break and energy to break of pure PP is 418% and 12 N.m, respectively. Only 10wt% loading of CE had a great impact on elongation and toughness of composites. Elongation at break decreased from 418% to about 8% and energy to break decreased from 12 N.m to 0.35 N.m. These observations clearly show that incorporation of particles causes a brittle behavior in the composites compared to ductile thermoplastic matrix, even at low fiber loadings. This is because particles or fibers restrict deformation capacity in elastic zone as well as plastic zone. Restricted

deformation capacity in the elastic zone causes increase in modulus whereas restricted deformation capacity in the plastic zone causes decreased elongation at break and toughness.

Figures 5.16 and 5.17 illustrate the deviation of strain at break and energy to break of CE, SD and WS composites with AS, MS and MAPP treatment, respectively. Considering error bars, AS and MS treatment did not change strain at break and energy to break of composites significantly for three types of composites, but MAPP significantly reduced the two responses. The reduction in strain at break was 33.5, 33.9,

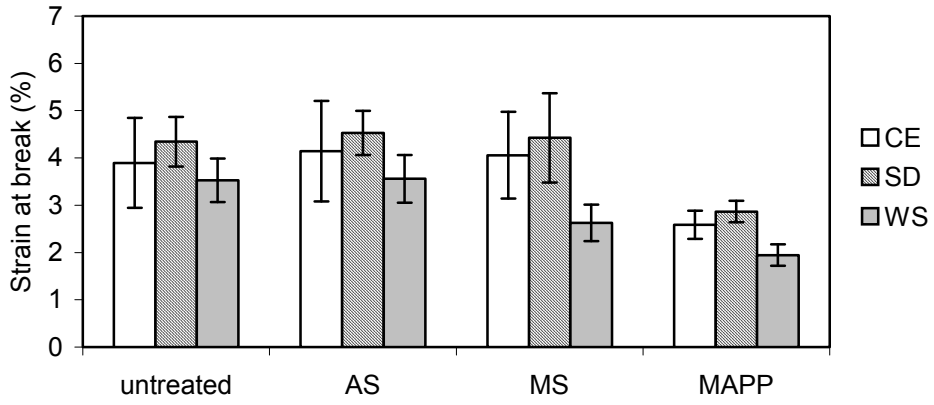

Figure 5.16. Effect of fiber and treatment type on strain at break of PP/CE, SD, WS composites at 30wt% fiber loading.

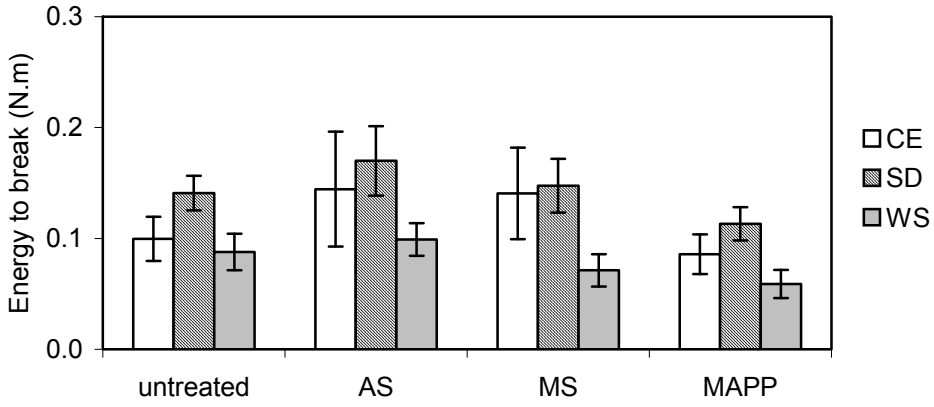

Figure 5.17. Effect of fiber and treatment type on energy to break of PP/CE, SD, WS composites at 30wt% fiber loading.

and 44.8% for CE, SD, and WS/PP composites, respectively. Similarly, reduction in energy to break was 10.0, 21.4 and 33.3% for for CE, SD, and WS/PP composites, respectively. MAPP have reduced strain at break and, consequently energy to break values of composites due to enhanced adhesion between fiber and matrix. Better adhesion yields to more restriction of deformation capacity of composites, thus catastrophic failure occurs after small strain deformations. It would be expected that silane coupling agents would decrease strain at break and toughness of composites due to enhancement of adhesion between polymer and fiber but it seems that limited enhancement of the interface was not reflected in toughness of the composites.

5.3. Morphological Properties of Composites

Effect of surface treatment on dispersion of fiber in the matrix, interfacial adhesion between fiber and matrix and fracture modes of the composites were studied by examining fracture surface of PP/CE,SD and WS composites at 30wt% fiber loading. Silane treatment was applied at 1% wt ratio with respect to fiber weight. MAPP was applied at a 5wt% ratio with respect to PP weight. Figure 5.18-20 illustrate fracture surfaces of CE, SD and WS without treatment or with 3 different surface treatments at 100x magnification, respectively. At the first sight, it can be easily observed that all types of fibers were well dispersed in the matrix, regardless of surface treatment employed. This observation proves that efficient mixing of fibers in the matrix was achieved via melt mixing of fibers and PP in Rheomixer and compression molding in the polymer press. In Figure 5.18, particulate structure of cellulose can be observed. Figures 5.19 and 5.20 reveal that SD and WS were predominantly in fiber form and WS has higher fiber length and aspect ratio than SD. SD and WS composites consist of fibers. It can be seen that fibers were oriented randomly along the matrix. When effect of surface treatments on fracture surface of composites were compared, it was observed that AS and MS did not cause a change on the fracture surface of composites for both CE, SD and WS composites whereas MAPP treatment changed fracture mode significantly. Comparison of surface treatments shows that surface roughness of composites treated with MAPP is significantly lower than that of untreated or AS and MS treated composites. Decreased surface roughness with employment of MAPP is a cause of enhanced stress transfer between fiber and matrix via enhanced fiber matrix

adhesion. Fiber or particle pull out from the matrix in the presence of a tensile load is an indicator of lack of adhesion between fiber and matrix and increases surface roughness of fracture surface. These observations were also confirmed by tensile test results. Tensile strength of composites significantly increased with employment of MAPP for all composite types. AS and MS did not yield a significant increase in tensile strength since adhesion could not be improved.

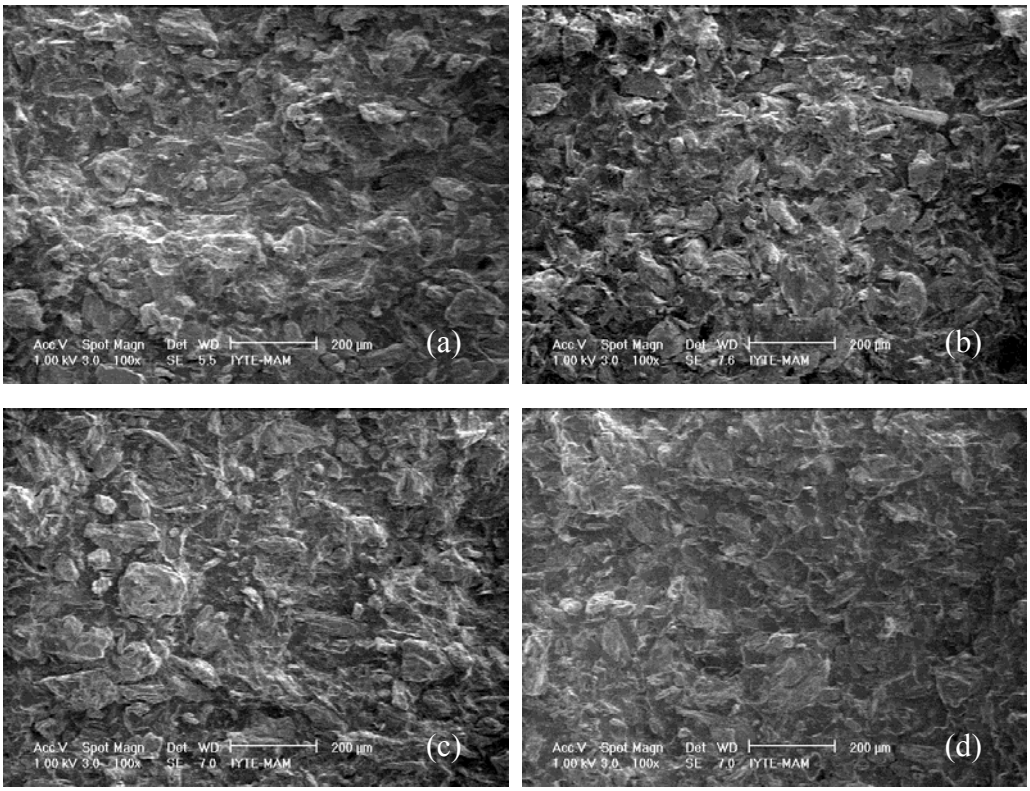

Figure 5.18. SEM micrographs of (a) untreated (b) AS treated (c) MS treated (d) MAPP treated CE/PP composites at 30 wt% loading and x100 magnification.

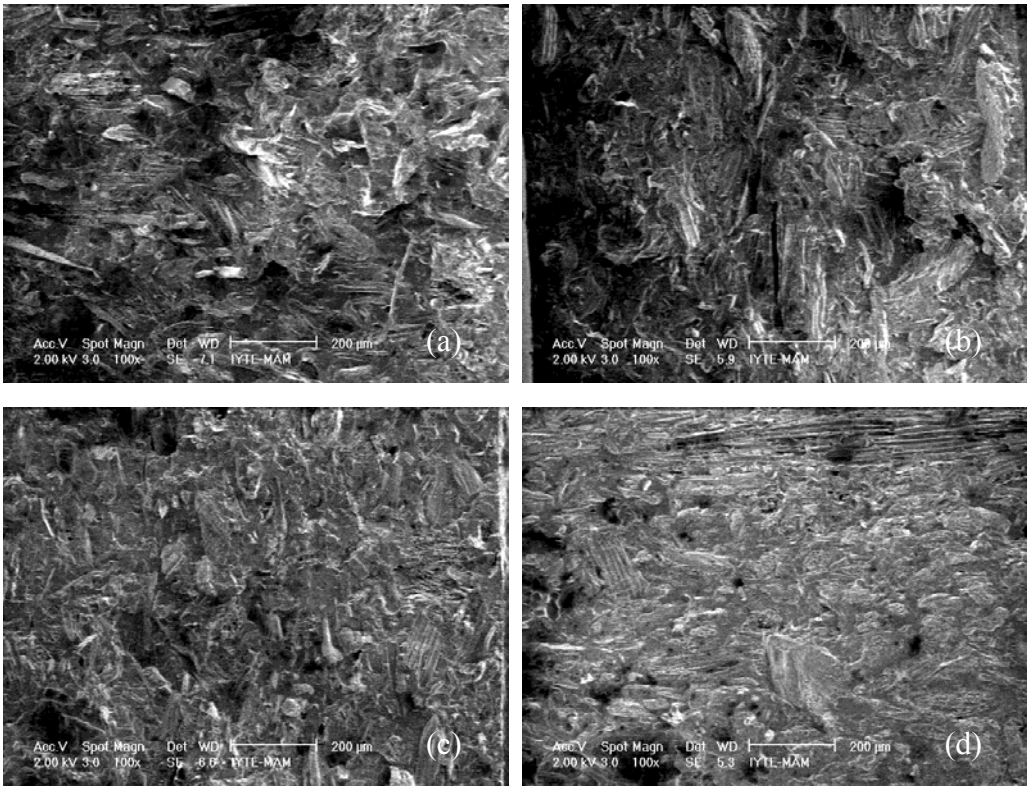

Figure 5.19. SEM micrographs of (a) untreated (b) AS treated (c) MS treated (d) MAPP treated SD/PP composites at 30 wt% loading and x100 magnification.

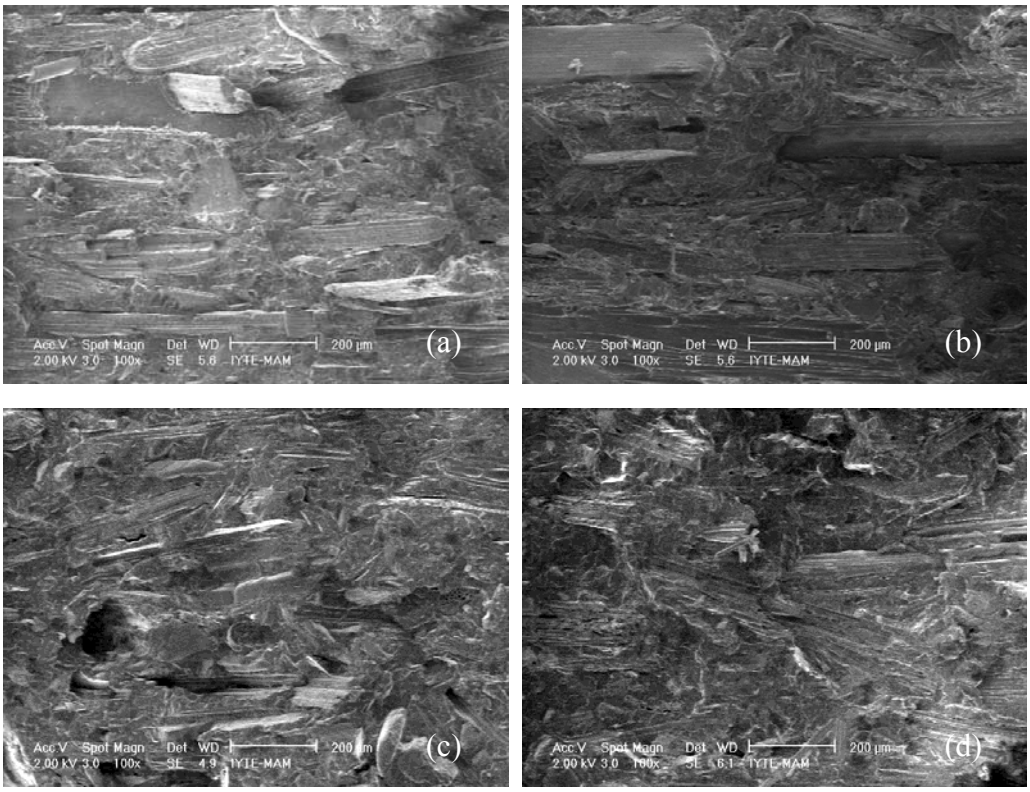

Figure 5.20. SEM micrographs of (a) untreated (b) AS treated (c) MS treated (d) MAPP treated WS/PP composites at 30 wt% loading and x100 magnification.

Figures 5.21-23 depict a more detailed view of the same composites in the same sequence at 1000 times magnification. Detailed view of fracture surface of composites enables a deeper understanding of interface and nature of fracture. As seen in Figure 5.21-(a-c), cellulose particles exhibited poor wetting by polymer matrix. Particles were not covered with a polymer layer and there were voids around the particles. This is a proof that PP was easily separated from C along the interface because of low interfacial adhesion. On the contrary, MAPP treated PP/CE composites were well embedded in the matrix with surface coverage by the matrix as seen in Figure 5.21-d. In Figure 5.22-a, fiber pull out accompanied by void formations could be observed for untreated PP/SD composites. AS and MS treatment improved interfacial adhesion to some extend. There is less fiber pull out and more interfacial adhesion as seen in Figure 5b,c. In addition to fiber pull out as the mode of fracture, fiber breakage can also occur for MAPP treated composites, as seen in Figure 5.23d. for PP/WS composites. This is an evidence of effective stress transfer between fiber and matrix.

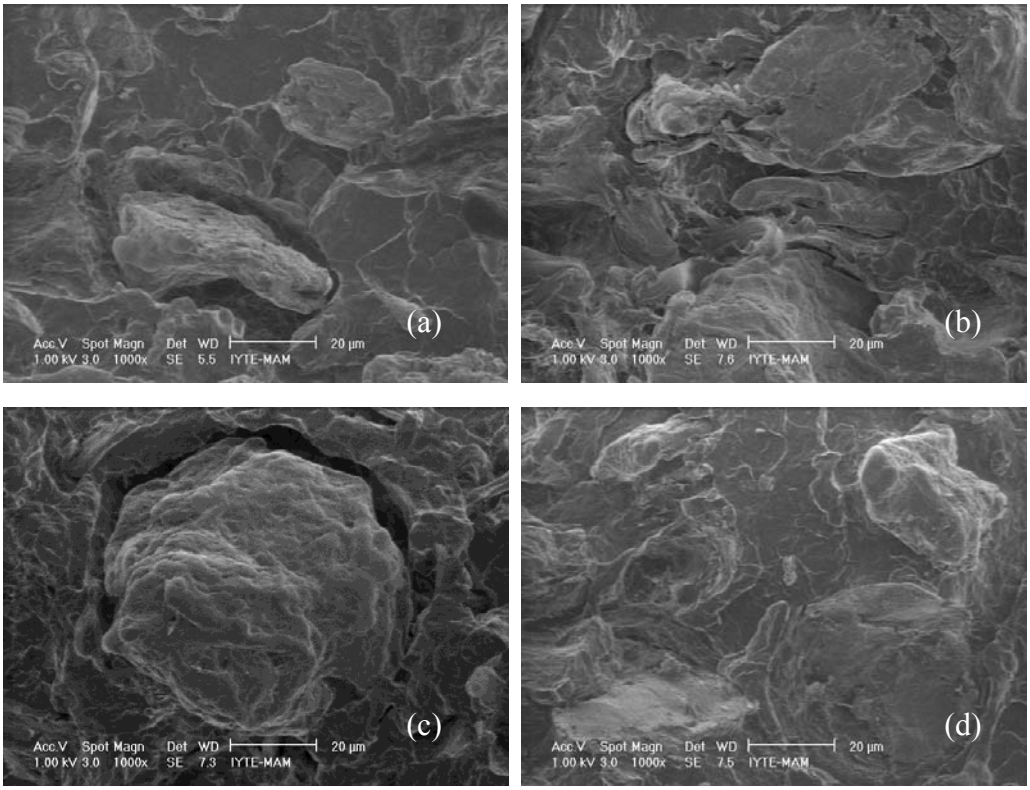

Figure 5.21. SEM micrographs of (a) untreated (b) AS treated (c) MS treated (d) MAPP treated CE/PP composites at 30wt% loading and x1000 magnification.

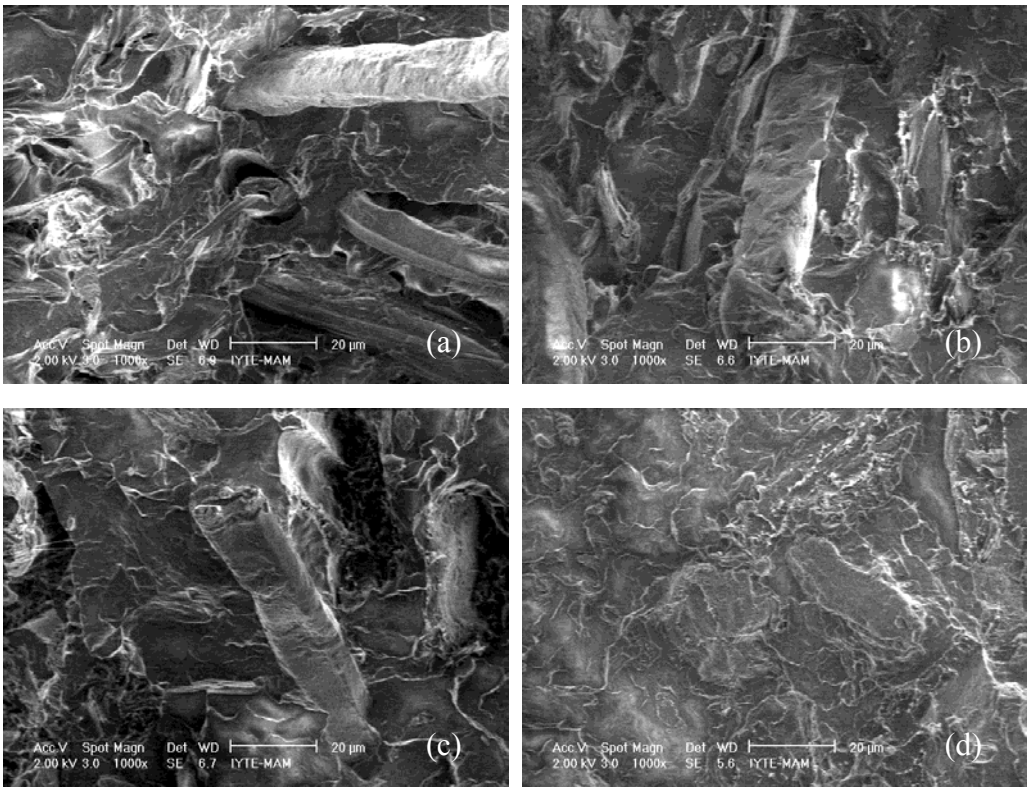

Figure 5.22 SEM micrographs of (a) untreated (b) AS treated (c) MS treated (d) MAPP treated SD/PP composites at 30wt% loading and x1000 magnification.

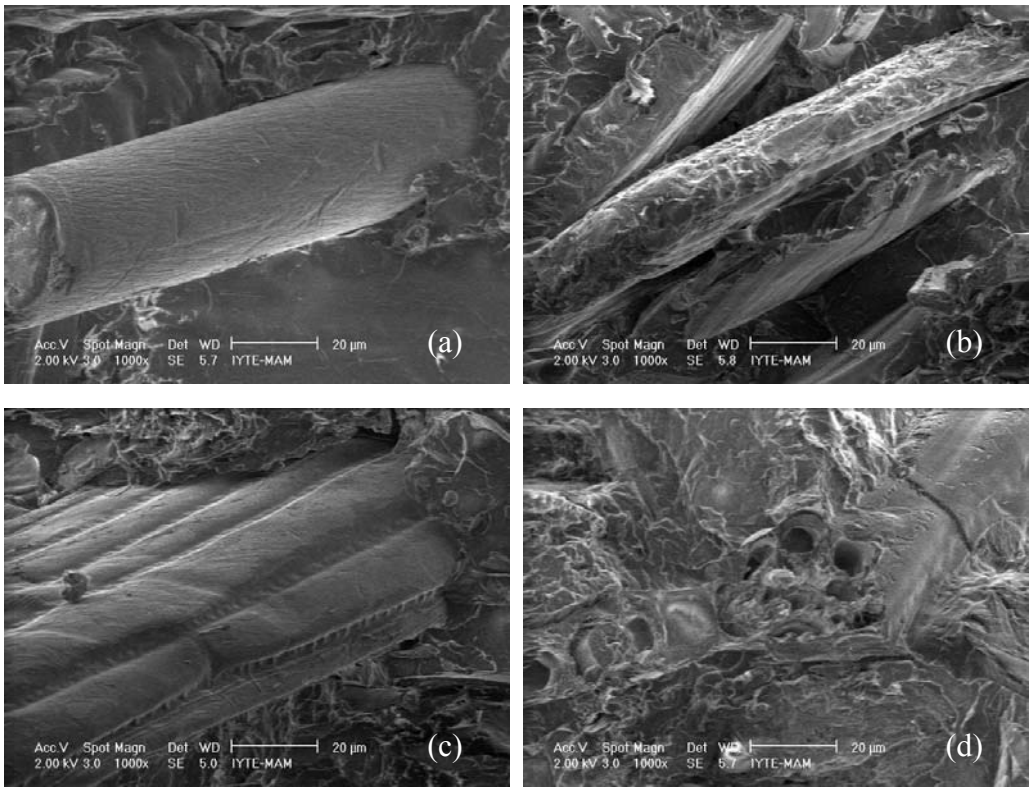

Figure 5.23. SEM micrographs of (a) untreated (b) AS treated (c) MS treated (d) MAPP treated WS/PP composites at 30wt% loading and x1000 magnification.

Mechanical properties had shown that there is a significant decrease in elongation at break and toughness of composites when MAPP treatment was employed. In the light of SEM observations, it is evident that MAPP decreased fiber pull-out by increasing fiber-matrix adhesion and decreased void formations around the fibers. Voids around the fibers and fiber pull out of the composites would have increased energy dissipation while fracture of composites, which has a positive impact on toughness of composites. It is obvious that voids around fibers increased the path of crack penetration in the transverse direction. Decreased surface roughness of fracture surface of composites with employment of MAPP is a direct evidence of decreased path distance during crack propagation, decreasing elongation at break and toughness of composites accordingly. Ichazo et al (2001) suggested another explanation to decreased elongation at break with employment of MAPP. They suggested that this behavior of elongation at break when composites contain MAPP can be due to acidic nature of functionalized compatibilizers since these compatibilizers can accelerate degradation of cellulose fibers at the processing temperature, and this, in turn leads to fragilization of cellulose fibers.

5.4. Water Sorption of Composites

Cellulose is a hydrophilic polymer, which is capable of forming hydrogen bonds with water molecules because of hydroxyl group in its chemical structure. When incorporated into PP matrix, cellulose is still capable of absorbing water. Water penetrates into interface between PP and cellulose that decreases interfacial adhesion between fiber and matrix. This phenomenon has a great negative impact on mechanical properties of composites. In this study, effect of fiber loading and coupling agents on water sorption of PP/CE,SD and WS composites were investigated. Figure 5.24 shows effect of CE loading on water sorption of PP/CE composites. It is clearly seen that water sorption increases with increasing CE loading due to increasing hydrophilicity of the composite as expected. The increase is almost in a linear fashion.

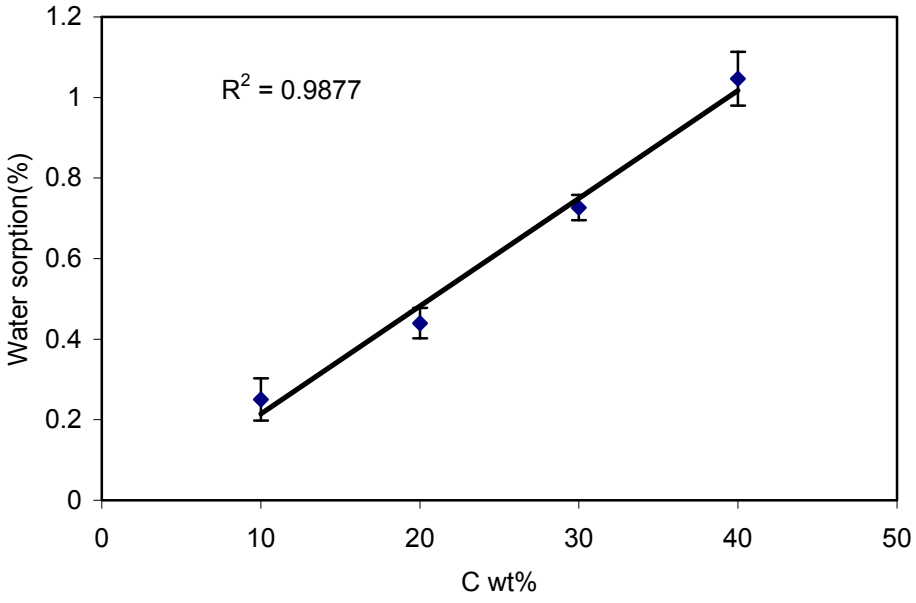

Figure 5.24. Effect of CE loading on water sorption of PP/CE composites.

Linearity in the graph proves that the composites did not exhibit agglomeration which would complicate water sorption tendency of composites with increasing fiber loading.

Figure 5.25 illustrates effect of coupling agent and fiber type on water sorption of composites at 30% fiber loaded composites. It was observed that three coupling agents decreased water sorption of composites at different levels for the three fiber types. The decline in water sorption of composites with respect to fiber and coupling type is shown in Table 5.3.

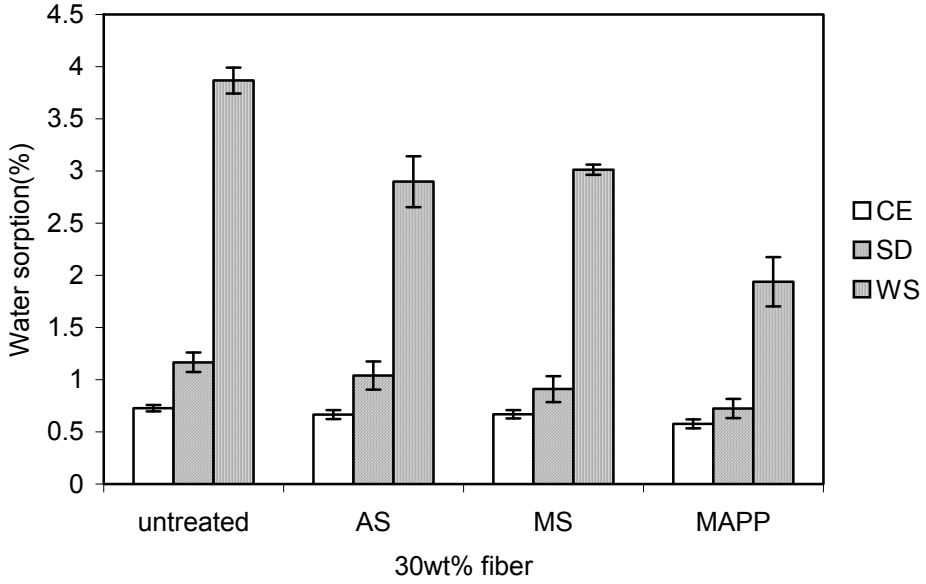

Figure 5.25. Effect of coupling agents and fiber type on water sorption of composites.

Table 5.3. % decrease in water sorption with changing coupling agent for CE, SD and WS loaded composites.

% decrease	AS	MS	MAPP
CE	8.5	7.8	20.5
SD	10.9	21.9	37.9
WS	25.1	22.1	49.8

From Table 5.3, it was observed that MAPP treatment exhibited the best performance in terms of decreasing water absorption of the composites. As mentioned before, all three coupling agents are capable of bonding to hydroxyl group of cellulose either by hydrogen or covalent bonds. Hydroxyl group reduction is accompanied by reduction in hydrophilicity. More hydrophobic nature yielded a decrease in water sorption of composites. Decrease in water sorption can be treated as an indicator of enhanced interfacial adhesion between fiber and matrix since tensile strength is in correlation with water sorption results, thus MAPP treatment caused higher tensile strength compared to silane treatment. Ichazo et al (2001) employed vinil-tris-2-metoxietoxi-silane and MAPP to PP/wood flour composites and they found that silane

and MAPP treatment have decreased water sorption 30 and 35% at 40% filler loading, respectively.

Comparison of water sorption results of three fiber types shows that WS is 3 and 5 times more capable of absorbing water compared to SD and CE, respectively. WS was also much more sensitive to coupling agents since enhancements in water sorption is much more pronounced compared to CE and WS. A possible cause of this observation could be greater porosity of WS fibers compared to CE and SD fibers. Fiber length is also greater in WS compared to SD. Void fraction experiments also showed that WS composites exhibited the highest void fraction. SD also have a higher void fraction than CE. Higher void fraction enables water molecules penetrate into the composite more easily. Coupling agents decreased void fraction which is a cause of restricted water penetration through matrix. Restriction of water penetration decreases water sorption of composites. This phenomenon can be treated as a dominating cause of decrease in water sorption with coupling agent employment which is also interconnected with adhesion phenomenon.

5.5. Density Measurements of Composites

Density measurements of composites, PP and MAPP were conducted with according to Equation 5.3 which is based on Archimedes principle. Theoretical densities of composites were calculated using densities of fibers measured by gas picnometer. Theoretical densities of composites were calculated employing Equation 5.3.

$$d_{theo} = \Sigma m_i / \Sigma (m_i/d_i) \quad (5.3)$$

where

d_{theo}= Theoretical density of composite

$m_{i=}$ Mass of component i in the composite

d_i= Density of component i in the composite.

Densities of fibers were listed in Experimental section previously. Densities of neat PP and MAPP were;

d_{PP}= 0.9022 g/cm^3

d_{MAPP}= 0.9011 g/cm^3

Void fractions (ε) of composites were determined by calculating the deviation in experimental density compared to theoretical density by using equation 5.4.

$$d_{exp} = (1 - \varepsilon)\, d_{theo} \qquad (5.4)$$

where d_{theo} is the theoretical density. Comparison of theoretical and experimental densities of PP/CE composites with changing fiber weight fraction is shown in Figure 5.26.

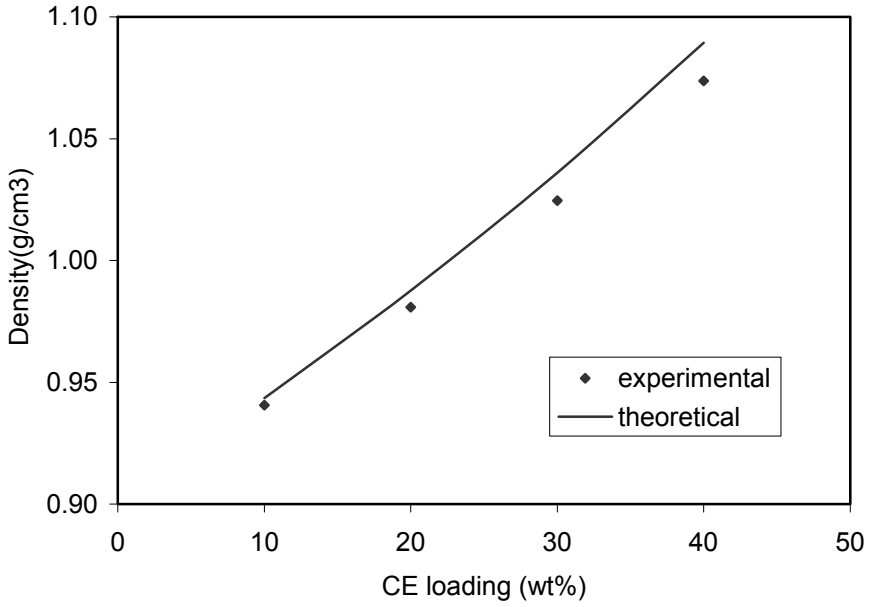

Figure 5.26. Experimental and theoretical densities of PP/CE composites with respect to CE loading.

Deviation of experimental density from theoretical density accounts for void fraction of composites. Deviation increases with increasing CE loading as a consequence of increase in void fraction. Figure 5.27 illustrates change in void fraction with changing CE loading. It was observed that void fraction increased from 0.3% to 1.4% with increasing CE loading from 10% to 40%. The increase is in a linear fashion. Linearity of void fraction suggests that mode of void formation is the same regardless of CE loading. Agglomeration of particles or dispersion incapability of the fiber in the matrix did not took place which would increase void formation tendency of composites. Void fractions of composites were directly proportional to water sorption

measurements. A greater void fraction with increasing fiber loading is accompanied with an increase in water sorption as mentioned in Chapter 3.

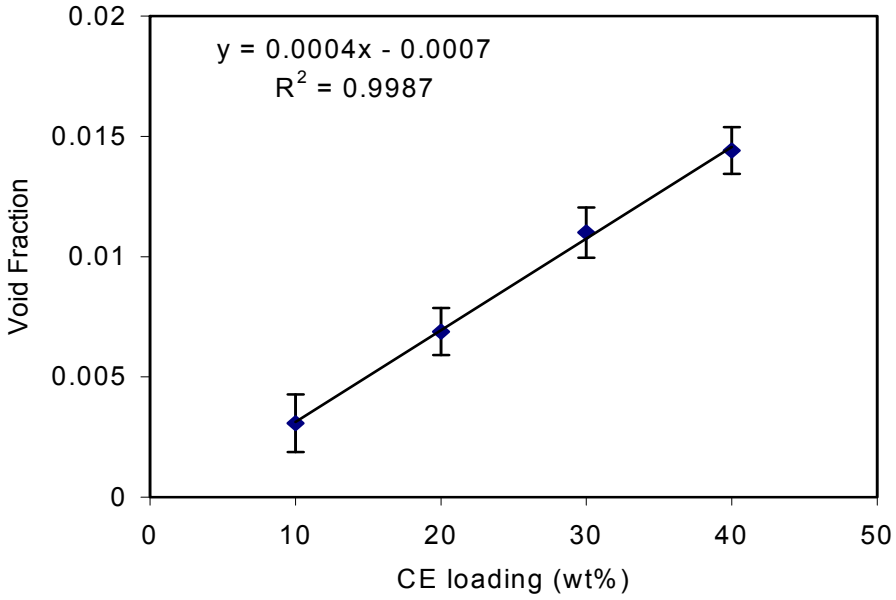

Figure 5.27. Effect of CE loading on void fraction of PP/CE composites.

Figure 5.28 shows effect of type of coupling agent and fiber type on void fraction of 30wt% loaded PP/fiber composites at optimum coupling agent concentration. It was observed that all three coupling agents decreased void fraction, MAPP established the highest void fraction decrease among three types of fibers. These results are consistent with mechanical tests and water sorption measurements. MAPP exhibited maximum tensile strength and minimum water sorption decline in all three types of PP/fiber composites due to better adhesion between fiber and matrix. WS exhibited the highest void fraction parallel to water sorption results. SEM observations also proved better adhesion and decreased void fraction via MAPP treatment.

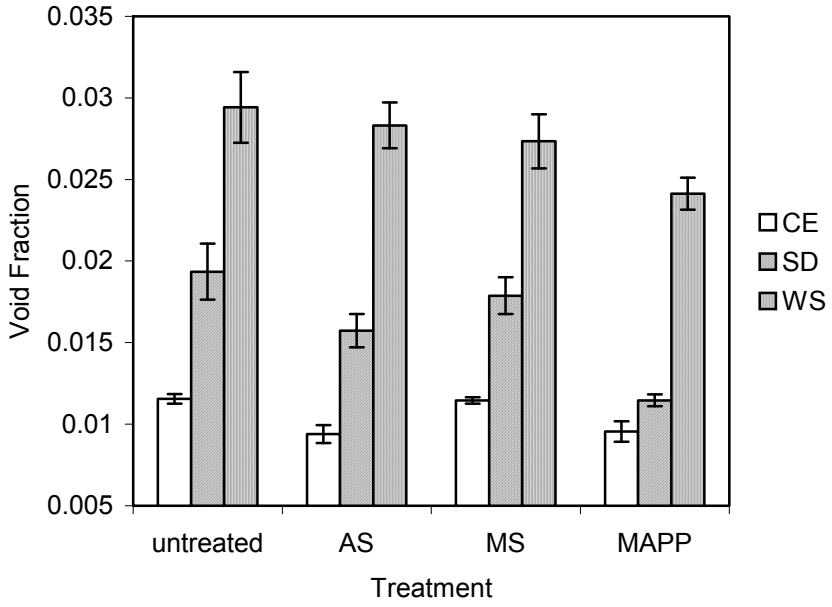

Figure 5.28. Effect of coupling agent and fiber type on void fraction of composites.

5.6. FTIR Analysis of Fibers and Composites

FTIR analysis was used in order to characterize chemical composition of fibers, PP and coupling agents. New bonds formed in the composites with the employment of coupling agents were also studied. Table 5.4 shows characteristic peaks associated in cellulose based compounds. Lignin and hemicellulose are other natural constituents of natural fibers. Figure 5.29 shows FTIR spectra of CE, SD and WS at two different wavenumber ranges.

As seen in Figure 5.29 and 5.30, there are additional peaks of WS and SD compared to CE. It has to be emphasized that CE is a synthetic compound and only contains cellulose whereas SD and WS are natural compounds and may contain constituents other than cellulose. The peak around 1734 cm^{-1} is specific to SD and WS and assigned to C=O stretching in hemicellulose. In addition, the peak specific to SD and WS at 1507 cm^{-1} is assigned to aromatic skeleton vibrations of lignin. The peaks observed for SD and WS at around 1460 cm^{-1} and 1420 cm^{-1} are assigned to CH deformation in lignin. These results prove that only constituent of CE is cellulose but WS and SD contains cellulose, lignin and hemicellulose in their chemical structure.

Table 5.4 Characteristic bands of natural fibers (Hinterstoisser and Salmen, 2000; Olssan and Salmen, 2004; Colom, 2003; Castellano, 2004; Pandey, 2003)

Wavenumber(cm^{-1})	Assignment
3100-3400	-OH hydrogen bonding stretching
2990	C-H stretching(cellulose)
1734	C=O stretching in xylans hemicellulose
1650	Free water
1505-1511	Aromatic skeleton in lignin
1462 and 1425	C-H deformation in lignin
1375	C-H deformation in cellulose
1335	-OH in plane bending (cellulose)
1158-1162	C-O-C vibrations (cellulose)
1122	C-O stretching(cellulose)
898	C-H deformation(cellulose)

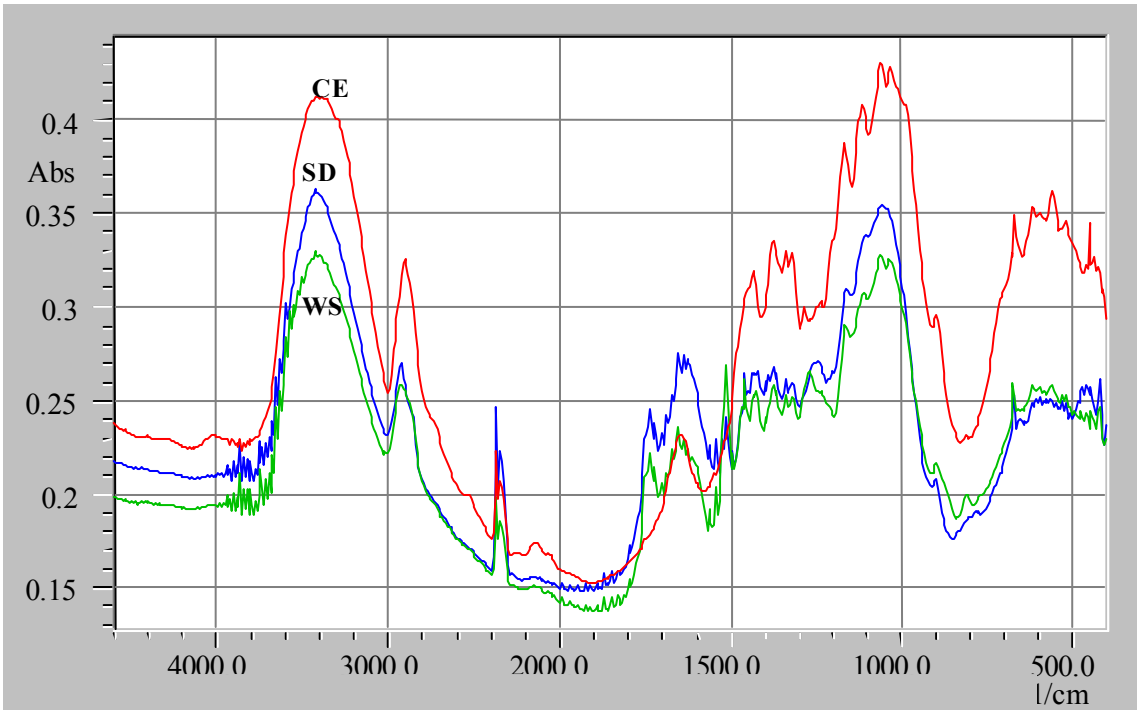

Figure 5.29. FTIR spectra of CE, SD and WS (400-4400 cm^{-1})

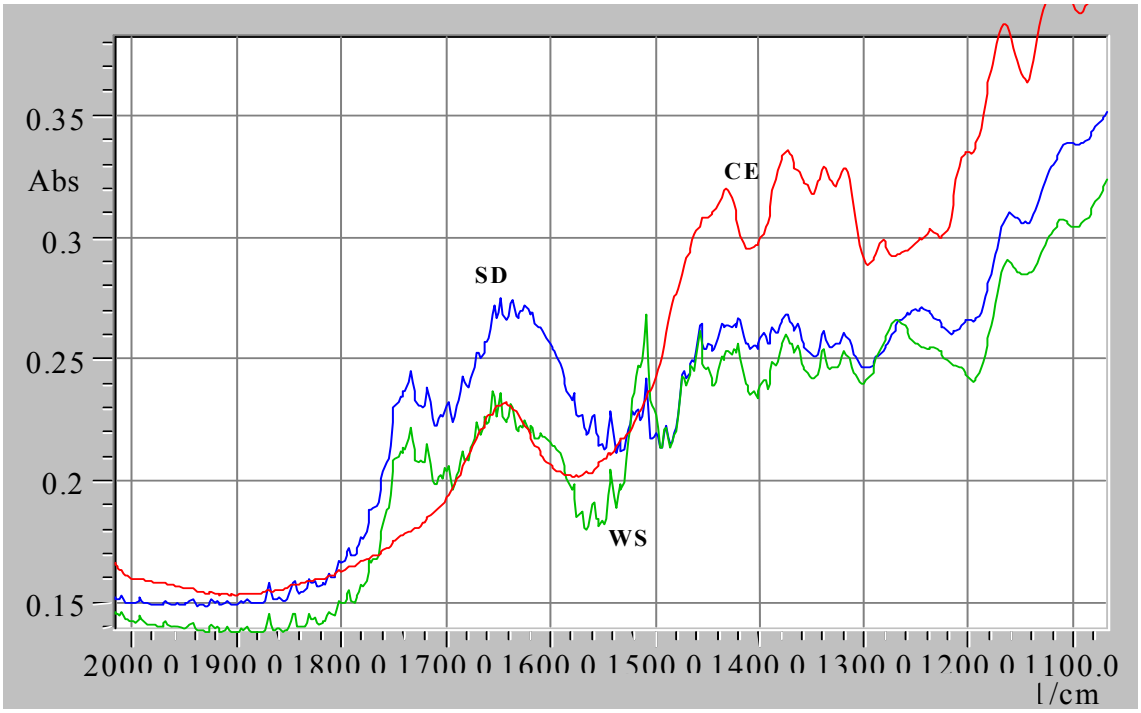

Figure 5.30. FTIR spectra of CE, SD and WS (1100-2000 cm^{-1})

In Figure 5.31, FTIR spectra of untreated, 1wt% AS and MS treated CE fibers were illustrated. The goal was to determine chemical changes occurred with employment of AS and MS. Chemical structures of AS and MS can be seen in Figure 4.2. Chemical structure as well as condensation reactions of silane coupling agents and bond formations between cellulose and coupling agents via surface treatment. was to be determined. Condensation reactions yields Si-O-Si linkage which have band at around 1135 cm^{-1}. Si-O-Cellulose has peak at 1200 cm^{-1}. In addition, Si-OCH_3 bonds has peaks around 1080-1100 cm^{-1}. Si-OH groups which are products of hydrolization reactions have peak at 1015 cm^{-1}. NH_2 group in AS has band around 1575 cm^{-1}(Castellano, 2004). FTIR specta of surface treated CE revealed none of these bands because amount of coupling agent is so low compared to fibers. Metin (2002) observed slight decreases in absorbtion band at 3400 cm^{-1} with silane treatment . The band at 3400 cm^{-1} is caused by OH vibrations and can be treated as a measure of hydrophilicity. The band at 2990 cm^{-1} belongs to C-H stretching of cellulose and do not change with silane treatment. Ratio of these two bands would be used to determine relative degree of hydrophilcity to depict effect of coupling agents on hydrophilicity.

Table 5.5. Variation of I_{3400}/I_{2990} with respect to silane coupling agents.

Treatment	I_{3400}/I_{2990}
Untreated CE	2.74
1wt% AS treated CE	2.17
1wt% MS treated CE	2.45

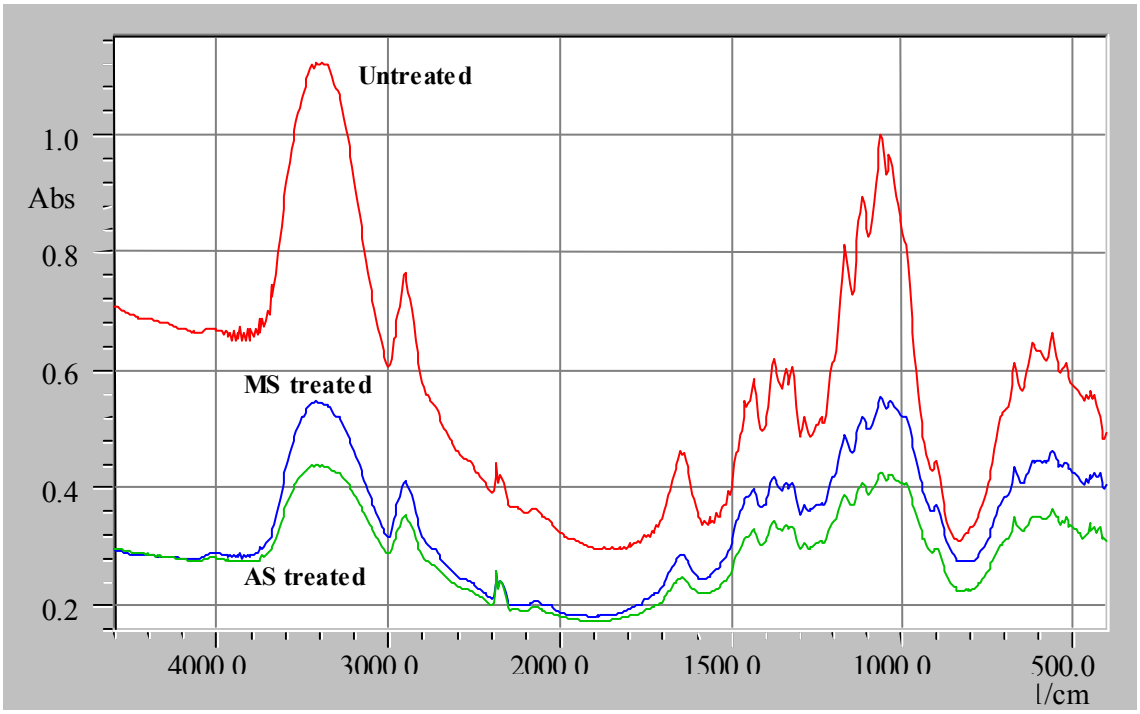

Figure 5.31. FTIR spectra of CE, untreated and treated with 1wt% AS and MS

As seen in Table 5.5 two, I_{3400}/I_{2990} decreases with employment of silane coupling agents. The decrease is much more pronounced for AS treated CE. These results reveal that AS and MS is capable of decreasing hydrophilicity of CE.

Table 5.6. Characteristic bands of polypropylene (Metin, 2002)

Wavenumber(cm^{-1})	Assignment
790, 1158	i-polypropylene
1131, 1199, 1230	s-polypropylene
995-997	t-polypropylene
2930	-CH_2 asymmetric stretching
2860	-CH_2 symmetric stretching
1470	-CH_2 deformation
2970	-CH_3 asymmetric stretching
2870	-CH_3 symmetric stretching
1460	-CH_3 asymmetric deformation
1375	-CH_3 symmetric deformation

FTIR spectra of composites with AS and MS treatments did not exhibit any changes because of the reasons mentioned above but MAPP treatment in PP/CE composites at 30wt% loadings, there were some new peaks associated with MAPP treatment due to stretching of carbonyl groups on MAPP, as seen in Fgures 5.32.and 33 (Bettini, 2000; Qiao, 2004; Qiu, 2004; Prachayawarakorn, 2003). The new bands observed are 1710 cm^{-1} characteristic of carbonyls from carboxylic dimer acid, 1785 and 1867 cm^{-1} characteristic of five-membered cyclic anhydride carbonyls (Bettini, 2000). Activation of carbonyl groups leads ester linkages between cellulose and maleic anhdride group of MAPP, thus chemical coupling of cellulose to PP is achieved.

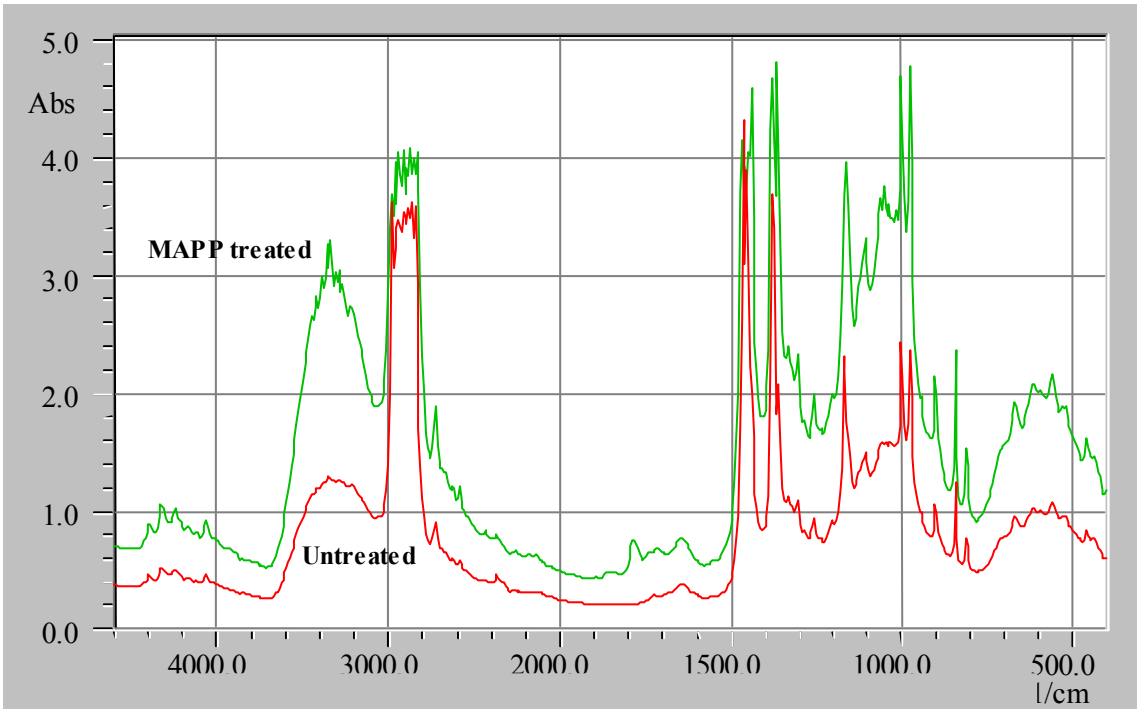

Figure 5.32. FTIR spectra of 30wt% PP/CE composites (a) untreated (b) treated with 10wt% MAPP (400-4400 cm^{-1})

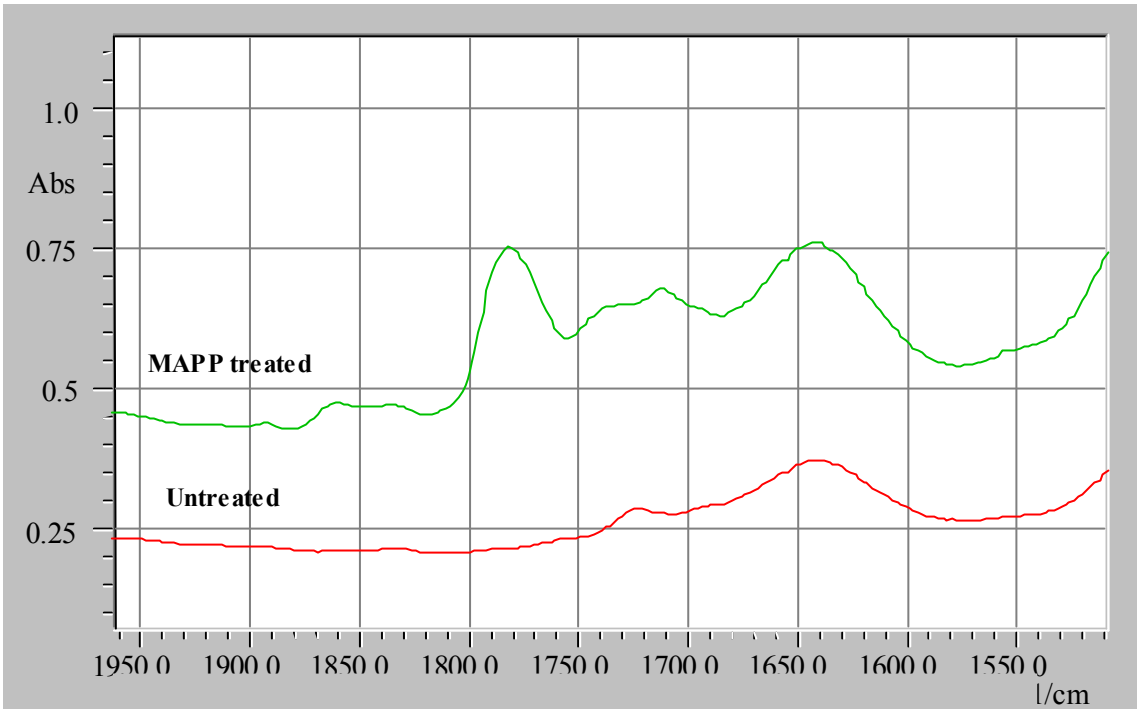

Figure 5.33. FTIR spectra of 30wt% PP/CE composites (a) untreated (b) treated with 10wt% MAPP (1500-1950 cm^{-1})

Chapter 6

CONCLUSIONS AND RECOMMENDATIONS

In this study, three natural fibers, namely cellulose (CE), sawdust (SD) and wheat straw (WS) were used as reinforcement for PP matrix. Three coupling agents, (3-aminopropyl)-triethoxysilane (AS), methacriloxy propyl trimethoxy silane (MS), and maleic anhydride grafted polypropylene (MAPP) were employed in order to enhance interfacial interactions between hydrophilic fiber and hydrophobic matrix. As a consequence, it was aimed to improve mechanical and water sorption properties of PP/fiber composites by enhancing interfacial interactions.

Torque data, which was a measure of rheological properties of composites, revealed that incorporation of fibers into PP increased stabilization torque of the composites. The extent of increase at 40wt% CE loading was about 11%. Silane treatments increased stabilization torque values up to 1 wt% silane treatment with respect to fiber weight, irrespective of the fiber employed due to increased interactions between fiber and matrix. MAPP treatment decreased stabilization torque due to plasticizing effect of MAPP.

Tensile tests were also conducted to investigate effect of fiber loading and type and coupling agents on tensile responses such as tensile strength, Young's Modulus, Strain at break and toughness. Tensile strength of the PP/fiber composites tends to decrease and Young's Modulus tends to increase with increasing fiber volume fraction. Comparison of three coupling agents proved that MAPP treatment exhibited the best performance in terms of tensile strength and Young's Modulus, especially for PP/SD composites. The increase in tensile strength with employment of MAPP was up to 50% for the PP/SD composites whereas AS and MS treatment provided at most 14.2% increase in tensile strength at 30wt% fiber loading. Pukanzsky and Nielsen models were used to evaluate interfacial interactions and adhesion between fiber and matrix. The improvement in adhesion between them with coupling agents was confirmed by these models. Young's Modulus increase in untreated composites was over 200% and MAPP treatment provided over 50% further increase in Young's Modulus. Optimum coupling agent concentration was found to be 1 wt% with respect to fiber and 5wt% MAPP with respect to PP for maximum mechanical properties. Strain at break and toughness of

composites declined drastically even at low fiber loadings. MAPP treatment give rise to decline in toughness due to enhanced interactions between fiber and matrix whereas silane treatment did not have a significant effect on toughness of PP/fiber composites. In the light of these measurements, interfacial interactions, thus stress transfer between fiber and matrix, were considerably improved via MAPP treatment. Silane treatments also had the same effect but to a lesser extend.

SEM studies confirmed mechanical test results, proving better adhesion with the employment of MAPP. Void and crack formations around the fibers were observed to decrease with MAPP treatment. Silane treatment did not provide an observable enhancement in adhesion between fiber and matrix.

Water sorption of the composites pointed out that water sorption of the composites increase in a linear fashion with increasing fiber loading. WS composites were capable of sorbing water 3-5 times more than SD and CE composites. Parallel to mechanical test results, MAPP performed superior performance in decreasing water sorption of composites. Up to 50% decrease in WS/PP composites was reported with employment of MAPP. AS and MS also exhibited decrease in water sorption due to decreased hydrophilicity of the fibers and enhanced interaction and void prevention via surface treatment of the fibers.

Density measurement results also confirmed water sorption and mechanical test results of the composites. Decreased void fraction with employment of coupling agents was observed in all fiber loaded composites. Parallel to water sorption tests, MAPP had decreased void fraction to a higher extend than silane treatments.

FTIR analysis put forward the decrease in hydrophilicity with silane treatment by comparing the band at 3400 cm^{-1}, which belongs to OH groups on cellulose, and The band at 2990 which is a characteristic peak of cellulose. The ratio of these two bands decreased from 2.74 to 2.17 for AS treatment and to 2.45 for MS treatment. FTIR results also showed that WS and SD contain hemicellulose and lignin other than cellulose whereas cellulose particulates were pure. New bands associated with carbonyl group on MAPP were determined when MAPP treated and untreated composites were compared. Consequently, mechanical test and water sorption results and scanning electron micrographs (SEM) of the PP/fiber composites indicated that PP composites containing SD trated with MAPP experienced maximum improved compatibility and interfacial adhesion between fiber and matrix.

All these results bring about the fact that SD treated with MAPP, which is a waste product would serve as a promising composite material to be used in the field of building material or outdoor applications because of its superior mechanical properties and limited water sorption. AS and MS treatment should further be studied to expose the high potential coupling efficiency. Parameters related to treatment condition such as mixing time, mixing temperature and curing of the fibers should be investigated since silanes were proven to have a good coupling efficiency for some cases in natural fiber reinforced thermoplastic composites.

Potential composite applications of other natural fibers abundant in Turkey should be investigated. Another need is a full characterization of the composites including flexural, impact, fatigue properties of composites. Weathering or fungal exposure can also be studied for the potential outdoor applications of natural fiber-thermoplastic composites.

REFERENCES

Albano C., Reyes J., Ichazo M., Gonzales J. Brito M., Moronta D., Analysis of the mechanical, thermal and morphological behaviour of polypropylene compounds with sisal fiber and wood floor, irradiated with gamma rays, *Polymer Degredation and Stability*, **76** (2002) 191-203

Amash A., Zugenmaier P., Morphology and properties of isotactic and oriented samples of cellulose fibre-polypropylene composites, *Polymer*, **41** (2000) 1589-1596

Asten A., Veenendaal N., Koster S., Surface characterization of industrial fibers with inverse gas chromatography, *Journal of Chromatography*, **888** (2000) 175-196

Battaille P., Ricard L., Sapieha S., Effect of cellulose fibers in polypropylene composites, *Polymer Composites*, **10** (1989) 103-108

Bettini S.H.P. and Agnelli J.A.M., Evaluation of methods used for analysing maleic anhydride grafted onto polypropylene by reactive processing, *Polymer Testing*, **19** (2000) 3-15

Bledzki A.K.and Gassan J., Composites reinforced with cellulose based fibres, *Progress in Polymer Science*, **24** (1999) 221-274

Castellano M., Gandini A., Fabbri P., Belgacem M.N., Modification of cellulose fibres with organosilanes: Under what conditions does coupling occur?, Journal of *Colloid and Interface science*, **273** (2004) 505-511

Cho K., Li F., Choi J., Crystallization and melting behavior of polypropylene and maleated polypropylene blends, *Polymer* **40** (1999) 1719-1729

Colom X., Carrasco F., Pages P., Canavate J., Effect of different treatments on the interface of HDPE/lignocellulosic fiber composites, *Composites Science and Technology*, **63** (2003) 161-169

Czvikovszky T., Hargitai H., Compatibilization of recycled polymers through radiation treatment, *Radiation Physics and Chemistry*, **55** (1999) 727-730

Denac M. And Musil V., The influence of thermoplastic elastomers on morphological, and mechanical properties of PP/talc composites, *Acta Chim. Slov*. **46** (1999) 55-67

Felix J.M., Gatenholm P., Schreiber H.P., Controlled interactions in cellulose-polymer composites, *Polymer Composites*, **14** (1993) No:6

Fernanda M., Coutinho B., Thasis H., Costa S., Carvalho L., Polypropylene-wood fiber composites: Effect of treatment and mixing conditions on mechanical properties, *John Wiley and Sons, Inc*, **21** (1997) 061227-09

Fernanda M.., Coutinho B., Thais H., Costa S., Performance of polypropylene-wood fiber composites, *Polymer Testing*, **18** (1999) 581-587

Gahleitner M., Melt Rheology of Polyolefins, *Prog. Polym. Sci*., **26** (2001) 895-944

Gassan J. and Bledzki A.K., Possibilities to improve the properties of natural fiber reinforced plastics by fiber modification –Jute polypropylene composites-, *Applied Composite Materials*, **7** (2000) 373-385

Gauthier R., Joly C., Coupas A.C., Gauthier H., Interfaces in polyolefin/cellulosic fiber composites: Chemical coupling, morphology, correlation with adhesion and aging in moisture, *Polymer Composites*, **19** (1998) 287-299

Gonzales A.V., Cervantes J.M., Olaya R., Franco P.J., Chemical modification of henequen fibers with organosilane coupling agent, *Composites Science and Technology*, **63** (2003) 861-869

Gurram S., Julson J.L., Muthukumarrapan K., Stokke D.D., Mahapatra A.K., Application of Biorenewable fibers in composites, 2002 ASEA/CSEA North Central Intersectional Conference.

Hinterstoisser B. and Salmen L., Application of dynamic 2D FTIR to cellulose, *Vibrational Spectroscopy*, **22** (2000) 111-118

Hornsby P.R., Rheology, compounding and processing of filled thermoplastics, in *Advances in Polymer Science*, Edited by J. Janjar (Springer, New York, 1999)

Hull D., Clyne T.W., *An Introduction to Composite Materials*, Cambridge University Press, Cambridge, 1996

Ichazo M.N., Albano C., Gonzales J., Perera R., Candal M.V., Polypropylene/wood flour composites: Treatment and properties, *Composite Structures*, **54** (2001) 207-214

Jancar J., Structure-Property relationships in thermoplastic matrices, in *Advances in Polymer Science*, Edited by J. Janjar (Springer, New York, 1999)

Jang B.Z., *Advenced Polymer Composites*, ASM International, United States of America, 1994, pp1-6

Joseph P.V., Koseph K., Thomas S., Effect of processing variables on the mechanical properties of sisal-fiber-reinforced polypropylene composites, *Composite Science and Technology*, **59** (1999) 1625-1640

Joseph P.V., Mathev G., Joseph K. ,Groeninckx G., Thomas S., Dynamic mechanical properties of short sisal fibre reinforced polypropylene composites, *Composites: Part A*, **34** (2003) 000-000

Karnani R, Krisnan M., Narayan R., Biofiber-reinforced polypropylene composites, *Polymer Engineering and Science*, **37** (1997) No:2

Keener T.J., Stuart R.K., Brown T.K., Maleated coupling agents for natural fiber composites, *Composites:Part A*, xx (2003) xxx-xxx

Manchado M.A., and Arroya M., Thermal and dynamic mechanical properties of polypropylene and short organic fiber composites, *Polymer* **41** (2000) 7761-7767

Metin D., Interfacial enhancement of polypropylene zeolite composites, M. Sc. Thesis, İzmir Institute of Technology, Chemical Eng Dept., İzmir, 2002

Michell A.J., Future prospects for wood cellulose as reinforcement in organic polymer composites, *Polymer Composites*, **10** (1989) 69-77

Mwaikambo L.Y., Martuscelli E., Avella M., Kapok/cotton fabric-polypropylene composites*, Polymer Testing*, **19** (2000) 905-918

Olssan A. and Salmen L., The association of water to cellulose and hemicellulose in paper examined by FTIR spectroscopy, Carbohydrate research, **339** (2004) 813-818

Pandey K.K. and Pitman A.J., FTIR studies of the changes in wood chemistry following decay by brown-rot and white-rot fungi, *International Biodetoriation and Biodegradation*, **52** (2003) 151-160

Park B. and Belatincz J.J., Short term flexural creep behavior of wood-fiber/polypropylene composites, *Polymer Composites,* **19** (1998) 377-382

Pickering K.L., Abdalla A., Ji C., McDonald A.G., Franich R.A., The effect of silane coupling agents on radiata pine fibre for use in thermoplastic matrix composites, *Composites: Part A*, **34** (2003) 915-926

Plueddemann E.P., Silane Coupling Agents, Plenum Press, New York, (1982)

Prachayawarakorn J. and Anggulalat K., Influence of Meranti sawdust aspect ratios and amount of loadings on mechanical and morphological properties of composites from polypropylene and Meranti sawdust, *Sonklanakarin Journal of Science and Technology*, **25** (2003) 595-606

Pukanszky B., Fekete E., Adhesion and surface modification, in *Advances in Polymer Science*, Edited by J. Janjar (Springer, New York, 1999)

Qiao W., Zhang Y., Zhang Y., Maleic anhydride grafted polypropylene as a coupling agent for polypropylene composites filled with ink-eliminated waste paper sludge flour, *Journal of Applied Polymer Science*, **91** (2004) 2320-2325

Qiu W., Zhang F., Endo T., Hirotsu T., Milling-induced esterification between cellulose and maleated polypropylene, *Journal of Applied Polymer Science*, **91** (2004) 1703-1709

Raj R.G., Kokta B.V., Daneult C., Polypropylene-wood fiber composites: Effect of fiber treatment on mechanical properties, *Journal of Polymeric Materials*, **12** (1989) 239-250

Rana A.K., Mandal A., Bandyopadhyay S., Short jute fiber reinforced polypropylene composites: Effect of compatibilizers, impact modifier and fiber loading, *Composites Science and Technology*, xx (2002) xxx-xxx

Rothon R.N., Mineral fillers in thermoplastics: Filler manufacture and characterization, in *Advances in Polymer Science*, Edited by J. Janjar (Springer, New York, 1999)

Rowel R.M., Caulfield D.F., Chen G., Recent advances in agro-fiber/thermoplastic composites, *Second International Symposium on Natural Polymers and Composites*, ISNaPol-98

Sae-Oui P., Thepsuwan U., Hatthapanit K., Effect of curing system on reinforcing efficiency of silane coupling agent, *Polymer Testing*, xx (2003) xxx-xxx

Sanadi A.R., Feng D., Caulfield D.F., Highly filled lignocellulosic reinforced thermoplasitcs, *18th International Symposium on Materials Science*,Denmark, 1997

Santos J., Gil M.H., Portugal A., Guthrie J.T., Characterization of the surface of a cellulosic multi-purpose office paper by inverse gas chromatography, *Cellulose*, **8** (2001) 217-224

Selke S.E., Wichman I., Wood fiber/polyolefin composites, *Composites:Part A*, xx (2003) xxx-xxx

SpecialChem, Additive developments aid growth in wood-plastic composites, ww.specialchem4polymers.com, 2002

Suarez J.C.M., Coutinho M.B., Sydenstricker T.H, SEM studies studies of tensile fracture surfaces of polypropylene-sawdust composites, *Polymer Testing*, **22** (2003) 819-824

Takase S. and Shiarishi N., Studies on composites from wood and polypropylene, *Journal of Applied Polymer Science*, **37** (1989) 645-659

Tjong S.C., Xu Y., Meng Y.Z., Composites based on maleated polypropylene and methyl cellulosic fiber: Mechanival and thermal properties, *Journal of Applied Polymer Science*, **72** (1999) 1647-1653

Tshabalala M.A., Determination of the acid-basecharacteristics of lignocellulosic surfaces by inverse gas chromatography, *Jourrnal of Applied Polymer Science*, **65** (1997) 1013-1020

Valadez A., Uc J.M., Olayo R., Franco P.J., Effect of fiber surface treatment on the fiber-matrix bond strength of natural fiber reinforced composites, *Composites: Part B*, **30** (1999) 309-320

Wambua P., Ivenis J., Verpoest I., Natural fibres:can they replace glass reinforced plastics?, *Composites Science and Technology*, **63** (2003) 1259-1264

Wielage B., Lampke T., Uschick H., Soergel F., Processing of natural-fiber reinforced polymers and the resulting dynamic-mechanical properties, *Journal of Materials Processing Technology*, **139** (2003) 140-146

Zafeiropoulos N.E., Baillie C.A., Hodqkinson J.M., Engineering and characterization of interface in flax fiber/polypropylene composite materials, *Composites:Part A*, **33** (2002) 1185-1190

APPENDICES

APPENDIX A

Mechanical Properties of CE/PP Composites

Treatment	wt % (fiber)	Stress @ Peak (N/mm²)	Strain @ Peak (%)	Energy to Break (N.m)	Stress @ Break (N/mm²)	Strain @ Break (%)	Youngs Modulus (N/mm²)
Untreated	10	28.486	6.24	0.437	27.04	10.24	1816.90
		27.683	5.72	0.361	26.50	8.56	1926.19
		26.941	4.96	0.264	26.23	6.44	2161.80
		27.351	5.4	0.298	25.95	7.88	2015.87
		27.603	5.4	0.248	27.08	6.2	2034.44
	ave.	27.61	5.54	0.32	26.56	7.86	1991.04
	st.dev	0.57	0.47	0.08	0.50	1.65	128.64
	20	23.147	3.52	0.18	22.03	4.88	2617.19
		23.717	3.44	0.195	19.50	5.88	2744.00
		23.443	3.76	0.249	22.12	6.72	2481.47
		23.527	3.52	0.143	23.22	4.12	2660.16
		23.255	3.32	0.223	21.81	5.92	2787.80
	ave.	23.42	3.51	0.20	21.74	5.50	2658.12
	st.dev	0.22	0.16	0.04	1.36	1.01	119.46
	30	22.701	2.72	0.105	22.29	3.04	3321.69
		21.464	2.56	0.083	21.28	2.91	3336.98
		19.58	2.8	0.076	19.05	5.2	2783.16
		20.84	2.77	0.109	19.41	4.01	2994.34
		18.671	2.68	0.125	17.76	4.32	2772.78
	ave.	20.65	2.71	0.10	19.96	3.90	3041.79
	st.dev	1.58	0.09	0.02	1.81	0.95	277.03
	40	18.035	1.91	0.071	17.63	2.36	3758.08
		19.809	2.2	0.093	19.04	3	3583.63
		17.532	1.81	0.044	17.42	2	3855.10
		19.186	1.8	0.043	19.19	1.8	4242.24
		19.014	1.84	0.07	18.29	2.44	4112.81
	ave.	18.72	1.91	0.06	18.31	2.32	3910.37
	st.dev	0.92	0.17	0.02	0.80	0.46	266.52
AS 1%	30	20.646	2.32	0.082	20.39	2.96	3541.86
		23.363	2.48	0.135	20.64	3.84	3749.38
		23.889	2.96	0.113	23.64	3.4	3212.10
		23.239	3	0.211	21.78	5.24	3083.04
		21.16	3.24	0.181	19.92	5.28	2599.28
	ave.	22.46	2.80	0.14	21.27	4.14	3237.13
	st.dev	1.45	0.38	0.05	1.49	1.07	443.42
MS 1%	30	23.529	3.16	0.144	22.97	4.12	2963.46
		21.826	2.92	0.164	20.64	4.68	2974.91
		23.631	3.16	0.193	22.15	5.08	2976.31
		20.576	2.6	0.115	20.07	3.68	3149.71
		22.295	2.36	0.087	21.62	2.72	3759.92
	ave.	22.37	2.84	0.14	21.49	4.06	3164.86
	st.dev	1.27	0.35	0.04	1.16	0.92	341.51
MAPP 5%	30	26.818	2.32	0.108	26.32	2.72	4600.67
		27.986	2.6	0.098	27.97	2.88	4284.01
		29.558	2.28	0.065	29.56	2.67	5159.69
		26.167	2.16	0.087	26.08	2.56	4821.51
		26.544	2.1	0.071	26.54	2.1	5030.72
	ave.	27.41	2.29	0.09	27.30	2.59	4779.32
	st.dev	1.38	0.19	0.02	1.46	0.30	348.89

Treatment	wt % (fiber)	Stress @ Peak (N/mm²)	Strain @ Peak (%)	Energy to Break (N.m)	Stress @ Break (N/mm²)	Strain @ Break (%)	Youngs Modulus (N/mm²)
AS 0.5%	30	21.122	2.56	0.111	20.05	3.66	3283.81
		20.65	2.89	0.154	19.84	4.14	2843.84
		21.545	2.36	0.105	19.65	3.76	3633.44
		19.98	2.47	0.107	18.24	3.57	3219.45
		22.264	2.5	0.16	20.43	5.01	3544.43
	ave.	21.11	2.56	0.13	19.64	4.03	3304.99
	st.dev	0.87	0.20	0.03	0.84	0.59	310.50
AS 2.5%	30	20.41	2.21	0.106	19.84	2.99	3675.65
		21	2.83	0.135	20.01	3.97	2953.36
		21.75	2.65	0.148	20.91	4.36	3266.60
		19.51	2.56	0.135	18.56	4.51	3033.20
		20.64	2.29	0.114	19.83	3.81	3587.21
	ave.	20.66	2.51	0.13	19.83	3.93	3303.20
	st.dev	0.82	0.26	0.02	0.84	0.60	322.50
MS 0.5%	30	20.11	2.36	0.112	19.75	3.01	3391.43
		21.12	2.54	0.098	20.65	2.89	3309.35
		20.65	2.83	0.137	20.17	3.24	2904.13
		22.04	2.51	0.144	21.02	3.98	3494.79
		19.91	2.88	0.161	19.07	4.47	2751.45
	ave.	20.77	2.62	0.13	20.13	3.52	3170.23
	st.dev	0.86	0.22	0.03	0.76	0.68	323.96
MS 2.5%	30	20.47	2.24	0.108	20.01	2.65	3637.08
		21.68	2.41	0.117	21.31	2.98	3580.35
		19.562	2.91	0.147	18.97	3.43	2675.49
		20.11	2.21	0.088	19.76	2.94	3621.62
		21.127	2.66	0.12	21	3.42	3161.11
	ave.	20.59	2.49	0.12	20.21	3.08	3335.13
	st.dev	0.83	0.30	0.02	0.95	0.34	417.97
AS 1%	10	26.897	5.72	0.352	25.92	8.68	1871.50
		28.622	5.44	0.762	26.395	15.36	2094.04
		26.951	5.88	0.466	25.78	10.48	1824.23
		28.45	6.12	0.477	26.688	11.52	1850.18
		28.8	5.88	0.422	27.643	9.76	1949.39
	ave.	27.94	5.81	0.50	26.49	11.16	1917.87
	st.dev	0.94	0.25	0.16	0.74	2.57	109.00
	20	25.614	4.08	0.204	25.1	5.4	2498.62
		24.502	4.64	0.364	22.954	9.08	2101.68
		24.83	4.08	0.293	23.457	7.72	2422.14
		24.462	3.92	0.311	22.72	8.2	2483.64
		24.788	3.66	0.151	24.136	4.04	2695.53
	ave.	24.84	4.08	0.26	23.67	6.89	2440.32
	st.dev	0.46	0.36	0.09	0.96	2.09	215.30
	30	20.646	2.32	0.082	20.39	2.96	3541.86
		23.363	2.48	0.135	20.64	3.84	3749.38
		23.889	2.96	0.113	23.64	3.4	3212.10
		23.239	3	0.211	21.78	5.24	3083.04
		21.16	3.24	0.181	19.92	5.28	2599.28
	ave.	22.46	2.80	0.14	21.27	4.14	3237.13
	st.dev	1.45	0.38	0.05	1.49	1.07	443.42
	40	20.1	1.88	0.057	19.833	1.92	4255.21
		19.943	1.84	0.073	18.4	2.6	4313.76
		18.804	1.82	0.069	18.38	2.56	4112.08
		18.047	2.04	0.111	17.38	3.88	3520.93
		17.673	1.91	0.073	16.473	2.6	3682.65
	ave.	18.91	1.90	0.08	18.09	2.71	3976.93
	st.dev	1.09	0.09	0.02	1.26	0.71	354.86

Treatment	wt % (fiber)	Stress @ Peak (N/mm²)	Strain @ Peak (%)	Energy to Break (N.m)	Stress @ Break (N/mm²)	Strain @ Break (%)	Youngs Modulus (N/mm²)
MS 1%		27.593	5.76	0.412	25.963	10.48	1906.60
		28.348	6	0.598	24.883	15.28	1880.42
	10	27.655	6.64	0.656	25.007	16.04	1657.63
		26.314	6.28	0.546	24.919	14.32	1667.67
		28.491	6.6	0.504	27.153	12.24	1718.09
	ave.	27.68	6.26	0.54	25.59	13.67	1766.08
	st.dev	0.86	0.38	0.09	0.98	2.28	118.92
		24.034	4.12	0.189	22.917	5.88	2321.73
		22.932	3	0.119	22.223	3.76	3042.31
	20	24.063	4.52	0.221	22.92	6.88	2118.82
		23.378	3.6	0.153	22.72	4.72	2584.57
		23.482	4.08	0.245	22.376	7.32	2290.65
	ave.	23.58	3.86	0.19	22.63	5.71	2471.62
	st.dev	0.48	0.58	0.05	0.32	1.48	359.91
		23.529	3.16	0.144	22.97	4.12	2963.46
		21.826	2.92	0.164	20.64	4.68	2974.91
	30	23.631	3.16	0.193	22.15	5.08	2976.31
		20.576	2.6	0.115	20.07	3.68	3149.71
		22.295	2.36	0.087	21.62	2.72	3759.92
	ave.	22.37	2.84	0.14	21.49	4.06	3164.86
	st.dev	1.27	0.35	0.04	1.16	0.92	341.51
		18.017	2.26	0.078	17.942	2.96	3172.91
		17.906	2.12	0.091	17.441	3.25	3361.60
	40	19.42	2.48	0.098	18.659	3.19	3116.60
		18.731	2.06	0.1	18.118	2.79	3618.90
		18.32	2.14	0.107	17.25	3.11	3407.18
	ave.	18.48	2.21	0.09	17.88	3.06	3335.44
	st.dev	0.62	0.17	0.01	0.56	0.19	200.31
MAPP 5%		26.642	6.48	0.513	25.268	12.92	1636.35
		26.065	6.04	0.478	24.64	11.68	1717.53
	10	25.97	6.48	0.467	24.563	12.12	1595.07
		25.985	6.28	0.618	24.193	15.52	1646.82
		27.666	6.32	0.402	25.584	10.2	1742.26
	ave.	26.47	6.32	0.50	24.85	12.49	1667.60
	st.dev	0.73	0.18	0.08	0.56	1.96	60.70
		24.822	4.36	0.391	22.445	10.56	2265.86
		25.109	3.56	0.194	23.921	5.44	2807.13
	20	26.167	3.6	0.275	24.509	6.8	2892.91
		24.407	4.52	0.233	23.316	6.56	2149.11
		24.98	4	0.247	23.87	6.4	2485.51
	ave.	25.10	4.01	0.27	23.61	7.15	2520.10
	st.dev	0.65	0.43	0.07	0.78	1.97	325.90
		26.818	2.32	0.108	26.32	2.72	4600.67
		27.986	2.6	0.098	27.97	2.88	4284.01
	30	29.558	2.28	0.065	29.56	2.67	5159.69
		26.167	2.16	0.087	26.08	2.56	4821.51
		26.544	2.1	0.071	26.54	2.1	5030.72
	ave.	27.41	2.29	0.09	27.30	2.59	4779.32
	st.dev	1.38	0.19	0.02	1.46	0.30	348.89
		27.738	1.82	0.061	27.738	1.82	5334.23
		27.926	1.91	0.071	27.926	1.91	5117.33
	40	26.985	1.71	0.057	26.985	1.71	5523.25
		27.327	1.89	0.066	27.327	1.89	5060.56
		26.785	1.8	0.064	26.785	1.8	5208.19
	ave.	27.35	1.83	0.06	27.35	1.83	5248.71
	st.dev	0.48	0.08	0.01	0.48	0.08	185.06

APPENDIX B

Mechanical Properties of SD/PP Composites

Treatment	wt % (fiber)	Stress @ Peak (N/mm²)	Strain @ Peak (%)	Energy to Break (N.m)	Stress @ Break (N/mm²)	Strain @ Break (%)	Youngs Modulus (N/mm²)
Untreated		27.857	5.4	0.303	27.3	7.2	2053.16
		27.845	5.8	0.391	26.945	8.84	1910.74
	10	26.472	6.32	0.429	25.652	9.72	1667.07
		27.143	5.96	0.395	26.243	9.64	1812.57
		25.173	5.24	0.26	24.867	6.76	1912.00
	ave.	26.90	5.74	0.36	26.20	8.43	1871.11
	st.dev.	1.12	0.43	0.07	0.98	1.38	142.69
		25.048	5.04	0.24	24.481	6.56	1978.00
		24.676	4.68	0.269	24.014	7.08	2098.51
	20	25.297	3.96	0.213	23.572	5.48	2542.48
		23.443	4.4	0.19	23.207	5.44	2120.53
		23.533	5.32	0.29	22.333	7.76	1760.55
		23.586	4.88	0.197	23.366	5.68	1923.61
	ave.	24.26	4.71	0.23	23.50	6.33	2070.61
	st.dev.	0.84	0.48	0.04	0.73	0.96	265.42
		21.305	3.8	0.149	20.842	4.8	2231.42
		20.618	3.64	0.146	20.253	4.68	2254.39
	30	20.786	3.32	0.159	20.056	4.68	2491.82
		21.095	3.28	0.13	20.8	3.92	2559.70
		21.42	2.96	0.12	21.189	3.64	2880.12
	ave.	21.04	3.40	0.14	20.63	4.34	2483.49
	st.dev.	0.34	0.33	0.02	0.46	0.53	264.21
		19.048	3.16	0.106	18.984	3.56	2399.08
		18.086	2.64	0.105	17.754	3.2	2726.60
	40	18.31	3	0.127	18.026	4.2	2429.13
		18.762	2.64	0.093	18.325	3.36	2828.51
	ave.	18.55	2.86	0.11	18.27	3.58	2595.83
	st.dev.	0.43	0.26	0.01	0.53	0.44	214.28
AS 1%		23.323	3.16	0.151	22.631	4.4	2937.52
		24.43	3.96	0.21	23.821	5	2455.34
	30	22.473	3.6	0.167	22.241	4.48	2484.52
		21.867	3.36	0.131	21.659	3.84	2590.20
		22.984	3.76	0.191	22.4	4.92	2432.88
	ave.	23.02	3.57	0.17	22.55	4.53	2580.09
	st.dev.	0.96	0.32	0.03	0.80	0.47	208.70
MS 1%		23.851	3.44	0.136	23.764	3.68	2759.51
		21.445	3.52	0.139	21.19	4.36	2424.75
	30	22.834	3.4	0.155	22.772	4.08	2672.92
		21.754	2.96	0.169	21.2	6	2925.03
		22.157	3.68	0.176	21.606	5	2396.33
		21.821	3.04	0.11	21.559	3.44	2856.83
	ave.	22.31	3.34	0.15	22.02	4.43	2672.56
	st.dev.	0.89	0.28	0.02	1.03	0.94	220.44
MAPP 5%		32.161	2.92	0.132	32.161	2.92	4383.59
		30.355	2.52	0.089	30.355	2.52	4794.16
	30	31.36	2.84	0.106	31.28	3.04	4394.82
		32.07	2.68	0.116	32.07	2.68	4762.63
		32.496	2.92	0.112	32.496	2.92	4429.25
		31.419	3.12	0.124	31.419	3.12	4007.94
	ave.	31.64	2.83	0.11	31.63	2.87	4462.06
	st.dev.	0.77	0.21	0.01	0.78	0.23	289.35

Treatment	wt % (fiber)	Stress @ Peak (N/mm²)	Strain @ Peak (%)	Energy to Break (N.m)	Stress @ Break (N/mm²)	Strain @ Break (%)	Youngs Modulus (N/mm²)
AS 0.5%	30	22.175	3.21	0.16	21.911	4.7	2749.42
		21.617	3.44	0.147	20.055	4.81	2501.04
		20.22	3.66	0.121	19.51	4.41	2198.79
		20.711	2.99	0.132	19.9	4.01	2756.85
		22.851	3.74	0.2	20.87	5.66	2431.74
	ave.	21.51	3.41	0.15	20.45	4.72	2527.57
	st.dev.	1.07	0.31	0.03	0.96	0.61	234.40
AS 2.5%	30	20.17	3.05	0.155	19.51	4.17	2632.02
		21.105	3.56	0.165	20.56	5.02	2359.49
		19.621	4.01	0.198	18.56	6.2	1947.42
		19.31	2.99	0.124	18.98	3.56	2570.36
		22.032	3.66	0.131	21.36	4.21	2395.83
	ave.	20.45	3.45	0.15	19.79	4.63	2381.02
	st.dev.	1.12	0.43	0.03	1.15	1.02	268.11
MS 0.5%	30	22.01	3.56	0.161	21.56	4.01	2460.67
		21.12	3.21	0.14	20.71	3.88	2618.62
		21.55	2.98	0.17	21.32	3.56	2878.15
		21.11	3.92	0.164	20.82	5.14	2143.31
		20.42	2.77	0.142	20.01	4.1	2933.99
	ave.	21.24	3.29	0.16	20.88	4.14	2606.95
	st.dev.	0.59	0.46	0.01	0.60	0.60	322.88
MS 2.5%	30	20.65	2.91	0.15	20.25	3.55	2824.30
		21.04	3.54	0.169	20.81	4.7	2365.51
		19.86	3.24	0.13	19.46	4.21	2439.59
		19.77	3.28	0.171	19.51	5.01	2398.92
		21.34	3.71	0.181	20.94	6.07	2289.30
	ave.	20.53	3.34	0.16	20.19	4.71	2463.53
	st.dev.	0.70	0.31	0.02	0.70	0.94	209.08
MAPP 2.5%	30	30.253	2.92	0.105	30.253	2.92	4123.53
		33.908	3.24	0.128	33.908	3.24	4165.24
		29.651	3.02	0.109	29.651	3.02	3907.65
		30.545	3.12	0.112	30.545	3.12	3896.45
		29.36	2.99	0.105	29.36	2.99	3908.12
	ave.	30.74	3.06	0.11	30.74	3.06	4000.20
	st.dev.	1.83	0.12	0.01	1.83	0.12	132.53
MAPP 10%	30	28.813	1.96	0.081	28.813	1.96	4311.12
		28.253	2.08	0.084	28.253	2.08	4195.78
		27.16	2.32	0.09	27.16	2.32	4659.34
		28.442	1.72	0.075	28.442	1.72	5099.06
		29.941	2.84	0.113	29.941	2.84	4195.96
	ave.	28.52	2.18	0.09	28.52	2.18	4492.25
	st.dev.	1.00	0.43	0.01	1.00	0.43	388.79

APPENDIX C

Mechanical Properties of WS/PP Composites

Treatment	wt % (fiber)	Stress @ Peak (N/mm²)	Strain @ Peak (%)	Energy to Break (N.m)	Stress @ Break (N/mm²)	Strain @ Break (%)	Youngs Modulus (N/mm²)
Untreated	10	28.431	6	0.297	28.138	7.68	1885.92
		26.633	5.44	0.319	25.455	8.24	1948.52
		25.434	5.84	0.216	25.338	6.04	1733.34
		27.097	5.8	0.221	27.009	6.08	1859.41
		26.11	6.04	0.358	25.379	8.92	1720.49
	ave.	26.74	5.82	0.28	26.26	7.39	1829.54
	st.dev.	1.13	0.24	0.06	1.26	1.29	99.21
	20	22.104	3.52	0.118	21.889	3.76	2499.26
		20.8	3.36	0.143	20.452	4.36	2463.81
		21.766	4.16	0.148	21.49	4.8	2082.42
		19.882	4.28	0.181	19.506	6.04	1848.84
		22.136	3.26	0.103	22.122	3.51	2702.49
	ave.	21.34	3.72	0.14	21.09	4.49	2319.36
	st.dev.	0.98	0.47	0.03	1.09	1.00	345.52
	30	18.04	3.04	0.081	17.92	3.28	2361.95
		18.065	3.04	0.11	17.723	4.04	2365.09
		16.933	3.24	0.082	16.933	3.48	2080.04
		17.855	3.32	0.098	17.671	3.92	2140.45
		16.654	2.64	0.068	16.292	2.92	2510.72
	ave.	17.51	3.06	0.09	17.31	3.53	2291.65
	st.dev.	0.67	0.26	0.02	0.68	0.46	177.46
	40	18.57	2.80	0.114	17.78	3.84	2639.31
		17.507	2.12	0.052	17.507	2.12	3286.69
		18.48	2.28	0.102	17.96	3.28	3225.89
		16.529	2.04	0.055	16.529	2.04	3224.78
		18.361	2.84	0.083	18.142	3.04	2573.13
	ave.	17.89	2.42	0.08	17.58	2.86	2989.96
	st.dev.	0.87	0.38	0.03	0.63	0.77	351.98
AS 1%	30	19.455	2.92	0.103	19.052	3.48	2651.74
		19.422	2.76	0.083	19.003	3.36	2800.71
		18.898	2.84	0.094	18.82	3.16	2648.38
		19.457	3.56	0.122	19.143	4.44	2175.25
		19.286	2.88	0.093	19.171	3.36	2665.22
	ave.	19.30	2.99	0.10	19.04	3.56	2588.26
	st.dev.	0.24	0.32	0.01	0.14	0.51	239.42
MS 1%	30	19.61	2.44	0.086	19.306	2.76	3198.68
		21.114	2.72	0.076	21.114	2.72	3089.48
		19.614	2.68	0.078	19.172	2.96	2912.83
		19.402	2.55	0.068	19.402	2.74	3028.23
		18.021	1.96	0.048	18.021	1.96	3659.37
	ave.	19.55	2.47	0.07	19.40	2.63	3177.72
	st.dev.	1.10	0.31	0.01	1.11	0.39	288.41
MAPP 5%	30	27.793	2.28	0.077	27.793	2.28	4851.59
		25.175	1.88	0.053	25.175	1.88	5329.60
		25.862	1.8	0.058	25.862	1.8	5718.38
		25.793	1.82	0.048	25.793	1.82	5640.45
	ave.	26.16	1.95	0.06	26.16	1.95	5385.00
	st.dev.	1.13	0.23	0.01	1.13	0.23	393.27

Treatment	wt % (fiber)	Stress @ Peak (N/mm²)	Strain @ Peak (%)	Energy to Break (N.m)	Stress @ Break (N/mm²)	Strain @ Break (%)	Youngs Modulus (N/mm²)
AS 0.5%	30	19.536	3.08	0.11	19.348	3.52	2524.46
		18.634	2.64	0.099	18.234	3.4	2809.22
		20.762	2.77	0.111	20.66	3.2	2983.13
		20.32	2.8	0.094	20.32	2.8	2888.34
		20.763	3.84	0.158	20.517	4.52	2152.00
	ave.	20.00	3.03	0.11	19.82	3.49	2671.43
	st.dev.	0.91	0.48	0.03	1.02	0.64	337.12
AS 2.5%	30	18.568	2.96	0.108	18.219	3.64	2496.64
		19.972	2.84	0.096	19.916	3.16	2798.89
		18.518	2.68	0.084	18.505	2.92	2750.06
		18.724	3	0.102	18.566	3.64	2484.05
	ave.	18.95	2.87	0.10	18.80	3.34	2632.41
	st.dev.	0.69	0.14	0.01	0.76	0.36	165.33
MS 0.5%	30	20.217	3.12	0.101	20.067	3.56	2578.96
		17.857	3.4	0.109	17.686	4.08	2090.32
		18.053	3.04	0.119	17.162	4.6	2363.52
		18.717	2.64	0.088	18.702	2.97	2821.73
	ave.	18.71	3.05	0.10	18.40	3.80	2463.63
	st.dev.	1.07	0.31	0.01	1.28	0.70	311.41
MS 2.5%	30	18.167	3.04	0.093	17.876	3.52	2378.44
		16.157	3	0.115	15.607	4.28	2143.50
		15.185	2.76	0.084	15.185	3.27	2189.72
		16.16	3	0.088	16.12	3.36	2143.89
	ave.	16.42	2.95	0.10	16.20	3.61	2213.89
	st.dev.	1.25	0.13	0.01	1.18	0.46	111.83
MAPP 2.5%	30	26.407	1.2	0.042	26.407	1.2	8758.32
		23.366	1.12	0.033	23.366	1.12	8303.28
		29.251	1.68	0.127	29.251	1.68	6929.70
		26.747	1.51	0.102	4.722	1.51	7049.87
		26.474	2.04	0.064	26.474	2.04	5165.03
	ave.	26.45	1.51	0.07	22.04	1.51	7241.24
	st.dev.	2.09	0.37	0.04	9.90	0.37	1403.01
MAPP 10%	30	24.214	2.24	0.079	22.103	2.24	4302.31
		26.841	1.84	0.057	26.841	1.84	5805.83
		26.259	1.92	0.06	26.259	1.92	5443.27
		27.174	2.04	0.069	27.174	2.04	5301.59
		26.456	2.45	0.066	26.456	2.45	4297.75
	ave.	26.19	2.10	0.07	25.77	2.10	5030.15
	st.dev.	1.16	0.25	0.01	2.08	0.25	691.41